**An asymptomatic and persistent enteric virus is restricted from causing disease by the host immune system in a STAT1-dependent manner**

by

Heather Filyk

B.Sc., Queen's University, 2015

A THESIS SUBMITTED IN PARTIAL FULFILLMENT OF

THE REQUIREMENTS FOR THE DEGREE OF

MASTER OF SCIENCE

in

THE FACULTY OF GRADUATE AND POSTDOCTORAL STUDIES

(Microbiology and Immunology)

THE UNIVERSITY OF BRITISH COLUMBIA

(Vancouver)

October 2017

**Abstract**

Mammalian evolution has occurred while hosting mutualistic, commensal, and pathogenic micro- and macro-organisms for millennia. The virome can provide beneficial immune-stimulating signals or it can provide detrimental immune-stimulating signals that impact host health. Mechanisms that are important for relaying signals from the virome to the immune system are not well understood. Here I investigate the importance of a signalling molecule, Signal Transducer and Activator of Transcription-1 (STAT1), in controlling the immune response to an asymptomatic and persistent virus infection by murine Norovirus strain CR6 (CR6). By evaluating clinical parameters and virus-specific adaptive immune responses I was able to better understand how the host can coordinate appropriate immune responses to persistent enteric virus infections. Moreover, I confirmed that host-virome signals could limit CR6 burdens and systemic dissemination in immunosufficient mice. I conclude with a new perspective of how CR6 persists asymptomatically; by therapeutically limiting CR6 replication, I uncovered that unlike other persistent virus infections CR6 persistence may not be due to the apparent weak immune responses against it. Importantly, CR6 persistence requires STAT1 signalling, because deficient signalling leads to uncontrolled virus replication and ultimately host mortality, which limits virus transmission potential.

## Lay Summary

Humans have a large number of viruses inside their intestines, but the influence of these viruses on human health is not well understood. Animal models are useful in enabling a better understanding of how viruses interact with their human hosts. In my experiments, I infected mice with a virus that establishes a persistent intestinal infection in normal mice, without causing illness. I then investigated the role of a molecule (STAT1) in maintaining host health following virus infection. The mice missing STAT1 developed virus-induced disease and an uncontrolled immune response, which suggested to me that STAT1 is important for host responses to this intestinal virus. These findings contribute to basic scientific research while future applications may not be directly foreseeable, they may be applicable in vaccine design against intestinal viruses or fecal matter transplants.

## Preface

For this project I was responsible for the design, execution, and analysis of the data for all experiments, under the supervision of Dr Lisa Osborne. A tool I used to analyze the concentration of cytokines from data collected by cytometric bead array was synthesized by my lab mate Andrew Sharon, using the SOLVER script on Excel (Brown, 2001). Dr Lisa Osborne, Andrew Sharon, Blair Hardman, and Hannah Robinson all helped with tissue processing and lymphocyte collection during various experiments.

Histology slides were prepared by Jana Hodasova at the University of British Columbia Center for Comparative Disease and were analyzed by Dr. Ian Welch in discussion with myself.

This project required animal ethics approval for the murine Norovirus model. All experiments we performed in accordance with recommendations from the Canadian Council for Animal Care. The Animal Care Committee of the University of British Columbia approved all protocols (A15-0122, A15-0161). Biosafety protocols were approved by the University of British Columbia Biosafety Committee (B15-0113).

The anti-viral drug, 2'CMC, was graciously provided by collaborators Joana Duarte Da Rocha Pereira and Johan Neyts (Rega Institute for Medical Research, Belgium).

Fig 1.1 and Fig 1.2 have been published in **Filyk, H. A.** & Osborne, L. C. The Multibiome: The Intestinal Ecosystem's Influence on Immune Homeostasis, Health, and Disease. *EBioMedicine* **13,** 46-54 (2016). doi: 10.1016/j.ebiom.2016.10.007. The figure concepts were designed and created by myself with input from Dr. Lisa Osborne. Juliane Poschinski created graphics of the cell types and generously gave us permission to use them.

**Table of Contents**

**Abstract** ..... ii

**Lay Summary** ..... iii

**Preface** ..... iv

**Table of Contents** ..... v

**List of Tables** ..... x

**List of Figures** ..... xi

**List of Symbols** ..... xii

**List of Abbreviations** ..... xiii

**Acknowledgements** ..... xviii

**Dedication** ..... xix

**Chapter 1: Introduction** ..... 1

**1.1 Immune-mediated control of intestinal commensals and pathogens** ..... 1

**1.2 Norovirus and its influence on immune homeostasis** ..... 3

**1.3 Comparison of human and murine Norovirus** ..... 3

**1.4 The intestinal immune system** ..... 5

**1.4.1 Th1 cells** ..... 7

**1.4.2 Th2 cells** ..... 7

**1.4.3 Th17 cells** ..... 8

**1.4.4 Treg cells ..... 8**

**1.5 The antiviral state: STAT1 signalling ..... 12**

**1.5.1 MNV and IFN signalling ..... 12**

**1.5.1.1 Type I IFN ..... 13**

**1.5.1.2 MNV and Type I IFN ..... 14**

**1.5.1.3 Type II IFN ..... 14**

**1.5.1.4 MNV and Type II IFN ..... 15**

**1.5.1.5 Type III IFN ..... 15**

**1.5.1.6 MNV and Type III IFN ..... 15**

**1.6 MNV and the immune response ..... 16**

**1.6.1 Innate immunity to CR6 ..... 16**

**1.6.2 Adaptive immunity to CR6 ..... 17**

**1.7 STAT1 signalling in T cells ..... 19**

**1.7.1 STAT1 signalling in $CD4^+$ T cells ..... 19**

**1.7.2 STAT1 signalling in $CD8^+$ T cells ..... 20**

**1.8 Conclusion ..... 21**

**Chapter 2: Methods ..... 23**

**2.1 *in vivo* murine Norovirus CR6 infection model ..... 23**

**2.1.1 Mouse strains and housing conditions ..... 23**

**2.1.2 MNV CR6 generation and quantification of MNV CR6 stocks ..... 23**

**2.1.2.1 MNV CR6 generation ..... 23**

**2.1.2.2 Viral stock quantification ..... 24**

**2.1.3 Infection conditions ..... 24**

**2.1.4 *in vivo* antibody depletion conditions ..... 25**

**2.1.5 Antibiotic treatment ..... 25**

**2.2 *in vivo* MNV CR6 post-infection analysis ..... 26**

**2.2.1 Tissue histology ..... 26**

**2.2.2 Lymphocyte recovery ..... 26**

**2.2.2.1 Spleen and lymphocytes ..... 26**

**2.2.2.2 Colon and cecum ..... 26**

**2.2.2.3 *ex vivo* lymphocyte stimulation ..... 27**

**2.2.2.4 MNV-specific $CD4^+$ T cell enrichment ..... 27**

**2.2.3 Flow cytometry ..... 28**

**2.2.3.1 Surface and intracellular staining ..... 28**

**2.2.3.2 Flow cytometry data acquisition and analysis ..... 29**

**2.2.4 Serum cytokine detection ..... 29**

**2.2.4.1 Cytometric bead array ..... 29**

**2.2.5 Quantitative PCR ..... 29**

**2.2.5.1 RNA isolation and cDNA generation ..... 29**

**2.2.5.2 Measurement of viral loads by qPCR ..... 30**

**2.2.5.3 Gene expression qPCR ..... 30**

**2.2.6 Intestinal permeability assays ..... 31**

**2.2.6.1 Serum FITC-dextran assay ..... 31**

**2.2.6.2 Fecal serum albumin assay ..... 32**

**2.3 Statistical analyses ..... 32**

**Chapter 3: Results ..... 33**

**3.1 STAT1 limits systemic enteric CR6 viral replication and virus-induced disease .... 33**

**3.2 CR6-induced weight loss is associated with systemic histopathology in *Stat1$^{KO}$* mice .... 38**

**3.3 STAT1 limits the expansion and function of CR6-specific CD8$^{+}$ T cells *in vivo* ..... 39**

**3.4 IFNγ is produced by different cell types in CR6-infected *Stat1$^{het}$* compared to *Stat1$^{KO}$* mice .... 43**

**3.5 STAT1 directs transcription factor expression in CR6-specific CD4$^{+}$ T cells ..... 44**

**3.6 STAT1 directs cytokine production by CD4$^{+}$ T cells post CR6 infection ..... 47**

**3.7 STAT1 directs CD4$^{+}$ T cell differentiation after receiving type 1-associated stimulation .... 48**

**3.8 IL-17A neutralization does not change clinical outcomes or immune signatures of CR6-infected *Stat1$^{KO}$* mice .... 52**

**3.9 STAT1 signalling regulates systemic cytokine production following CR6 infection 55**

**3.10 STAT1 signalling does not regulate properties of Treg cells during CR6 infection .... 57**

**3.11 Enteric CR6 infections do not cause a detectable disturbance in the intestinal barrier .... 59**

**3.12 Antiviral treatment prevents clinical signs, but does not impair the immunological signature of CR6-infected *Stat1$^{KO}$* mice .... 62**

**Chapter 4: Conclusion .... 65**

**4.1 Discussion .... 65**

**4.2 Summary .... 75**

**4.3 Research applications and future directions .... 77**

**References** ..... **80**

**Appendices** ..... **93**

**Appendix A Flow cytometry gating strategy used in experiments** ..... **93**

**Appendix B CD8$^{+}$ T cell frequencies expanded in CR6-infected *Stat1*$^{KO}$ mice, but do not display a role in protection or immunopathology.** ..... **94**

**Appendix C Antibiotic treatment does not change CR6-induced morbidity or altered immune responses observed in infected *Stat1*$^{KO}$ mice** ..... **95**

**Appendix D CD4 T cells not responsible for CR6-infection induced morbidity or altered immune responses** ..... **96**

**Appendix E IL-17A-neutralization in CR6-infected *Stat1*$^{KO}$ mice reduced Th17 serum cytokines, compared to control treated mice** ..... **97**

**List of Tables**

Table 2.1 Primers used for RT-qPCR…… 31

**List of Figures**


Figure 1.1 T helper cell subsets: pathogen specificity and cytokine response……10

Figure 1.2 T helper subsets cross regulate to coordinate appropriate immune responses to pathogens……11

Figure 3.1 STAT1 limits chronic CR6-infection induced weight loss, mortality, and virus dissemination……..……..35

Figure 3.2 STAT1 limits acute CR6-infection induced weight loss, mortality, and virus dissemination……..37

Figure 3.3 CR6-induced weight loss is associated with systemic histopathology in *Stat1*$^{KO}$ mice……39

Figure 3.4 STAT1 limits CR6-specific CD8$^{+}$ T cell frequencies and cytokine production…….…..42

Figure 3.5 STAT1 is important for generating IFNγ producing CD4$^{+}$ T cells, regardless of infection status……44

Figure 3.6 STAT1 is important for directing Th1 differentiation during CR6-specific T cell activation……..……46

Figure 3.7 STAT1-deficient Th cells produce IL-17A and do not produce IFNγ……...48

Figure 3.8 Th1 skewing conditions directs away from type 1 cytokine production by *Stat1*$^{KO}$ CD4$^{+}$ T cells *in vitro*……..……51

Figure 3.9 IL-17A is not directly responsible for CR6-induced disease observed in *Stat1*$^{KO}$ mice...……54

Figure 3.10 CR6-infected *Stat1*$^{KO}$ mice have increased serum cytokines, compared to *Stat1*$^{het}$ mice……56

Figure 3.11 Treg differentiation and function are not dependent on STAT1 signaling during CR6 intestinal infection……..……58

Figure 3.12 Barrier integrity maintained during CR6 infection, regardless of STAT1 signaling……61

Figure 3.13 Uncontrolled CR6 replication responsible for CR6-induced morbidity, but not altered immune responses observed in infected *Stat1*$^{KO}$ mice..……...64

**List of Symbols**

| | |
|---|---|
| α | Alpha |
| | Anti |
| β | Beta |
| γ | Gamma |
| λ | Lambda |
| μ | Micron |
| I | One |
| II | Two |
| III | Three |
| % | Percent |
| $Gene^{-/-}$ | Genetic Deletion of a Gene |
| $Gene^{KO}$ | |
| $Gene^{+/-}$ | Genetic Heterozygote of a Gene |
| $Gene^{het}$ | |

**List of Abbreviations**

| | |
|---|---|
| 2CMC | 2'-*C*-Methylcytidine |
| Ab | Antibody |
| ACK | Ammonium-Chloride-Potassium |
| APC | Allophycocyanin |
| BMDC | Bone Marrow-Derived Dendritic Cell |
| C57BL/6 | C57 Black 6 |
| CBA | Cytokine Bead Array |
| CD | Cluster of Differentiation |
| CID | Chronic Inflammatory Disease |
| CR6 | Murine Norovirus strain CR6 |
| CTCM | Complete Tissue Culture Media |
| CW3 | Murine Norovirus strain CW3 |
| DC | Dendritic Cell |
| dH2O | Distilled Water |
| DMEM | Dulbecco's Modified Eagle's Medium |
| EDTA | Ethylenediaminetetraacetic Acid |
| ELISA | Enzyme-Linked Immunosorbent Assay |
| FACS | Fluorescence-Activated Cell Sorting |
| FBS | Fetal Bovine Serum |
| FITC | Fluorescein Isothiocyanate |

| | |
|---|---|
| Foxp3 | Forkhead Box P3 |
| GALT | Gut-Associated Lymphoid Tissue |
| GAS | Gamma-Activated Sequences |
| GATA3 | GATA Binding Protein 3 |
| GF | Germ Free |
| GI | Gastrointestinal |
| H&E | Hematoxylin and Eosin |
| HIV | Human Immunodeficiency Virus |
| HPRT | Hypoxanthine-guanine phosphoribosyltransferase |
| HRP | Horse Radish Peroxidase |
| huNoV | Human Norovirus |
| i.p. | Intra-Peritoneal |
| IBD | Inflammatory Bowel Disease |
| IBS | Irritable Bowel Syndrome |
| ICS | Intracellular Stain |
| IEC | Intestinal Epithelial Cell |
| IEL | Intraepithelial Lymphocyte |
| IFN | Interferon |
| IFNAR | Interferon alpha Receptor |
| Ig | Immunoglobulin |
| IL | Interleukin |
| IRF9 | Interferon Response Factor 9 |

| | |
|---|---|
| ISGF3 | Interferon-Stimulated Gene Factor 3 |
| ISRE | Interferon-Stimulated Response Elements |
| JAK | Janus Kinase |
| kDa | Kilodalton |
| LCMV | Lymphocytic Choriomeningitic Virus |
| L.o.D. | Limit of Detection |
| LPL | Lamina Propria Lymphocyte |
| M cell | Microfold Cell |
| MDA | Melanoma Differentiation-Associated |
| MHC | Major Histocompatibility Complex |
| mi | micro |
| MIP | Macrophage Inflammatory Protein |
| MLN | Mesenteric Lymph Node |
| MNV | Murine Norovirus |
| mRNA | Messenger Ribonucleic Acid |
| MUC | Mucin |
| NCS | Newborn Calf Serum |
| NK | Natural Killer |
| pfu | Plaque Forming Units |
| pi | Post Infection |
| *p.o.* | Per Os |
| PBS | Phosphate-Buffered Saline |

| | |
|---|---|
| PCR | Polymerase Chain Reaction |
| PE | Phycoerythrin |
| PMA | Phorbol 12-myristate 13-acetate |
| *Rag* | Recombination-Activating Gene |
| REG | Regenerating Islet-Derived Protein |
| RIG-I | RIG-I-like Receptor |
| RNA | Ribonucleic Acid |
| RORγt | Retinoic Acid-Related Orphan Receptor-gamma t |
| RPMI | Roswell Park Memorial Institute |
| RT | Room Temperature |
| RT-PCR | Real Time Polymerase Chain Reaction |
| SA | Serum Albumin |
| SD | Standard Deviation |
| SIV | Simian Immunodeficiency Virus |
| ss | Single Stranded |
| STAT | Signal Transducer and Activator of Transcription |
| T-bet | T-box Transcription Factor |
| TCR | T Cell Receptor |
| TGF | Transforming Growth Factor |
| Th | T helper |
| Tjp | Tight junction protein |
| TLR | Toll-Like Receptor |

| | |
|---|---|
| TNF | Tumor Necrosis Factor |
| Treg | T Regulatory Cell |
| UBC | University of British Columbia |
| *vs.* | Versus |
| WT | Wild Type |

**Acknowledgements**

I deeply appreciate my parents for their continual love and support, from childhood to my existential young adulthood. They have been consistent in their encouragement to try my best and enjoy life. I thank my siblings, for keeping their youngest sister humbled yet confident to go out and explore the world. I am also thankful to my friends, both near and far, for being there and contributing so much to this wonderful adventure.

This thesis could not have come to fruition without my supportive lab and its wonderful members. I especially appreciate all the guidance and mentorship my supervisor, Dr Lisa Osborne, provided me. This thesis could not have been written without your support.

I would like to thank my committee members, Dr Ken Harder and Dr Bruce Vallance, for providing direction and stimulating new ideas during the progression of my thesis. Moreover, I thank NSERC for providing funding for my stipend for the second year of my MSc thesis.

Blair Hardman, Andrew Sharon, Hannah Robinson, Wallace Yuen, and Jung Hee Seo, I appreciate you all so much. To have such enthusiastic, quick-witted, and courteous lab members makes leaving difficult, I could not have asked for a better environment to do science in.

Finally, I must acknowledge the nature that surrounds Vancouver, especially the coastal mountains. Creative thoughts, new perspectives, meanings, and inspirations were often conjured up on weekend trips to the coastal mountains. I made beautiful friendships in the mountains, where we endured suffering and also celebrated meaningless accomplishments and failures in elation. At no point was my time in graduate school cripplingly arduous or filled with apathy, thanks to these natural cathedrals.

For my late grandfather Maurice Strong, who instilled in me the desire and courage to pursue meaningful work and to live consciously.

“Don't accept that you can't make a difference, because if you can't make a difference, you won't make a difference” – Maurice Strong

# Chapter 1: Introduction

## 1.1 Immune-mediated control of intestinal commensals and pathogens

Mammalian evolution has occurred while hosting mutualistic, commensal, and pathogenic micro- and macro-organisms for millennia. The presence of these organisms has resulted in reciprocal interactions between these colonizing species and the host immune system. A largely mutualistic relationship exists between the host and its bacterial microbiota, which have been shown to promote numerous physiological functions including intestinal vascularization and epithelial cell function, nutrient absorption, and inhibition of pathogen invasion (Brestoff and Artis, 2013; Hooper et al., 2012; Stappenbeck et al., 2002). Moreover, crosstalk between intestinal bacterial communities and the host fundamentally influences immune homeostasis, host-protective immunity, and disease-associated inflammation (Belkaid and Hand, 2014; Brestoff and Artis, 2013). Sequencing technologies have revolutionized our understanding of which bacteria colonize the intestine (Filyk and Osborne, 2016). Moreover, extensive investigation of germ-free (GF), gnotobiotic (selectively colonized), and antibiotic-treated small animal models have provided insight into how intestinal bacteria interact with the host (Filyk and Osborne, 2016). However, the microbiome includes more than just bacteria, there are also viruses, archaea, fungi, and protists; but thus far, these entities and their influence on host homeostasis and disease have been less thoroughly investigated (Filyk and Osborne, 2016).

Constituents of the virome are present in order of magnitudes higher than the bacterial microbiome and several lines of evidence support the hypothesis that virome-derived signals influence host immunity and physiology. First, GF mice colonized with a persistent eukaryotic virus (Murine Norovirus strain CR6) is sufficient to restore some of the characteristic defects in

immune tissue development and intestinal pathogen protection that were previously thought to result from lack of bacterial-derived signals (Kernbauer et al., 2014). Next, depleting the murine virome with broad-spectrum (DNA and RNA) antiviral treatment exacerbated DSS-induced colitis in WT mice, indicating that the intestinal virome may mitigate the severity of intestinal inflammation through Toll-like receptors (TLR) 3 and TLR7 (Yang et al., 2016). There is also evidence that the host actively controls the intestinal virome, Human Immunodeficiency Virus (HIV) and Simian Immunodeficiency Virus (SIV)-induced acquired immunodeficiency leads to an expansion in other viruses in those affected with immunodeficiency (Handley et al., 2012; Monaco et al., 2016). Finally, immune responses to a number of enteric viruses have been associated with autoimmunity (enteroviruses with Type 1 Diabetes and Reovirus with celiac disease) (Bouziat et al., 2017; Richardson and Horwitz, 2014). Thus, in certain contexts the virome can contribute to the development or progression of various chronic inflammatory diseases (CIDs), such as autoimmunity.

During homeostasis, the immune system resists and/or tolerates the enteric virome (Schneider and Ayres, 2008). The concept of tolerance differs from that of resistance in that resistance occurs to limit pathogen burden by utilizing immune defenses, whereas tolerance aims to limit collateral damage from an overt immune response to a non-life threatening pathogen (Schneider and Ayres, 2008). Our understanding of how members of the eukaryotic virome can influence host health, while remaining asymptomatically persistent, is still being parsed. The overall objective of my thesis is to better understand host mechanisms that regulate immune responses to an asymptomatic and persistent enteric virus, murine Norovirus strain CR6.

## 1.2 Norovirus and its influence on immune homeostasis

Norovirus infections are the most common cause of gastroenteritis globally and a significant cause of morbidity and mortality (Bartsch et al., 2016). Noroviruses normally cause acute disease, with severe diarrhea; however, immunocompromised and some immunocompetent persons can be persistently infected and shed the virus for years (Bok and Green, 2012; Woodward et al., 2015). It has been postulated by numerous groups that chronically infected individuals may act as reservoirs for emerging strains, leading to new outbreaks (Karst et al., 2014). At mucosal interfaces, such as the gastrointestinal (GI) tract, acute and persistent Norovirus infection are theorized to have the ability to cause profound long-term effects on the host's immune system (Woodward et al., 2015). Supporting this claim, epidemiological studies have found that Norovirus infections were associated with increased prevalence of post-infectious irritable bowel syndrome (IBS) and inflammatory bowel disease (IBD) in human populations (Pensabene et al., 2015; Zanini et al., 2012). We are beginning to uncover that infections, like Norovirus, not only cause acute disease, but also can act as environmental triggers for CIDs by influencing the host's immune homeostasis after inducing inflammation.

## 1.3 Comparison of human and murine Norovirus

Both human (huNoV) and murine Norovirus (MNV) are non-enveloped icosahedral positive-sense single stranded RNA viruses, spread via the fecal-oral route (Karst et al., 2014). In humans, a typical huNoV infection involves acute onset of symptoms followed by 24-72 hours of diarrhea and vomiting. A major discrepancy in the pathogenesis of human *vs* murine Norovirus infection is that wild-type mice do not develop severe diarrhea post-MNV infection (Karst et al., 2014). However, this small animal model has a number of similarities to the huNoV and can be used to interrogate host-virus interactions. For instance, the replication mechanisms

of huNoV and MNV are relatively similar; MNV can replicate once inside human cells. Therefore, only the MNV attachment receptor, murine CD300lf, confers species-specific tropism (Orchard et al., 2016). In addition, although huNov infections are typically acute, chronic infections can also be established. Similarly, there are two strains of MNV, which emulate either the acute or chronic human infection. The CW3 strain models acute huNoV infections; CW3 infects the entire length of the GI tract, disseminates systemically, causes acute disease, and intestinal damage (Karst et al., 2014). In contrast, the CR6 strain models chronic huNoV infections; CR6 persistently and asymptomatically infects mice, is restricted to the intestine, but causes little damage to intestinal tissue (Karst et al., 2014). This small animal model, although imperfect, is invaluable because it affords the ability to track, qualify, and quantify MNV specific immune responses in details not possible using human samples.

Investigating host-virome interactions requires an appropriate model. Strains of MNV can be endemic in animal research facilities and can be considered a "commensal" murine enteric virus (Kernbauer et al., 2014). MNV is endemic to mouse populations, 22.1% of mouse research colonies in both the United States and Canada contained animals that were seropositive for MNV (Hsu et al., 2005). Importantly CW3 and CR6, according to initial studies, do not cause major disruptions in the bacterial microbiota – thus, observations made during infection are likely due to the virus's direct effect on the host (Nelson et al., 2013). Moreover, mice with a genetic susceptibility to IBD only developed symptoms in CR6-endemic facilities or when deliberately exposed to CR6 when the microbiota were present, indicating this asymptomatic constituent can act as an environmental trigger for murine IBD (Cadwell et al., 2010). In summary, persistent strains of MNV are examples of eukaryotic intestinal virome constituents that are common to mice and can directly influence host immune homeostasis and disease. These

factors make CR6 an attractive virus model to explore mechanisms by which the host interacts with the virome.

### 1.4 The intestinal immune system

The intestinal immune system has evolved various ways to protect the host from pathogens. The intestine's physical and chemical nature offers large changes in pH, proteolytic enzymes, mucus lining with antimicrobial peptides, and competitive ecological environments, which all act as a defense in some capacity.

In the cecum and colon, the epithelial layer is relatively flat, with absorptive intestinal epithelial cells (IECs), microfold (M) cells, and goblet cells creating the cellular barrier between the host and the intestinal lumen. In the colon, goblet cells produce a thick dual-layer mucus to protect the intestinal epithelial layer from mechanical damage and microbial threat (Mowat and Agace, 2014). If, for example, a viral pathogen penetrates through the epithelial layer, typically via M cells, it will encounter the gut-associated lymphoid tissue (GALT), a dendritic cell (DC)-rich area for processing and presentation to the adaptive immune system. Cecal and colonic patches are lymphocyte rich areas in the murine cecum and colon (Mowat and Agace, 2014; Owen et al., 1991). These areas specialize in priming and promoting adaptive T and B cell responses to luminal antigens. Upon activation, B cells differentiate into plasma cells that secrete antigen-specific IgA into the lumen to help keep commensal populations controlled and protect against secondary infections (Mowat and Agace, 2014). The GALT of the cecum and colon drain into the mesenteric lymph nodes, where antigen-specific $CD4^+$ and $CD8^+$ T cells are primed and then home to the intestinal tissue (Carter and Collins, 1974). The microbiota is typically sensed and processed by the immune system during homeostasis. In this setting, regulatory signals

shape the adaptive immune response against commensal microbiota, promoting tolerant immune responses (Belkaid and Hand, 2014).

$CD8^+$ T cells home to the intestinal epithelium and are referred to as intraepithelial lymphocytes (IELs) (Sheridan and Lefrançois, 2010). IELs are comprised of antigen-specific (conventional) IELs, which represent tissue-resident effector and memory $CD8^+$ T cells and limited-specificity IELs (Sheridan and Lefrançois, 2010). Antigen specific IELs scour the epithelium after antigen exposure in close contact with enterocytes to monitor any alterations and assure the integrity of the intestinal epithelium (Jabri and Ebert, 2007). Conventional IELs are promoted if antigen is presented along with pro-inflammatory signals and these cells can have potent cytotoxic effects and prevent the systemic spread of pathogens (van Wijk and Cheroutre, 2010).

The lamina propria of the intestine contains a diverse array of $CD4^+$ T cells, also known as T helper cells. T helper (Th) cells are aptly named as they differentiate into specific subtypes according to signals they receive from DCs to help coordinate an appropriate immune response to each specific threat. Th cells produce arrays of cytokines and chemokines that direct B cell antibody (Ab) class-switching and differentiation to Ab-secreting plasma cells, activate macrophages and DCs, and recruit innate cells to the area of inflammation (Zhu and Paul, 2008). Important Th subtypes are the Th1, Th2, Th17, and T regulatory (Treg) cells, summarized in Figure 1.1 by the pathogens they respond to and major cytokines they produce (Filyk and Osborne, 2016). The major subjects are outlined below, categorized by activating signals and general function.

### 1.4.1 Th1 cells

$CD4^+$ Th1 cells are involved in type 1 immunity, the response coordinated against viral infections and intracellular pathogens. Th1 differentiation begins by signalling through Signal Transducer and Activator or Transcription-1 (STAT1) to promote the transcription of Tbet, the master transcription factor of Th1 differentiation and function (Zhu and Paul, 2008). Once differentiated, Th1 cells produce cytokines interferon-γ (IFNγ), IL-2, and TNFα (Maldonado et al., 2009). Th1 function is amplified by interleukin (IL)-12 signaling through STAT4 to increase IFNγ production.

The purpose of type 1 immunity, in a viral context, is to induce an antiviral state, encourage antigen presentation, promote IgG antibody production, and stimulate cytotoxic $CD8^+$ T cell activation and memory cell formation (Williams et al., 2006; Zhu and Paul, 2008). $CD8^+$ T cells destroy infected cells by specifically binding major histocompatibility complex I (MHC I) proteins that contain a pathogen's peptide presented by an infected cell and releasing cytotoxic effector molecules, which initiates pro-apoptotic programming. Moreover, IgG can neutralize viral particles and promote opsonization by activated macrophages and DCs or can coat cells to promote nature killer (NK) cell cytotoxic activity.

### 1.4.2 Th2 cells

$CD4^+$ Th2 cells are involved in allergic responses and parasitic immunity. Th2 differentiation begins by signalling through STAT6 to promote the transcription of GATA3, the master transcription factor of Th2 differentiation and function. IFNγ suppresses Th2 differentiation (Maldonado et al., 2009). Th2 cells secrete type 2 cytokines (IL-4, IL-5, and IL-13) to promote IgE antibody secretion and mast cell and eosinophil recruitment (Kopf et al.,

1993; Swain et al., 1990; Zhu and Paul, 2008). Th2 responses are not specific to viral threats; in fact, Th2 responses directly antagonize antiviral Th1 immune responses, which can impair adaptive antiviral immunity and reactivate latent viral infections (Fig 1.2) (Osborne et al., 2014; Reese et al., 2014).

### 1.4.3 Th17 cells

$CD4^+$ Th17 cells are involved in extracellular bacterial and fungal immunity. Th17 differentiation begins by signalling through STAT3 to promote the transcription of RORγt, the master transcription factor of Th17 differentiation and function (Zhu and Paul, 2008). IL-4 and IFNγ suppress Th17 differentiation (Zhu and Paul, 2008). Th17 cells contribute to mucosal barrier strength, protecting the host from microbial invasion (Stockinger and Omenetti, 2017). Th17-derived IL-22 promotes mucus production and antimicrobial peptides REGIIIβ and REGIIIγ, while Th17-derived IL-17 direct the cellular location of some tight junction proteins to maintain barrier integrity (Kolls et al., 2008; Lee et al., 2015). Th17 cells can promote IgA production in Peyer's patch germinal centers (Hirota et al., 2013). IL-17A and IL-17F both attract and activate neutrophils, which target extracellular mucosal microbes and help prevent their systemic spread (Zhu and Paul, 2008). However, Th17-dependent neutrophil recruitment and pro-inflammatory cytokine release in non-mucosal tissues has not been observed under homeostatic conditions and can cause collateral damage to the host (Stockinger and Omenetti, 2017).

### 1.4.4 Treg cells

$CD4^+$ Treg cells are involved in maintaining tolerance to self and microbial commensal antigens. Treg differentiation begins by signalling through STAT5 to promote the transcription

of Foxp3, the master transcription factor of Treg differentiation and function (Zhu and Paul, 2008). Treg cells limit inflammation by producing cytokines IL-10 and TGFβ (Zhu and Paul, 2008). IL-10 inhibits many immune cell activities including those of Th1, Th2, and Th17 cells (Fig 1.2). Tregs are particularly important in the colon, where the microbial burden is at its highest density, but where the majority of microbes are symbiotic with the host (Mowat and Agace, 2014). Importantly, Norovirus-triggered microbiota-driven intestinal inflammation is limited by IL-10 production (Basic et al., 2014).

Many colonic $CD4^+$ T cells are primed by DCs in the mesenteric lymph nodes, after which they home to the intestinal tissue. Compared to other regions of the GI tract, the cecum and colon have the highest ratio of Treg to Th17 cells, reflecting the specialized need to tolerate and regulate inflammation from the high density of microbes in this part of GI tract (Denning et al., 2011). Th1 and Th2 subtypes do not vary significantly along the GI tract (Denning et al., 2011). These $CD4^+$ Th cells shape the microenvironment in which the immune system responds to both commensals and intestinal pathogens, including enteric viruses.

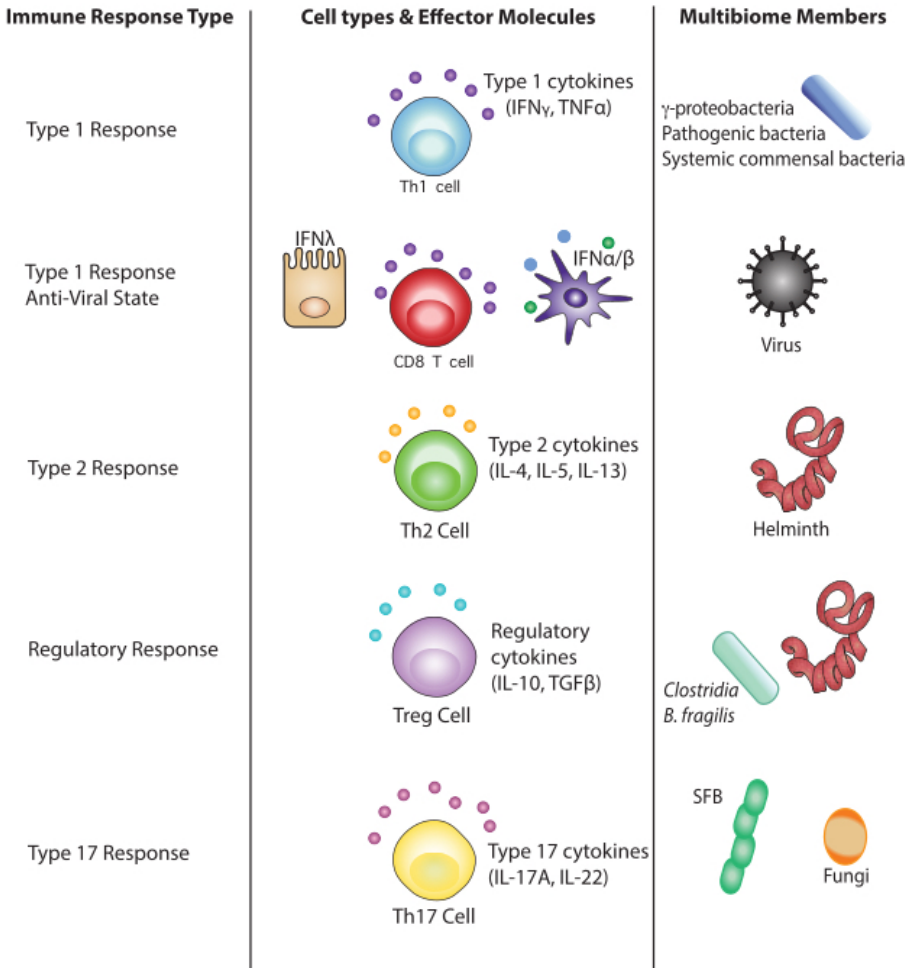


**Figure 1.1 T helper cell subsets: pathogen specificity and cytokine response.** Type 1 pro-inflammatory cytokines and cells target intracellular microbes, including bacterial pathogens, opportunistic commensal bacterial infection and viruses. IFNs are critical components of the antiviral immune response. Type 1 responses are pro-inflammatory and can cause collateral damage to the host if the immune response is not balanced and regulated. Type 2 immune responses are triggered by helminth infections. Type 2 responses coordinate worm expulsion and rapid wound healing; however, it can lead to fibrosis if the immune response is not balanced and regulated. Regulatory responses are promoted by certain bacterial species (some Clostridia species, B. fragilis), and helminth infections. Their broad immunosuppressive actions contribute to self-tolerance and commensal multibiome-tolerance. They are also initiated during the resolution phase of type 1, 2, and 17-promoting infections. Type 17 responses are triggered by extracellular bacterial pathogens, fungi and some epithelial cell binding commensal bacterial species. Type 17-associated cytokines promote mucosal barrier function, but are also widely implicated in autoimmune and CIDs.

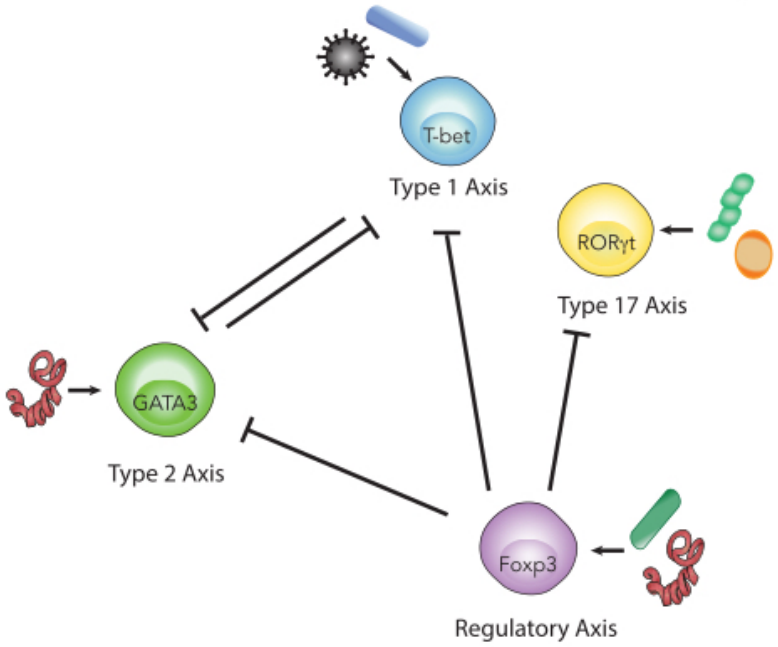


**Figure 1.2 T helper subsets cross regulate to coordinate appropriate immune responses to pathogens.** This illustration simplifies and illustrates T helper subset interactions and their ability to regulate or inhibit the activation or function of another subset. During an appropriate immune response, T helper subset regulation is crucial to restrict pathogen burdens, avoid immunopathology, and generate good memory responses. Immune cross-regulation is mediated through a variety of mechanisms including cytokines, chemokines, receptor interactions, and transcription factor expression. Certain pathogens promote the expansion of different subsets of Th cells, which in turn inhibit, promote, and/or balance the other subsets. T-bet expressing Th1 (activated in response to bacteria and viruses) and GATA3 expressing Th2 cells (helminth-induced), antagonize each other. Some bacterial species and helminths promote Foxp3-expressing Tregs, which in turn limit the activation of Th1, Th2 and Th17 cells.

## 1.5 The antiviral state: STAT1 signalling

Interferons (IFNs) induce cell-intrinsic antiviral states in infected and neighbouring cells to protect from virus infections (Ivashkiv and Donlin, 2014). There are three families of IFNs, all of which signal through STAT1 to induce the antiviral state. The precise antiviral state of an individual cell is dependent on context: IFN family, cell type, virus type, co-infections, and other environmental factors can all influence the response. The antiviral state reduces virus replication and spread, encourages antigen presentation, controls inflammatory responses, coordinates cytokine release, and promotes high-affinity antigen-specific T and B memory cell formation (Ivashkiv and Donlin, 2014). The commensal microbiota induces tonic signalling through IFN receptors and calibrates systemic IFN responses, which creates a state of preparedness and protects the host from viral infections at systemic sites (Abt et al., 2012; Kawashima et al., 2013). Thus, IFNs act to clear viral infections by acting early and rapidly and coordinating appropriate immune responses.

### 1.5.1 MNV and IFN signalling

Fourteen years ago, researchers at the University of Washington noticed that their colony of *Stat1*$^{-/-}$ *Rag1*$^{-/-}$ mice demonstrated significant rates of morbidity and mortality and determined that an infectious agent was the cause. They isolated a virus from affected animals and through sequencing alignment determined that it was a previously unknown member of the Norovirus family, amounting to the discovery of murine Norovirus (MNV) (Karst et al., 2003; Mumphrey et al., 2007). Since then, multiple strains of MNV have been discovered, and many murine knockout models have been investigated in the context of MNV infection; however few show clinical symptoms. The few proteins and pathways shown to be important for controlling MNV

infections are MDA5, IFNAR, IFNλR and STAT1—each involved in establishing or propagating the antiviral state—and RAG1, necessary for B and T cell development (Baldridge et al., 2015; Chachu et al., 2008a; Karst et al., 2003; McCartney et al., 2008; Nice et al., 2015, 2016; Tomov et al., 2013). Several studies have highlighted the importance of STAT1 signalling in the context of MNV infection: in $Stat1^{KO}$ mice the acute strain CW3 results in rapid lethality (Karst et al., 2003); an attenuated strain results in gastric bloating and diarrhea (Kahan et al., 2011); and persistent infection with MNV strain O7 results in severe diffuse inflammation and necrosis of the liver and enlarged spleen with pale foci (Shortland et al., 2014). These studies suggest that STAT1, which integrates all types of IFN signalling, will play an important role in establishing a coordinated immune response in an otherwise immunosufficient host. The above studies are relatively recent investigations and our understanding of the immune response to CR6 is far from comprehensive, the immune response to CR6 is still insufficiently characterized.

#### 1.5.1.1 Type I IFN

Type I IFNs (IFNα and IFNβ) are produced and sensed by both immune and non-immune cell types, therefore most cell types can induce an antiviral state to protect against virus infection (Ivashkiv and Donlin, 2014). IFNα and IFNβ bind the IFNα receptor (IFNAR), which leads to the phosphorylation of STAT1 and STAT2 (Levy and Darnell Jr., 2002). Phosphorylated STAT1 and STAT2 form a heterodimer and move to the nucleus to form a complex with interferon response factor 9 (IRF9), called the IFN-stimulated gene factor 3 (ISGF3) (Levy and Darnell Jr., 2002). This complex binds to interferon-stimulated response elements (ISREs), a particular sequence of nucleotides upstream of hundreds of antiviral genes. By directing the upregulation and downregulation of hundreds of proteins, STAT1 signalling enforces the antiviral state. The

antiviral state inhibits viral protein translation and synthesis, degrades cytoplasmic nucleic acids, alters metabolism, and induces apoptosis (Ivashkiv and Donlin, 2014).

#### 1.5.1.2 MNV and Type I IFN

The inability to signal through the IFNα/β receptor allows the intestinally-restricted CR6 infection to disseminate to the spleen (Baldridge et al., 2015). Intriguingly, the inability to signal through IFNAR does not result in CR6-induced disease or increased viral titers in the stool (Nice et al., 2015). This suggests that IFNAR signalling is not the primary factor for host control of CR6 replication in the colon, but is important for confining CR6 infections to the colon. The immune responses in the genetic mutants have not been thoroughly investigated.

#### 1.5.1.3 Type II IFN

Type II IFN (IFNγ) is produced by immune cells (NK cells, innate lymphoid cells, $CD4^+$ and $CD8^+$ T cells) and acts mainly on immune cells to encourage antiviral immune responses. IFNγ signals through the IFNγ receptor (IFNGR) in a similar sequence to Type I IFNs. IFNGR signalling phosphorylates STAT1 molecules, which form homodimers that bind to gamma-activated sequences (GAS) upstream of a different set of antiviral genes (Levy and Darnell Jr., 2002). Again, these genes encourage the antiviral state and cell-mediated immunity to intracellular pathogens. IFNγ acts on macrophages and DCs to super-activate phagocytosis and professional antigen presentation functions (Schroder et al., 2004). IFNγ acts on $CD4^+$ T cells to promote Th1 differentiation, which in turn produce more IFNγ (Zhu and Paul, 2008). IFNγ signals to B cells to produce antiviral IgG and increases the potential for specific $CD8^+$ T cell generation (Schroder et al., 2004).

#### 1.5.1.4 MNV and Type II IFN

IFNγ signaling is important for innate immunity to MNV infections. Macrophages require IFNγ signaling through STAT1 to effectively inhibit CW3 replication (Maloney et al., 2012). However, adaptive IFNγ-mediated $CD8^+$ T cell cytotoxicity is less important for CW3 clearance, than perforin production (Chachu et al., 2008a). The role of IFNγ in innate and adaptive immunity to CR6 infections has not been thoroughly investigated; however, at day 7 post-infection, CR6 titers in the stool are similar in WT and *Ifngr1*$^{-/-}$ mice, indicating that IFNγ is not crucial for controlling CR6 replication in the colon (Baldridge et al., 2015). Moreover, CR6-infected mice lacking IFNGR signalling were not reported to show clinical signs (Baldridge et al., 2015). However, the specific role of IFNγ signalling during CR6 infection has not been investigated beyond these parameters and merits study, since IFNγ is key to clearing many viral infections (Schroder et al., 2004).

#### 1.5.1.5 Type III IFN

Type III IFNs (IFNλ) are produced by epithelial cells, and certain subtypes of monocytes, macrophages, and DCs, and act primarily on cells of epithelial origin (Yin et al., 2012). IFNλs signal through the IFNλ Receptor (IFNλR) in a sequence similar to IFNα/β signalling. IFNλR activation phosphorylates STAT1 and STAT2, which heterodimerize and ultimately upregulate hundreds of antiviral genes (Lee and Baldridge, 2017; Yin et al., 2012). The genes stimulated by IFNα/β and IFNλ largely overlap; however, targeting different cell types allows for more specific antiviral responses (Lee and Baldridge, 2017).

#### 1.5.1.6 MNV and Type III IFN

IFNλ signalling through IECs is critical for controlling CR6 intestinal viral replication and shedding (Baldridge et al., 2017; Nice et al., 2015). Exogenous IFNλ can cure persistent

CR6 infection in WT and T and B cell-deficient (*Rag1*$^{-/-}$) mice, which suggests that IFNλ clears the infection independently of the adaptive immune system (Nice et al., 2015). New evidence suggests that a viral protein from CR6 inhibits IFNλ signalling to promote its persistence in the host (Lee et al., 2017).

In conclusion, IFNAR and IFNλR are crucial for controlling CR6 infections, but there are no reports of histopathological lesions observed in mice with singular knockouts of these receptors, these observations are only reported when their common signalling molecule, STAT1, is absent (Baldridge et al., 2015; Nice et al., 2015; Shortland et al., 2014). An in-depth analysis of how STAT1 relays signals from CR6 to coordinate immune responses can increase our understanding of how asymptomatic persistent enteric viruses signal to the host immune system and influence systemic immunity.

## 1.6 MNV and the immune response

The immune response to any infection requires a carefully orchestrated response by multiple cell types. Likewise, a complex immune network acts to control MNV infections; no cell type is solely responsible for its control. In other words, the depletion or addition of one cell type can only partially reduce MNV replication. Moreover until 14 years ago, relatively recently for a common virus infection, there was no small-animal model to explore these questions (Karst et al., 2003, 2014). Our current understanding of the cellular immune response is outlined below.

### 1.6.1 Innate immunity to CR6

MNV overcomes the intestinal epithelial cell layer by M cell transcytosis or by directly infecting IECs (Kolawole et al., 2016; Lee et al., 2017). Both huNoV and CW3 induce minor intestinal inflammation and IEC apoptosis; however, CR6 does not appear to induce intestinal

inflammation (Karst et al., 2014). Extensive studies have investigated CR6 tropism for IECs with only one indicating viral antigen in IECs of infected *Stat1*$^{KO}$ mice (Karst et al., 2014). However, new data suggests that CR6 infects a small number of IECs in the intestinal tract and these cells act as a reservoir for its persistence (Lee et al., 2017). M cells are located near Peyer's patches, CR6 translocation through M cells provides direct access to professional antigen-presenting cells (APCs), such as B cells, DCs, and macrophages, which CR6 displays tropism for (Karst et al., 2014). It is likely that CR6-infected WT APCs can superactivate, destroy, and present CR6 to the adaptive immune system, without spreading the virus systemically (Karst et al., 2014).

### 1.6.2 Adaptive immunity to CR6

DCs sense MNV ssRNA in the cytoplasm via MDA5 – other proteins that likely sense MNV, but have not been fully investigated are RIG-I and TLR7 (McCartney et al., 2008). Mice infected with CR6 develop a specific T cell response in the intestine and MLN, by day eight post-infection (Tomov et al., 2013). Mice lacking B and T cells (*Rag1*$^{-/-}$) mice are less susceptible to CR6 infection, which is likely due, in part, to the virus's tropism for B cells (Karst et al., 2014). However, once infected, *Rag1*$^{-/-}$ mice display consistently higher CR6 titers in the stool than WT mice, indicating the importance of adaptive immune cells in controlling CR6 infections (Nice et al., 2015). More studies have investigated the role of CD4$^{+}$ and CD8$^{+}$ T cells in controlling CW3 infections, and loss-of-function studies have demonstrated that both types of T cells are important in controlling CW3 titers during a primary infection (Chachu et al., 2008a). Moreover, transferring antigen-specific CD8$^{+}$ T cells into CW3-infected *Rag1*$^{-/-}$ mice reduces viral loads (Tomov et al., 2013). These studies indicate that CD4$^{+}$ and CD8$^{+}$ T cells contribute to controlling CW3 infections. However, differences exist between the adaptive immune response to CW3 and CR6 infections (Tomov et al., 2013). CR6-specific CD8$^{+}$ T cells are less abundant at

day eight post-infection compared to CW3-specific $CD8^+$ T cells (Tomov et al., 2013). Moreover, CR6-specific $CD8^+$ T cell responses are limited to the intestinal compartment, reflecting the location of CR6 infection in WT mice (Tomov et al., 2013). Finally, CR6-specific $CD8^+$ T cells are less functional compared to CW3-specific $CD8^+$ T cells, the majority of CR6-specific $CD8^+$ T cells produce only Granzyme B, while CW3-specific $CD8^+$ T cells co-produce cytokines (IFNγ, TNFα, MIP1a, and Granzyme B), all of which enhance the cytotoxic potential of $CD8^+$ T cells (Tomov et al., 2013). The importance of CR6-specific T cell responses have been less thoroughly investigated; however, one study has looked at the importance of impaired T cell responses to CW3 and CR6 (Osborne et al., 2014). This study showed that when CR6-specific $CD8^+$ IELs were decreased there was higher fecal CR6 shedding, which suggests a role for CR6-specific $CD8^+$ T cells in controlling CR6 infections (Osborne et al., 2014). Therefore, T cell specific responses are likely important for controlling CR6 infections.

DCs also promote B cell antibody responses to MNV (Elftman et al., 2013). CW3-specific antibodies reduce viral titers and, when transferred to naïve mice, can also partially protect from a primary infection (Chachu et al., 2008b; Zhu et al., 2013). The clearance of CW3 requires $CD4^+$ T cells, $CD8^+$ T cells, and B cells (Chachu et al., 2008a; Tomov et al., 2013). Importantly, initiating an effective secondary immune response against CW3 requires a primary $CD4^+$ T cell and an antibody response (Zhu et al., 2013).

Collectively, these data suggest that STAT1 will play important roles in coordinating both innate and adaptive pathways of antiviral immunity to CR6. Given collective knowledge from previous experiments with CW3, without STAT1 signaling macrophages and DCs probably cannot control replication and may promote its extra-intestinal spread. Moreover, without STAT1 signalling, IECs would not be able to receive and relay IFNλ signals and would be

unable to control CR6 replication. The inability to control CR6 replication can cause inflammation by signalling through TLRs and activating many immune cells, but most groups report no clinical signs or death. It is unknown whether the adaptive immune response could play a protective role in *Stat1*$^{KO}$ mice since CR6-specific adaptive immune responses are not well understood. A focus of my thesis project is to characterize the T cell response to enteric CR6 infection and the role of STAT1 in coordinating these T cell responses.

### 1.7 STAT1 signalling in T cells

My thesis project employs a whole body murine knockout of STAT1, with a focus on the function of T cells in response to CR6 infection. I will briefly describe the current state of knowledge about STAT1 signalling in T cells and what other virus infection models have uncovered about T cell responses to infection during STAT1 deficiency.

#### 1.7.1 STAT1 signalling in CD4$^+$ T cells

STAT1 promotes Th1 differentiation. T cell receptor (TCR) signalling, along with IFNγ signalling, recruits and phosphorylates STAT1, which establishes a transcriptional state for Th1 differentiation (Maldonado et al., 2009). DCs activate through MDA5 and IFN signalling and produce IL-12, which activates NK cells (Zhu and Paul, 2008). Activated NK cells produce IFNγ, which signals through STAT1 in the responding CD4$^+$ T cell to upregulate T-bet expression (Murphy and Reiner, 2002). In the systemic lymphocytic choriomeningitic virus (LCMV) model, a lack of STAT1 signalling establishes a lethal CD4$^+$ T cell-mediated disease, characterized by elevated serum cytokine levels and multi-organ immune pathology (Hofer et al., 2012). Depleting CD4$^+$ T cells reduced pathology and prevented mortality (Hofer et al., 2012). Humans with gain of function STAT1 mutations have decreased Th17 cells, making them more susceptible to yeast and fungal infections (Toubiana et al., 2016). Moreover, some STAT1 gain

of function patients have more severe mucocutaneous viral infections, for unknown reasons but possibly due to enhanced type 1 immune responses, that can respond with overt inflammation (Toubiana et al., 2016). In contrast, patients with defective STAT1 signalling exhibited decreased IFNγ production by $CD4^+$ T cells and NK cells (Sim et al., 2016). During chronic LCMV infections, IFNAR signalling in APCs increases IL-10 production and regulates $CD4^+$ T cell responses, which prevents LCMV clearance (Wilson et al., 2013). To our knowledge, studies have not yet investigated the importance of $CD4^+$ T cell responses to CR6 infection. Thus, it is unknown if STAT1 deficiency will result in reduced resolution of inflammation during chronic CR6 infection. One aspect of my thesis will be to assess the quantity and quality of the $CD4^+$ T cell response in both STAT1-sufficient and deficient CR6-infected mice.

### 1.7.2 STAT1 signalling in $CD8^+$ T cells

In a number of cell types, STAT1-dependent Type I IFN signalling is anti-proliferative, which is counterproductive to mounting a robust $CD8^+$ T cell response that is necessary for viral clearance. In the context of virus-specific $CD8^+$ T cell activation, STAT1 has been reported to act as both a positive and negative regulator of cellular proliferation, suggesting that $CD8^+$ T cells must have ways to overcome canonical IFN-STAT1 anti-proliferative effects. For example, LCMV infections are potent IFN inducers and $CD8^+$ T cells demonstrate down-regulation of STAT1 expression, which is required to increase $CD8^+$ T cell proliferation and an effective T cell response against LCMV (Gil et al., 2012). Two reported mechanisms of STAT1-inhibition in virus-specific $CD8^+$ T cells include the induction of an miRNA (miR-155), which broadly suppresses STAT1 signalling (Gracias et al., 2013) and preferential signalling through STAT4 (Gil et al., 2012). In highly inflammatory settings, STAT1-mediated inhibition of $CD8^+$ T cell proliferation may act as a regulatory mechanism to protect from infection-induced inflammation

(Ivashkiv and Donlin, 2014). In comparison, vaccinia virus infections are poor type 1 IFN inducers and the infection requires STAT1 for promoting the survival of clonally expanded $CD8^+$ T cells (Quigley et al., 2008). These conflicting data suggest context-dependent roles for STAT1 in regulating antiviral $CD8^+$ T cell immunity. CR6 is a relatively poor IFN-1 inducer and is associated with weak $CD8^+$ T cell responses (Tomov et al., 2013). It is currently unknown whether or how STAT1 signaling in CR6-specific $CD8^+$ T cells will be important for coordinating the immune response to CR6 infections.

The immune response to MNV requires the coordination of many arms of the immune system. Studies of immune responses to other types of viral infections have not been accurate in predicting the immune response to MNV infections, possibly due to differing routes of infection (the GALT is unique from systemic or lung lymphoid tissues). Finally, B cells, $CD4^+$ T cells, and $CD8^+$ T cells are all required for the efficient clearance of CW3 (Zhu et al., 2016); however, the adaptive immune response to CR6 is much less understood, although STAT1 likely plays an important role in coordinating it.

### 1.8 Conclusion

Complex immunological networks allow the host to maintain appropriate immune responses to virus infections. However, there is still more to learn with respect to these networks and persistent enteric virus interactions. **We hypothesize that STAT1 signalling is a critical factor for the host immune system's ability to respond to and restrict murine Norovirus strain CR6.** To test this hypothesis I will first assess disease parameters of acute and chronic CR6 infections in STAT1-sufficient and deficient hosts. Next, I will assess CR6- specific immune responses in STAT1-sufficient and deficient hosts. If this hypothesis were true, we would expect to see CR6-induced disease and dysregulated immune responses. Little is

understood about the ability of intestinal viruses to influence host physiology and these experiments may reveal new insights into whether host-signalling pathways coordinate responses to an asymptomatic intestinal eukaryotic virus. Understanding how host cells respond to and communicate with the eukaryotic intestinal virome may unveil mechanisms behind Norovirus-induced enteropathy in immunocompromised patients. Lastly, these experiments could provide rationale to consider the virome when developing future microbiome-manipulating therapies; for example, fecal transplants.

# Chapter 2: Methods

## 2.1 *in vivo* murine Norovirus CR6 infection model

### 2.1.1 Mouse strains and housing conditions

Mice were housed at the University of British Columbia (UBC) specific pathogen-free Centre for Disease Modeling. MNV-free C57BL/6 *Stat1*$^{het}$ mice (The Jackson Laboratory, strain B6.129S(Cg)-*Stat1*$^{tm1Dlv}$*/J* (012606) were used to establish a colony of *Stat1*$^{het}$ and *Stat1*$^{KO}$ breeder pair. *Stat1*$^{het}$ and *Stat1*$^{KO}$ littermates were aged-matched within each experiment, and were 6-12 weeks of age for all experiments. Experimental protocols were approved by the UBC Animal Care Committee and Biosafety Committee. Mice were kept on a 12-hour day/night cycle and were fed standard lab chow. PCR genotyping was performed using the follow primers (IDT): WT Forward: 5'-GAGATAATTCACAAAATCAGAGAG-'3, KO Forward: 5'-TAATGTTTCATAGTTGGATATCAT-'3 and Common Reverse: 5'-CTGATCCAGGCAGGCGTTG-'3 and GoTaq DNA polymerase (Promega) according to manufacturer's instructions on a SimplyAmp thermocycler (Applied Biosystems) with the following amplification settings: 2 min at 94°C, and 30 cycles of 30 seconds at 94°C, 30 seconds at 50°C and 30 seconds at 72°C, 2 min at 72°C.

### 2.1.2 MNV CR6 generation and quantification of MNV CR6 stocks

#### 2.1.2.1 MNV CR6 generation

Virus was grown as described (Tomov et al., 2013). Briefly, plasmids containing the genome of virus strain MNV-1.CR6 (GenBank accession number EU004676) were used to generate viral stocks. Viral stocks were produced by transfecting 293T cells (ATCC) using

FuGENE-HD reagent (Promega) according to the manufacturer's protocol (with a FuGENE/DNA ratio of 5:2). After 48 h at 37°C, transfected 293T cells were lysed by freezing (-80$^{o}$C) and thawing. Thawed supernatant was transferred to 2x10$^{6}$ RAW 264.7 cells per well for 48 hours. After 48 h, RAW 264.7 cells were freeze-thawed, centrifuged and the virus-containing supernatant was removed and stored at -80°C. All cell lines were maintained at 37°C and 5% $CO_2$ in RPMI 1640 (Sigma) containing 10% fetal bovine serum, 2 mM L-glutamine (VWR), 100 IU/ml penicillin, and 100 g/ml streptomycin (Invitrogen) (complete tissue culture media (CTCM)).

#### 2.1.2.2 Viral stock quantification

RAW 264.7 cells were plated at 2x10$^{6}$ cells per well overnight. 10-fold dilutions of virus stocks were prepared in complete DMEM medium and 0.5 mL was plated in duplicate on RAW 264.7 cells. Virus-coated plates were incubated for 1 hr at room temperature (RT) on a rocking platform. Diluted virus was aspirated and 2 mL overlay media (RPMI, 10 mg/ml methylcellulose, 5% FBS, 2 mM L-glutamine, 100 IU/ml penicillin, 100 µg/ml streptomycin) was added. Plates were incubated for 72 hr at 37°C and 5% $CO_2$. To visualize plaques, overlay media was removed and cells were washed once with PBS and fixed and strained (20% ethanol with 0.1% crystal violet) for 1 hr at RT on a rocking platform, and then washed with water. Plaques were counted and viral titers were calculated based on the dilution factor of the well with the best resolution of plaques.

### 2.1.3 Infection conditions

Mice were infected by oral gavage with 10$^{4}$ pfu of MNV CR6 diluted in sterile PBS. Naive mice were sham-infected by oral gavage (*p.o.*) with sterile PBS (Sigma). Mice were monitored over 8 to 30 days, depending on experimental time point. Mice were euthanized at

humane endpoint if body weight reached 80% of initial weight (or weight loss >20% of initial body weight).

### 2.1.4 *in vivo* antibody depletion conditions

To neutralize cytokines, anti-(α)IL-17A antibodies (clone 17F3, BioXcell) were diluted in sterile PBS (Sigma) and administered *i.p.* at 500ug per mouse, one day before MNV CR6 infection and days 2 and 5 post-infection.

To deplete cells, αCD4 (clone GK1.5, UBC AbLab) or αCD8a antibodies (clone 53.67, UBC AbLab) were diluted in sterile PBS (Sigma) and administered *i.p.* at 400 ug per mouse, on the day of infection and days 3 and 6 post-MNV CR6 infection. To ensure adequate depletion, tissues were analyzed by flow cytometry with antibodies of different specificities, anti-CD4 BV650 (clone RM4-5, BD Biosciences) and αCD8β (clone H35-17.2, ThermoScientific). For all mAb treatment experiments, IgG1 isotype control antibodies (clone MOPC-21, bioXcell) were administered with the same dosing regimen and schedule as the treatment.

### 2.1.5 Antibiotic treatment

Mice were given an antibiotic cocktail mixture by oral gavage 4 hours before infection and then supplemented into their sterile drinking water (Vancomycin 0.25mg/mL, Neomycin 0.5 mg/mL, Gentamycin 0.5 mg/mL, Ampicillin 0.5 mg/mL, Metranidizole 0.125 mg/mL, sucralose ((Splenda) 4 mg/mL). Antibiotic efficacy was assessed by agar plates with fecal streaks. Control mice received sterile drinking water supplemented with sucralose ((Splenda) 4 mg/mL).

## 2.2 *in vivo* MNV CR6 post-infection analysis

### 2.2.1 Tissue histology

Samples were collected in 10% Formalin at a 10:1 formalin:tissue ratio. The large intestine was flushed with PBS before submersion into 10% formalin. The spleen was submerged in 10% Formalin. All samples were stored in Formalin in the dark prior to being processed by Jana Hodasova at the Histochemistry Service Laboratory at the University of British Columbia Biomedical Research Centre. Tissue sections were analyzed in consultation with Dr. Ian Welch, Director, Veterinary Services & Research Support and University Veterinarian, UBC. Histology images were acquired with an Olympus BX51 microscope and an Olympus DP73 microscope camera lens.

### 2.2.2 Lymphocyte recovery

#### 2.2.2.1 Spleen and lymphocytes

Spleens and Lymph nodes were harvested in 2 mL RPMI-CTCM at 4°C and homogenized through 70 μm nylon mesh filters to a single-cell suspension. Spleens were incubated for 5 min with ammonium-chloride-potassium (ACK) lysing buffer, to lyse red blood cells.

#### 2.2.2.2 Colon and cecum

Intestinal lymphocytes were harvested from the caecum and colon. The intestines were dissected, fat and luminal contents were removed, then cut longitudinally, washed in cold PBS, and placed in 20 mL RPMI-CTCM on ice. To remove epithelial cells, intestines were incubated in pre-warmed (37$^{o}$C) epithelial stripping buffer (PBS with 5 mM EDTA, 1 mM dithiothreitol, 5% fetal bovine serum, 100 IU/ml penicillin, and 100 g/ml streptomycin) and shaken at 200 rpm for 10 min at 37°C, supernatant was discarded. To obtain intraepithelial lymphocytes (IEL),

intestines were incubated again in stripping buffer and shaken at 200 rpm for 20 min at 37°C. Supernatants containing IELs were passed through a 70-um cell strainer, washed in 2% NCS RPMI, resuspended in 20 mL 2% NCS containing 40% Percoll, and subjected to centrifugation at 600 *g* at RT for 20 min (without acceleration or break). Supernatants were carefully removed and cell pellets were washed in RPMI-CTCM. After IEL stripping, lamina propria lymphocytes (LPL) were isolated by incubating intestines in cell culture medium containing 0.5 mg/ml collagenase-dispase (Sigma) and 20 mg/ml DNase I (Sigma) shaken at 200 rpm for 20 min at 37°C. LPL were passed through a 70-μm cell strainer and washed.

#### 2.2.2.3 *ex vivo* lymphocyte stimulation

For peptide-specific cytokine responses, $2x10^6$ lymphocytes were stimulated with 0.4 μg/ml MHC class I-restricted peptides ($P1^{519Y}$) or 0.8 μg/ml MHC class II-restricted peptides ($Nterm^{28}$, $Nterm^{46}$, $NTPase^{622}$, $Pro^{991}$, $Pol1^{630}$, $P1^{496}$) for 5 hr at 37°C in the presence of 10 μg/ml brefeldin A (BFA) (Sigma) and GolgiStop containing monensin at a dilution of 1:1500 (BD Biosciences). For polyclonal cytokine responses, lymphocytes were stimulated with 0.1 μg/ml PMA and 1 μg/ml ionomycin (Sigma) in the presence of BFA and GolgiStop for 5 hr at 37°C. Cells were incubated in Dulbecco's Modified Eagle's Medium (DMEM) CTCM. Intracellular cytokine and effector molecule staining was performed using Cytofix/Cytoperm and Permeabilization Buffer (BD Biosciences). Transcription factor staining was performed using Foxp3 Transcription Factor Fixation and Permeabilization Buffer (eBiosciences), according to manufacturers instructions.

#### 2.2.2.4 MNV-specific $CD4^+$ T cell enrichment

To detect MNV-specific $CD4^+$ T cell population, MNV tetramer-specific MHC II IAb tetramers, specific for an epitope within the MNV capsid ($P1^{496}$) were used. Given the low

frequency of these cells, detection requires a positive selection. Cells from spleen, peripheral, and mesenteric lymph nodes were pooled in 2 mL RPMI-CTCM at 4°C and homogenized through 70 μm nylon mesh filters to a single-cell suspension. The cells were stained with fluorochrome-conjugated MHC II tetramers and subjected to magnetic bead enrichment process, as described previously (Moon et al., 2007).

### 2.2.3 Flow cytometry

#### 2.2.3.1 Surface and intracellular staining

The following primary antibodies and reagents were used for surface staining (clone, supplier): CD8α PE-Cy7 (53-6.7, BioLegend), CD44 APC-Cy7 (IM7, BioLegend), CD4 BV650 (RM4-5, BD Biosciences), TCRβ PerCP-Cy5.5 (H57-597, BioLegend), TCRβ PE/Dazzle 594 (H57-597, BioLegend), CD45.2 Alexa Fluor (104, BioLegend), MHCI H-2Kb PE (AF6-88.5.5.3, eBioscience), MHCII I-A/I-E APC (M5/114.15.2, eBioscience). MHCI tetramers specific for MNV CR6 capsid Kb-P1$^{519F}$ were prepared as previously described ((Tomov et al., 2013)) or provided by the NIH Tetramer Core Facility. MHCII IAb tetramers specific for MNV CR6 capsid P1$^{496-513}$ (YIAVSYSGSGPLTFPTDG) were generated by the NIH Tetramer Core Facility.

The following primary antibodies and reagents were used for intracellular staining (clone, supplier): TNFα PE (MP6-XT22, BioLegend), IL-17A PE/Dazzle 594 (TC11-18H10.1, BioLegend), T-bet Brilliant Violet 421 (4B10, BioLegend), IL-10 APC (JES516E3, BioLegend), IFNγ eFluor450 (XMG1.2, eBioscience), Foxp3 Alexa Fluor 488 (FJK-16s, eBioscience), RORγt PerCP-eFluor 71 (B2D, eBioscience).

#### 2.2.3.2 Flow cytometry data acquisition and analysis

Samples were collected on an LSR II with four lasers (BD Bioscience) using FACS Diva software. Data files were analyzed using FlowJo software (version 10.1r3, Tree Star Inc.). For all analyses, dead cells that stained positive for LIVE/DEAD Fixable Aqua Dead Cell Stain (Invitrogen, Molecular Probes) were excluded. Appendix A is an example of my gating strategy.

### 2.2.4 Serum cytokine detection

#### 2.2.4.1 Cytometric bead array

Concentrations of serum cytokines were assessed using the Cytometric Bead Array Mouse Inflammation kit and Mouse Th Cytokine panel (BioLegend LEGENDPlex) according to manufacturer's instructions. Blood was collected from euthanized mice in the absence of clotting factors, centrifuged at 10000 x g for 10 min at 4°C, and cleared supernatant (serum) was removed and stored at -80°C. Samples were run on the LSR II (BD Bioscience) using FACS Diva software and analyzed using FlowJo software. Analysis was performed by running a SOLVER script synthesized on Excel (Brown, 2001).

### 2.2.5 Quantitative PCR

#### 2.2.5.1 RNA isolation and cDNA generation

Cells, colon, spleen, liver, lung, and brains were harvested and stored at -20°C in RNAlater (Ambion). Samples were thawed and weighed before homogenization in lysis buffer using steel beads and the TissueLyser II (Qiagen) (6 min, x 35 beats/sec). RNA was isolated using PureLink RNA Mini Kit (ThermoFisher Scientific) according to manufacturer's instructions. cDNA was prepared from RNA in a two-step process. First, sample RNA was incubated with random hexamers (Applied Biosystems) and 10mM dNTPs in 13 µl reactions for

5 min at 65°C using a SimplyAmp thermocycler (Applied Biosystems). Next, Invitrogen Superscript III Reverse Transcriptase (ThermoFisher Scientific), 5x first strand buffer, and 0.1M DTT were added to a final volume of 20 µl and reverse transcription carried out with the following amplification settings: 10 min at 25°C, 120 min at 37°C, and 5 min at 85°C for one cycle.

#### 2.2.5.2 Measurement of viral loads by qPCR

Viral loads in tissue samples were carried out by qPCR using TaqMan Universal PCR master mix (Applied Biosystems) in 8 µl reaction mixture volumes with 2 µl of sample, according to the manufacturer's instructions. Detection of MNV genome copies was performed using TaqMan (TermoFisher Scientific) amplification with primers MNV F4972 (5' - CAC GCC ACC GAT CTG TTC TG - 3'), R5064 (5' - GCG CTG CGC CAT CAC TC - 3') and probe 5001-5015 (6FAM - CGC TTT GGA ACA ATG - MGBNFQ) on a Quant Studio 3 Real-Time PCR System (Applied Biosystems), with the following amplification settings: 2 min at 50°C, 10 min at 95°C, and 50 cycles of 15 seconds at 95°C and 1 min at 60°C. All samples were assessed in triplicate. Absolute numbers of MNV genome copies were extrapolated from a standard curve and normalized to tissue weight.

#### 2.2.5.3 Gene expression qPCR

Tissue RNA and cDNA were prepared as above and diluted 1:4 in $dH_2O$. Gene expression analysis was performed using PowerUp SYBR Green Master Mix according to manufacturer's instructions (Applied Biosystems) on a Quant Studio 3 Real-Time PCR System (Applied Biosystems), with the following amplification settings: 2 min at 50°C, 10 min at 95°C, and 40 cycles of 15 seconds at 95°C and 1 min at 60°C, followed by a programmed melt curve

cycle. Gene expression was normalized to *hprt1* and is expressed as fold-induction relative to the average expression levels in naïve *Stat1*$^{het}$ mice.

**Table 2.1 Primers used for RT-qPCR**

| Host Gene Target | QuantiTect Primer Assay |
|---|---|
| *Hprt* | Mm_Hprt_1_SG |
| *Tgfb* | Mm_Tgfb1_1_SG |
| *Il10* | Mm_Il10_1_SG |
| *Tnfa* | Mm_Tnf_1_SG |
| *Il17a* | Mm_IL17a_1_SG |
| *Reg3g* | Mm_Reg3g_1_SG |
| *Reg3b* | Mm_Reg3b_1_SG |
| *Muc2* | Mm_Muc2_2_SG |
| *Il22* | Mm_Il22_1_SG |
| *Ifng* | Mm_Ifng_A_SG |

### 2.2.6 Intestinal permeability assays

#### 2.2.6.1 Serum FITC-dextran assay

Mice were gavaged with 100mg/mL kDa FITC-dextran (Sigma-Aldrich) adjusted to 60 mg/100g mouse, after mice were deprived of food for 4 hours. 4 hours post-gavage, serum was collected from mice by cheek bleed and measured for FITC concentration using a Perkin Elmer Victor X5 fluorescent plate reader. The plate was read with the excitation of 485 nm and

emission of 530 nm. Sample concentrations of FITC were extrapolated from a standard curve of FITC-dextran that was serially diluted in naïve mouse serum, using GraphPad Prism Software.

#### 2.2.6.2 Fecal serum albumin assay

The concentration of serum albumin in intestinal lumen contents were assessed using the Mouse Albumin ELISA Quantitation Set (Bethyl Laboratories Inc.), according to the manufacturer's protocol. Fecal matter were prepared at 10 mg feces per 100 µl sample diluent buffer and homogenized in a TissueLyser II (Qiagen). Samples sat at RT for 10 min before centrifugation at 1000 x g for 20 min at RT. 100 µl of supernatants were added to duplicate wells. The plate was read on a PerkinElmer 2030 VICTOR X5 multilabel reader at wavelength 450 nm, using WorkOut2.5 software. Sample concentrations of serum albumin were extrapolated from a standard curve using GraphPad Prism Software.

## 2.3 Statistical analyses

Statistical analyses were performed using GraphPad Prism (GraphPad Software, Version 6.0). For graphs displaying correlations, statistical comparisons were performed using two-tailed nonparametric Spearman correlation. For survival curves, statistical analyses were performed using the Log-rank (Mantel-cox) curve comparison test. All other data data was analyzed by unpaired, nonparametric two-tailed Mann-Whitney t-test, or nonparametric multiple-comparison Kruskal-Wallis test with Dunn's correction, as stated in figure captions. Error bars and ± symbols represent SEM. * $p < 0.05$, ** $p < 0.01$, *** $p < 0.001$, **** $p < 0.0001$.

## Chapter 3: Results

### 3.1 STAT1 limits systemic enteric CR6 viral replication and virus-induced disease

To address the hypothesis that STAT1 signalling is a critical factor for the host's ability to maintain immune homeostasis with murine Norovirus, strain CR6, I wanted to describe clinical signs, weight loss, and mortality, in CR6-infected STAT1-sufficient (*Stat1*$^{+/-}$, *Stat1*$^{het}$) and STAT1-deficient (*Stat1*$^{-/-}$, *Stat1*$^{KO}$) mice. Mice were infected with $1x10^4$ CR6 plaque forming units (pfu) per os (*p.o.*), by oral gavage and were euthanized at day 30 post-infection (pi), or at humane endpoint (weight loss of 20% or more). Persistently infected *Stat1*$^{het}$ littermate controls displayed no clinical signs over the 30-day infection (Fig 3.1a, b) and CR6 genome copies were detected in colons at day 30 (Fig 3.1c, d). Our observations are consistent with past studies that found CR6 is persistent and well tolerated in STAT1-sufficient (WT) mice (Tomov et al., 2013). In comparison, the majority (mean = 81.25%) of CR6-infected *Stat1*$^{KO}$ mice lost significant weight pi, while *Stat1*$^{het}$ mice maintained weight over time (Fig 3.1a). Moreover, a significant percentage of *Stat1*$^{KO}$ mice (mean = 69%) succumbed to infection (Fig 3.1b). A correlation between the day of humane endpoint and number of viral genome copies in the colon, and a trend in the spleen, was observed, suggesting that uncontrolled virus replication correlates with mortality (Fig 3.1c, d). *Stat1*$^{KO}$ mice that survived past day 20 pi had high colonic CR6 genome copies, but splenic CR6 genome copies were below the level of detection (Fig 3.1c, d). Moreover, although CR6 was cleared, the spleens of these animals showed signs of inflammation, splenomegaly and large white foci. Two *Stat1*$^{KO}$ mice spontaneously cleared CR6 infection lost no weight and lived until the end of experiment (Fig 3.1c, d). CR6-specific IgG was detected in the serum of these mice, confirming they had been infected (data not shown). In

conclusion, chronically CR6-infected *Stat1*$^{KO}$ mice either eventually succumbed to infection or spontaneously cleared infection.

Chronic LCMV promotes a regulatory immune response (decreased IFNγ and increased IL-10) to suppress the immune system and maintain a persistent infection (Wilson et al., 2013). This regulatory response is mediated through type 1 IFN signalling; by experimentally inhibiting type 1 IFN signalling, IFNγ levels were elevated, and mice cleared chronic LCMV infections (Wilson et al., 2013). To investigate if similar regulatory responses could be promoting the persistence of CR6 infections, RNA was isolated from the colons and spleens of infected mice. Colonic and splenic IFNγ transcript levels were significantly increased in CR6-infected *Stat1*$^{KO}$ mice compared to *Stat1*$^{het}$ mice (Fig 3.1e), whereas IL-10 transcript levels were not significantly different between infected groups (Fig 3.1f). Lastly, transcripts of a non-type 1 cytokine (IL-17A) were significantly increased in the colon and spleen of infected *Stat1*$^{KO}$ mice (Fig 3.1g). These observations do not reflect the dampened immune profile observed in chronic LCMV infections and suggest an alternative mechanism of CR6 persistence. Moreover, high expression of IFNγ and IL-17A may be indicative of an overly pro-inflammatory response, which could cause immunopathology and inflammation, even once virus could not be detected in the spleen past day 20.

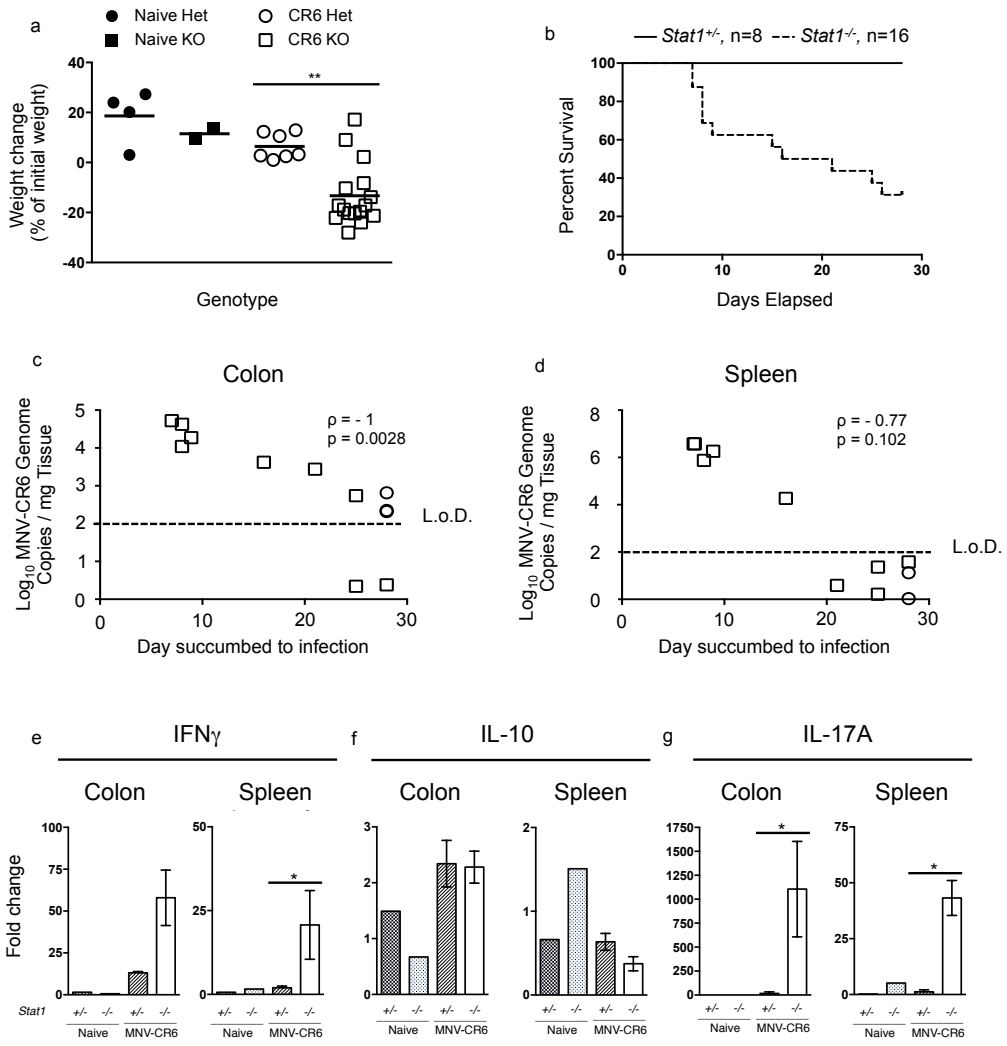


**Figure 3.1 STAT1 limits chronic CR6-infection induced weight loss, mortality, and virus dissemination.**

*Stat1*$^{het}$ *and Stat1*$^{KO}$ mice were given PBS or infected with $10^4$ pfu CR6 *p.o.* and euthanized on day 30 pi, or at humane endpoint. (a) weight change as a percentage difference from of initial (100%). (b) survival curve of CR6-infected mice. Comparison of detectable CR6 genome copies in colonic (c) and splenic (d) tissue versus day of humane endpoint in *Stat1*$^{het}$ (O) and *Stat1*$^{KO}$ (□ ) mice. Fold change of (e) *Il17a* (f) *ifng* and (g) *Il10* transcript expression of naïve *Stat1*$^{KO}$ mice, infected *Stat1*$^{het}$, or infected *Stat1*$^{KO}$ vs naïve *Stat1*$^{het}$ in spleen or colon as measured by qRT-PCR and normalized to *Hprt*. Data in (a, b) are compiled from two independent experiments. Data in (c, d, e, f, g) are representative data from two independent experiments displaying similar trends. Data from one mouse are represented by individual symbols, the line representing the mean. Statistical significance was determined by Mann-Whitney test (a, e, f, g) or Spearman's correlation coefficient test (b, d). ** = $p < 0.01$, n.s. = $p > 0.05$. L.o.D., Limit of Detection.

I designed all future experiments to end at day eight pi, given the observations that the majority of mice succumb to infection by day 30 and that past studies observed peak $CD8^+$ T cell responses at day 8 (Tomov et al., 2013). Therefore, I wanted to describe clinical signs, weight loss, and mortality, in CR6-infected *Stat1*$^{het}$ and *Stat1*$^{KO}$ mice at day 8 post-CR6 infection. Mice were infected with $1x10^4$ CR6 pfu by oral gavage and euthanized at day 8, or at humane endpoint. Consistent with observations in Fig 3.1, *Stat1*$^{het}$ littermate controls infected with CR6 showed no signs of morbidity, measured by weight loss (Fig 3.2a) or mortality (Fig 3.2b). Moreover, CR6 is restricted to intestinal tissue in *Stat1*$^{het}$ littermate controls (Fig 3.2c-f). CR6 genome copy numbers isolated from the colons trended higher in infected *Stat1*$^{KO}$ than *Stat1*$^{het}$ littermates (Figure 3.2c). In contrast to CR6-infected *Stat1*$^{het}$ mice, a proportion (mean = 37%) of *Stat1*$^{KO}$ mice displayed CR6-induced weight loss at day 8, and a smaller proportion of *Stat1*$^{KO}$ mice (mean = 15%) succumbed to CR6 infection by day 8 (Fig 3.2a, b). In all *Stat1*$^{KO}$ mice, CR6 disseminated to the spleen (Fig 3.2d). Moreover, in all *Stat1*$^{KO}$ mice that lost weight, CR6 also disseminated to the liver and lung (Fig 3.2e, f). These data suggest that weight loss is associated with systemic viral replication. In keeping with these data, we observed a significant positive correlation between weight loss and CR6 genome copies in the spleen (Fig 3.2g).

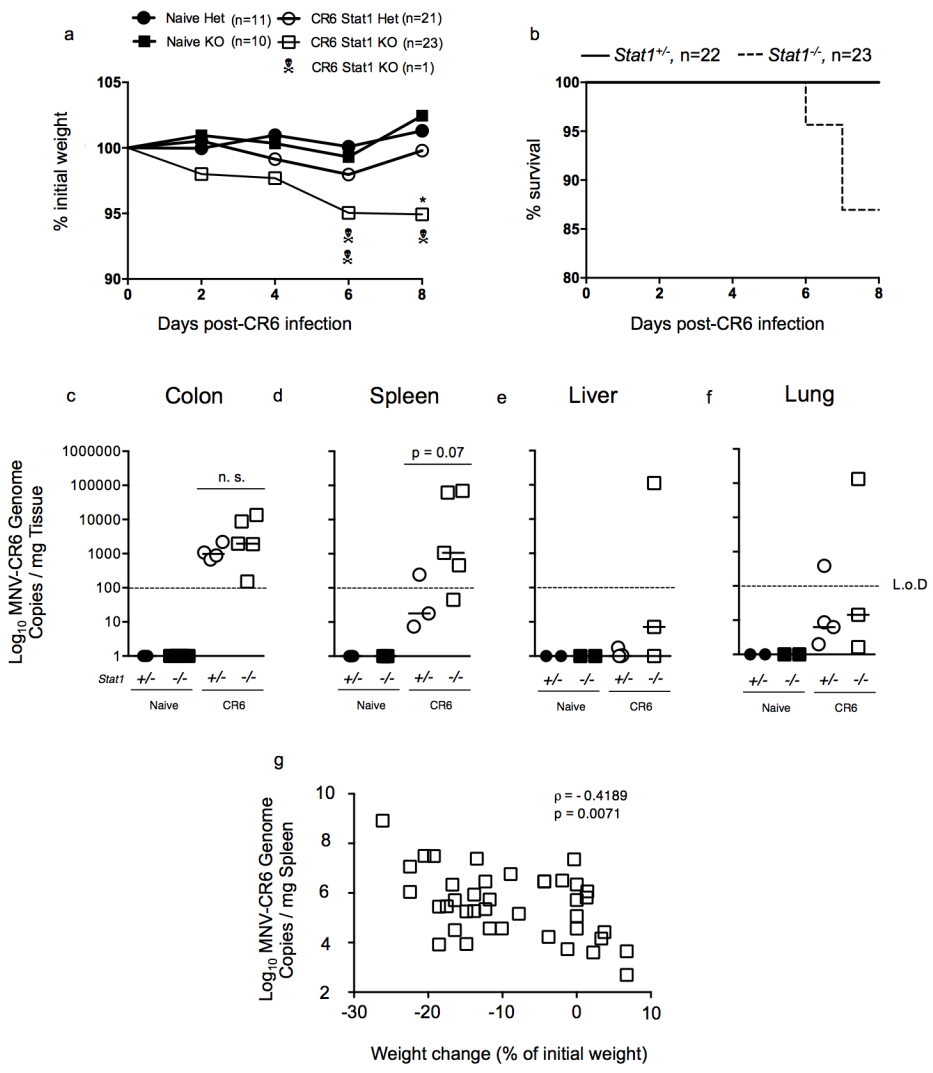


**Figure 3.2 STAT1 limits acute CR6-infection induced weight loss, mortality, and virus dissemination**.

*Stat1*$^{het}$ *and Stat1*$^{KO}$ mice were given PBS or infected with $10^4$ pfu CR6 *p.o.* and euthanized on day 8 pi (a) weight change as a percentage of initial weight at day 0. (b) survival curve of CR6-infected mice. Viral genome copies per mg specified tissue (c) colon (d) spleen (e) liver (f) lung. (g) Comparison of detectable CR6 genome copies in colonic tissue versus weight change at experiment endpoint. Data in (a, b) are compiled from six independent experiments. Data in (c, d, e, f) are representative data from three independent experiments displaying similar trends. Data in (g) are compiled from four independent experiments. Data from one mouse are represented by individual symbols, the line representing the median. Statistical significance was determined by Mann-Whitney test (c, d, e, f) or Spearman's correlation coefficient test (g). * = $p < 0.05$, n.s. = $p > 0.05$. L.o.D., Limit of Detection.

### 3.2 CR6-induced weight loss is associated with systemic histopathology in *Stat1*$^{KO}$ mice

Spleens taken from *Stat1*$^{KO}$ mice that lost weight were enlarged with white foci. Histological examination of the proximal colon, a site of CR6 infection, of naïve and infected *Stat1*$^{het}$ and *Stat1*$^{KO}$ mice showed no histological signs of inflammation (Figure 3.3a-d). The spleens of naïve mice showed no signs of histopathology (Figure 3.3e, f). The spleens of the CR6-infected *Stat1*$^{het}$ mice were mildly reactive; however, this is a normal response for any mouse spleen that is promoting an immune response to encountered antigen (Figure 3.3g). It should be noted that the spleens of healthy CR6-infected *Stat1*$^{KO}$ mice exhibited histological features that resembled those of CR6-infected *Stat1*$^{het}$ mice (not shown). However, spleens of *Stat1*$^{KO}$ mice that lost weight displayed significant histopathology (Figure 3.3h). These spleens showed signs of splenitis—white pulp areas showed neutrophil infiltration that surrounded follicles of apoptotic and dead cells, while red pulp areas had become sites of extensive extramedullary hematopoiesis. These histopathology signs, along with CR6 genome copies detected in the spleen, indicate CR6-induced splenitis in infected *Stat1*$^{KO}$ mice. Together, these results indicate that STAT1 is required for orchestrating an appropriate immune response and maintaining tissue homeostasis in the context of an otherwise avirulent enteric CR6 infection.

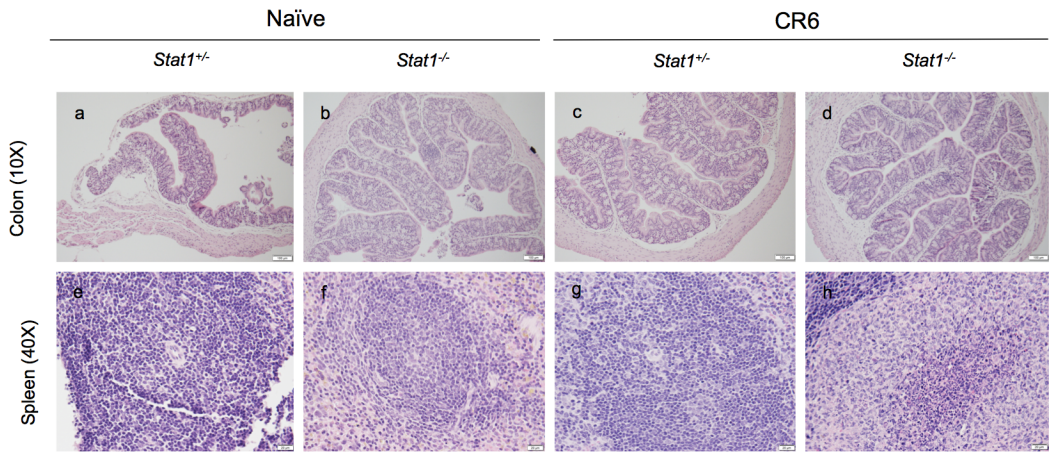


**Figure 3.3 CR6-induced weight loss is associated with systemic histopathology in *Stat1*$^{KO}$ mice**

*Stat1*$^{het}$ *and Stat1*$^{KO}$ were given PBS or infected with $10^4$ pfu MNV-CR6 *p.o.* and euthanized on day 8 pi. (a-d) the first cm of the proximal colon was flushed with PBS and subsequently stored in 10% Formalin. (e-h) spleen sections were collected and subsequently stored in 10% Formalin. Histology sections were H&E stained and analyzed with the help of Dr. Ian Welch

### 3.3 STAT1 limits the expansion and function of CR6-specific CD8$^+$ T cells *in vivo*

Given that CR6 disseminates systemically and replicates to high viral titers when STAT1 signaling is absent, we hypothesized that the systemic spread of CR6 may be due to impaired antiviral CD8$^+$ T cell responses, which are important cell types in controlling and clearing many virus infections. To test this hypothesis, IELs were isolated from the colon and cecum of naïve or infected mice and stained with a fluorescence-conjugated MHC I tetramer (Kb-P1$^{519F}$) that binds to a CR6 peptide-specific T cell receptor; thus, these tetramers stain CR6-specific CD8$^+$ T cells. In contrast to our hypothesis, we found increased frequencies of MNV-specific CD8$^+$ T cells in the IEL compartment (Fig 3.4a). To account for differences in leukocyte infiltration between genotypes, we measured CR6-specific CD8$^+$ T cells as a frequency of both CD8$^+$ T cells and

CD45.2$^+$ lymphocytes in the IEL compartment (Fig 3.4b, c). Compared to naïve mice, *Stat1$^{het}$* mice showed a significant expansion in CR6-specific TCRβ$^+$ CD8α$^+$ IELs, this indicates that *Stat1$^{het}$* mice produce an adaptive immune response to CR6 (Fig 3.4b, c). However, compared to infected *Stat1$^{het}$* mice, *Stat1$^{KO}$* mice exhibited significantly higher frequencies of CR6-specific IELs (Fig 3.4b, c) and a trend toward a higher frequency of CR6-specific CD8$^+$ T cells in the spleen ($p = 0.1$) and lamina propria ($p = 0.08$) (Appendix B a, b). To determine if *Stat1$^{KO}$* CR6-specific CD8$^+$ T cells were functional, we stimulated isolated lymphocytes with MNV peptides and measured cytokine responses. We observed increased frequencies of IFNγ$^+$ CR6-specific CD8$^+$ T cells post *ex vivo* MNV peptide-stimulation in both *Stat1$^{KO}$* spleens (Fig 3.4d) and colons (Fig 3.4e) compared to littermate *Stat1$^{het}$* organs. Further examination of effector molecules produced by CR6 peptide-stimulated CD8$^+$ splenocytes revealed a trend toward increased total numbers of CD8$^+$ T cells producing IFNγ$^+$, TNFα$^+$, and Granzyme B$^+$, but similar numbers of CD107a$^+$ and MIP1α$^+$ CD8$^+$ T cells in *Stat1$^{KO}$* mice compared to littermate *Stat1$^{het}$* mice (Fig 3.4f-j). These data indicate that STAT1-deficiency leads to increased frequencies and numbers of effector CR6-specific CD8$^+$ T cells, suggesting that impaired viral control is not a consequence of impaired CD8$^+$ T cell activation or function.

IFNγ production by CD8$^+$ T cells has been shown to cause immunopathology in other viral infection models in a STAT1-independent manner (Ramana et al., 2015; Zhao et al., 2000). Therefore, I sought to assess if increased CD8$^+$ T cell frequencies could be promoting weight loss, which would indicate immunopathology. However, in mice showing clinical disease (represented by weight loss, to the left of y-axis in Fig 3.4k), increased frequencies of IFNγ$^+$ CR6-specific CD8$^+$ T cells appeared to correlate with less severe disease (as measured by weight loss) in mice showing clinical signs (Fig 3.4k). Hence, once mice display clinical signs

(represented by weight loss), those with higher frequencies of functional IFNγ$^{+}$ CD8$^{+}$ T cells lost the least amount of weight by day 8. These data do not support the hypothesis of IFNγ-mediated immunopathology, but indicate that CD8$^{+}$ T cells may restrict viral replication and ameliorate CR6-induced disease. These observations set up a paradoxical situation. IFNγ could cause immunopathology or CR6-specific CD8$^{+}$ T cells could be protecting the host by helping control viral dissemination. To test this, I depleted CD8$^{+}$ T cells in CR6-infected *Stat1*$^{KO}$ mice, but this did not alter their susceptibility to morbidity or mortality, compared to *Stat1*$^{KO}$ mice that received IgG isotype (Appendix B c). Thus, CD8$^{+}$ T cells are probably not essential for protection from virus-induced disease nor contribute to immunopathology. However, this was a preliminary study and these results need to be repeated prior to deriving full conclusions.

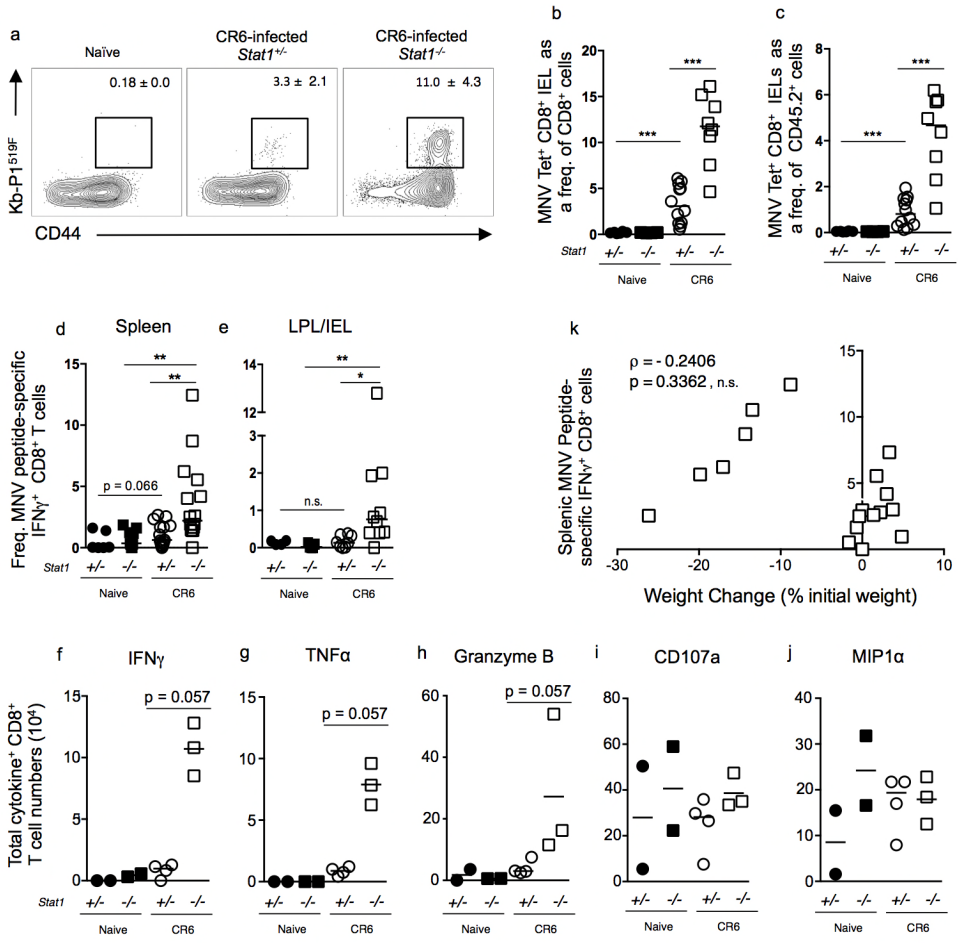


**Figure 3.4 STAT1 limits CR6-specific CD8+ T cell frequencies and cytokine production.** *Stat1*$^{het}$ *and Stat1*$^{KO}$ mice were given PBS or infected with $10^4$ pfu CR6 *p.o.* and analyzed on day 8 post-infection. (a) MNV-CR6 Kb-P1$^{519F}$ Tetramer$^+$ CD8$^+$ T cells as a frequency of (b) CD8$^+$ and (c) CD45.2$^+$ IELs. IFNγ$^+$ CD8$^+$ T cells responding to *ex vivo* MNV-specific peptide stimulation in (d) spleen and (e) IEL and LPL compartments. The frequency of IFNγ peptide producing cells was subtracted by the frequency of IFNγ$^+$ cells at baseline to generate a more accurate representation of MNV-specific CD8$^+$ T cells. (f-j) Total cell numbers of CD8$^+$ T cells from the spleen responding to *ex vivo* MNV-specific peptide stimulation for cytokines IFNγ$^+$, TNFα$^+$, Granzyme B$^+$, CD107a$^+$, and MIP1α$^+$. (k) Correlation between MNV-CR6 Kb-P1$^{519F}$ Tetramer$^+$ CD8$^+$ IEL frequency and percentage weight change from day 1. Data in (a) are representative flow plots used to generate the data in (b, c) which are compiled data from three independent experiments, $n$ = 4-6 naïve mice per genotype and $n$ = 12 *Stat1*$^{het}$ and $n$ = 8 *Stat1*$^{KO}$ infected mice. Data are compiled results from three (d) and two (e) independent experiments. Data in (k) are compiled data from CR6-infected *Stat1*$^{KO}$ mice from three independent experiments (n=18). Data in (f-j) are representative of two independent experiments. Data from one mouse are represented by individual symbols, the line representing the mean. Statistical

significance was determined by Mann-Whitney test (b, c, e, f), or Spearman's correlation coefficient test (f). * = $p < 0.05$, ** = $p < 0.01$, *** = $p < 0.001$.

### 3.4 IFNγ is produced by different cell types in CR6-infected *Stat1$^{het}$* compared to *Stat1$^{KO}$* mice

IFNγ is a signature effector cytokine of type 1 (antiviral) immune responses; we aimed to further investigate the role of STAT1 in regulating IFNγ production to CR6 infections. Following general lymphocyte stimulation (PMA and ionomycin), I used an unbiased gating strategy of all live lymphocytes to determine the identity of IFNγ$^+$ cell types in *Stat1$^{het}$* and *Stat1$^{KO}$* mice. There was no significant difference in the frequency of IFNγ$^+$ cells following stimulation between infected genotypes (Fig 3.5a). Live IFNγ$^+$ lymphocytes were analyzed for being CD8α$^+$, CD4$^+$, or other (CD8α$^-$CD4$^-$) cell types (Fig 3.5b). In contrast to the peptide-specific CD8$^+$ T cell data, *Stat1$^{KO}$* mice had similar numbers of non-specific IFNγ$^+$ CD8$^+$ cells and more IFNγ$^+$ other (CD8$^-$CD4$^-$) cells than *Stat1$^{het}$* mice (Fig 3.5c,f). These data indicate that *Stat1$^{KO}$* mice do not have increased non-specific IFNγ$^+$ CD8$^+$ T cells, which suggests that CR6-specific IFNγ$^+$ CD8$^+$ T cell expansion (Fig 3.4d) is not solely due to a loss in intrinsic STAT1-dependent regulation of CD8$^+$ T cells. These data also indicate that total numbers of IFNγ-producing "other" cells are increased when STAT1 signalling is deficient. Finally, only about 8% of IFNγ$^+$ *Stat1$^{KO}$* cells were CD4$^+$ cells, compared to 34% in *Stat1$^{het}$* mice; these frequency differences were also reflected in total cell numbers (Figure 3.5b, e). In conclusion, these data suggest that CD4$^+$ T cells are generally deficient at producing IFNγ when STAT1 signalling is absent. Since IFNγ is a key effector cytokine of the antiviral Th1 cellular response, this may indicate a defect in Th1 immunity.

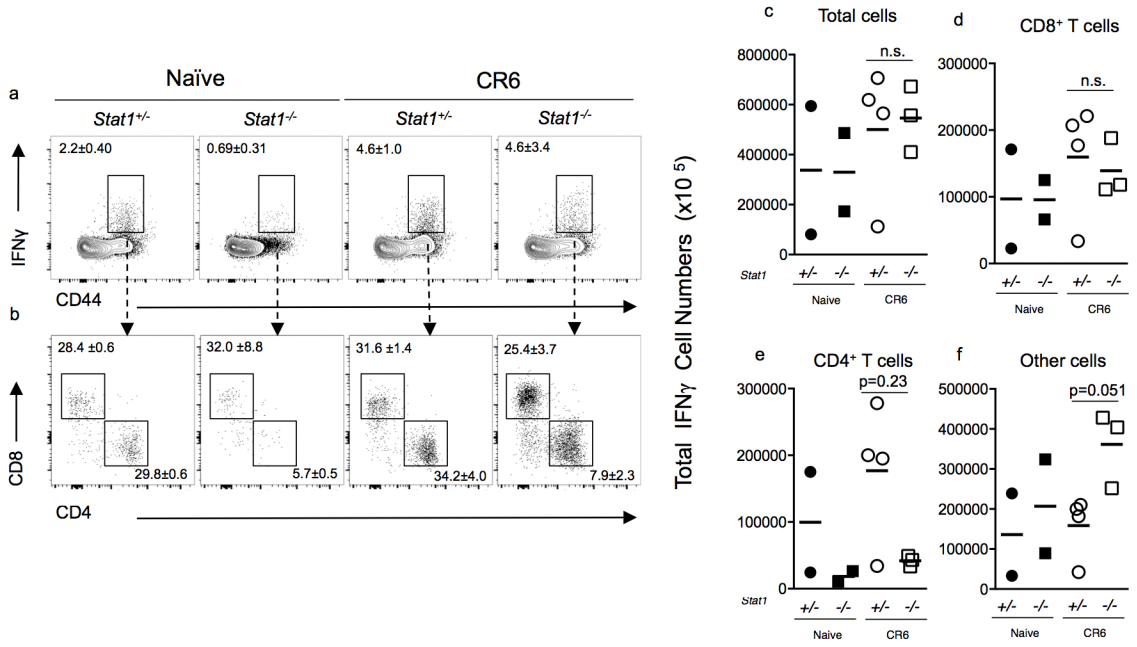


**Figure 3.5 STAT1 is important for generating IFNγ producing CD4$^+$ T cells, regardless of infection status.**
*Stat1$^{het}$ and Stat1$^{KO}$* mice were given PBS or infected with $10^4$ pfu MNV-CR6 *p.o.* and analyzed on day 8 pi. Splenocytes were isolated and treated with PMA and ionomycin for 5 hours in the presence of BFA and monensin, and the stained intracellularly for IFNγ. (a) IFNγ producing CD44$^{hi}$ live cells. (b) IFNγ producing cells, subsetted into CD4$^+$ T cells or CD8$^+$ T cells. Total cell numbers of IFNγ$^+$ producing (c) total cells (d) CD8$^+$ (e) CD4$^+$ or (f) CD8$^+$ CD4$^+$ cells in naïve *Stat1$^{het}$* and *Stat1$^{KO}$* mice (n = 2 per group) or CR6-infected *Stat1$^{het}$* and *Stat1$^{KO}$* (n = 4 per group) mice. Data are representative of three independent experiments. Data from one mouse are represented by individual symbols. Statistical significance was determined by Student's t test. * = $p < 0.05$, n.s. = $p > 0.05$.

## 3.5 STAT1 directs transcription factor expression in CR6-specific CD4$^+$ T cells

Figure 3.5e indicated a deficiency in IFNγ production by non-specifically stimulated CD4$^+$ T cells from *Stat1$^{KO}$* mice. Since Th1 responses are instrumental for coordinating immune responses against viruses, we investigated the accumulation, differentiation, and cytokine production of CR6-specific CD4$^+$ T cells. The role of CD4$^+$ T cells has not been thoroughly

investigated in the context of CR6 infections, although their selective depletion leads to delayed control of CW3 infections (Chachu et al., 2008). To detect the relatively rare CR6-specific $CD4^+$ T cell population, CR6 MHC II tetramer-specific $CD4^+$ T cells were enriched for, by using magnetic beads (Moon et al., 2007). Unlike CR6-specific *Stat1*$^{KO}$ $CD8^+$ T cell expansion, *Stat1*$^{het}$ and *Stat1*$^{KO}$ mice had similar numbers of CR6 MHC II tetramer-specific $CD4^+$ T cells (Fig 3.6a, b). To assess CR6-specific Th cell subsets, the expression of the canonical Th1 and Th17 transcription factors—T-bet and RORγt, respectively—were analyzed. T-bet expression levels and T-$bet^+$ $CD4^+$ T cell numbers were similar between *Stat1*$^{het}$ and *Stat1*$^{KO}$ CR6-specific $CD4^+$ T cells (Fig 3.6c, d). However, RORγt expression and RORγ$t^+$ $CD4^+$ T cell numbers were significantly increased in CR6-specific $CD4^+$ T cells from *Stat1*$^{KO}$ mice compared to *Stat1*$^{het}$ mice (Fig 3.6g, h). To determine if a role exists for STAT1 in bystander (non CR6-specific) $CD4^+$ T cell activation or differentiation, $CD4^+$ T cell T-bet and RORγt expression were analyzed in the tetramer negative magnetically-unbound fraction of cells. Bystander *Stat1*$^{KO}$ $CD4^+$ T cells showed no significant difference in T-bet and RORγ$t^+$ expression and total cell numbers ($p=0.19$), compared to bystander *Stat1*$^{het}$ $CD4^+$ T cells (Fig 3.6e-j). These data indicate that upon activation, CR6-specific $CD4^+$ T cells display a propensity to skew toward the Th17 subtype when STAT1 signalling is deficient.

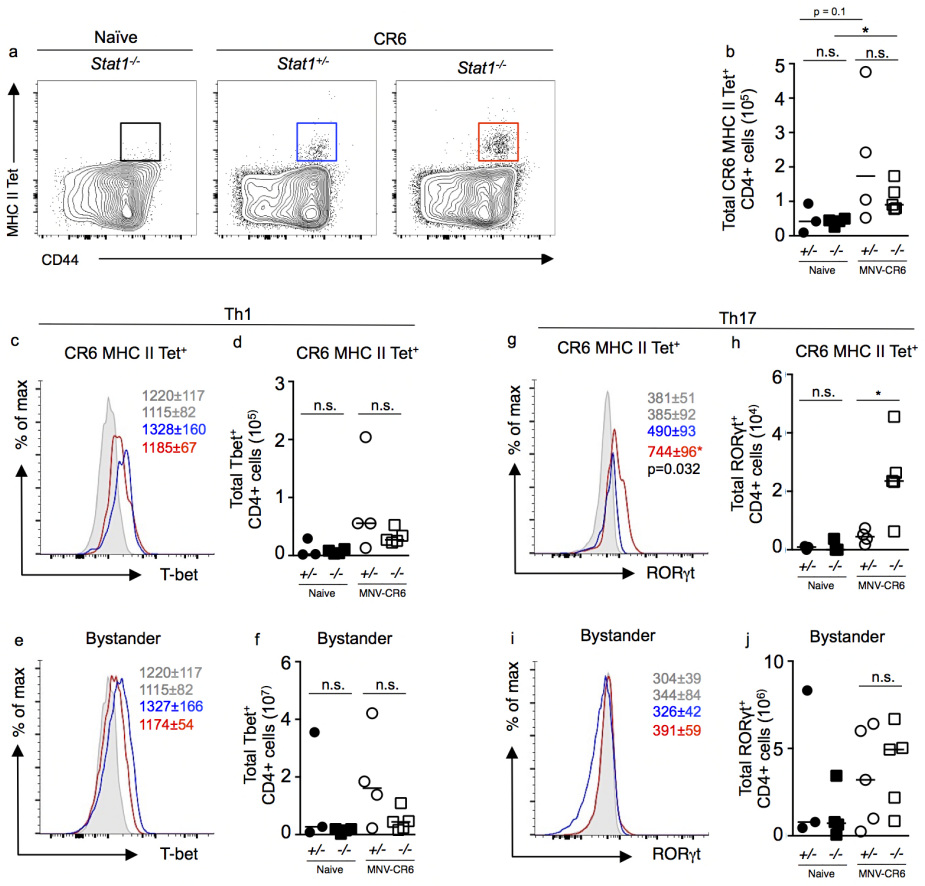


**Figure 3.6 STAT1 is important for directing Th1 differentiation during CR6-specific T cell activation.**

*Stat1*$^{het}$ *and Stat1*$^{KO}$ mice were given PBS or infected with $10^4$ pfu CR6 *p.o.* and spleens and lymph nodes were isolated on day 8 pi and subjected to tetramer pull-down and stained for flow cytometry. (a) MNV-CR6 MHC II Kb-P1$^{496}$ Tetramer$^+$ activated (CD44$^{hi}$) CD4$^+$ T cells (b) total number of MNV-CR6-specific CD4$^+$ T cells (c) Tetramer$^+$ CD4$^+$ T cells from *Stat1*$^{het}$ (blue) and *Stat1*$^{KO}$ (red) were analyzed for expression of T-bet. (d) Total numbers of T-bet$^+$ tetramer$^+$ CD4$^+$ T cells. (e) Tetramer negative "bystander" CD4$^+$ T cells from *Stat1*$^{het}$ (blue) and *Stat1*$^{KO}$ (red) were analyzed for expression of T-bet. (f) Total numbers of T-bet$^+$ tetramer negative CD4$^+$ T cells. (g) Tetramer positive CD4$^+$ T cells from *Stat1*$^{het}$ (blue) and *Stat1*$^{KO}$ (red) were analyzed for expression of RORγt. (h) Total numbers of RORγt$^+$ tetramer$^+$ CD4$^+$ T cells. (i) Tetramer negative "bystander" CD4$^+$ T cells from *Stat1*$^{het}$ (blue) and *Stat1*$^{KO}$ (red) were analyzed for expression of RORγt. (j) Total numbers of RORγt$^+$ tetramer negative CD4$^+$ T cells. Grey histograms of naïve (CD44$^{low}$) CD4$^+$ T cells. Data are representative of two independent experiments, each with *n=3-5* mice per group. Data from one mouse are represented by individual symbols. Statistical significance was determined by Mann-Whitney test * = $p < 0.05$, n.s. = $p > 0.05$. MFIs represented as the mean +/- standard deviation (SD).

### 3.6 STAT1 directs cytokine production by $CD4^+$ T cells post CR6 infection

To further investigate the role of STAT1 in $CD4^+$ T cell differentiation and function, we assessed cytokines produced by all $CD4^+$ T cells following CR6 infection. Stimulating (PMA/ionomycin) colonic $CD4^+$ T cells revealed a trend toward infection-induced increases in $IFN\gamma^+$ and $TNF\alpha^+$ $CD4^+$ LPLs and IELs from CR6-infected *Stat1*$^{het}$ mice (Fig 3.7a, c, d). There was no infection-induced increase $IFN\gamma^+$ and $TNF\alpha^+$ $CD4^+$ T cells in the spleen of CR6-infected *Stat1*$^{het}$ mice (Fig 3.7f, h, i), which reflects the localized nature of CR6 in WT hosts (Tomov et al., 2013). However, the frequency of colonic $IFN\gamma^+$ $CD4^+$ T cells from infected *Stat1*$^{KO}$ mice was significantly diminished compared to infected *Stat1*$^{het}$ littermate controls (Fig 3.7a, c). Notably, *Stat1*$^{KO}$ $CD4^+$ T cells exhibited a robust infection-induced increase in IL-$17A^+$ production in both the colon (Fig 3.7b, e) and spleen (Fig 3.7g, j) of *Stat1*$^{KO}$ mice, whereas little IL-17A production was observed in infected *Stat1*$^{het}$ mice (Fig 3.7b, e, g, j). Lastly, there were no differences in TNFα production by *Stat1*$^{het}$ and *Stat1*$^{KO}$ $CD4^+$ T cells from infected colons or spleens (Fig 3.7d, i), indicating that not all $CD4^+$ T cell functions are regulated by STAT1 signalling following CR6 infection. These data indicate increased IL-17A-producing (Th17) and decreased IFNγ-producing (Th1) $CD4^+$ T cells in CR6 infected *Stat1*$^{KO}$ mice, which is consistent with observations of increased $ROR\gamma t^+$ (Th17) and decreased T-$bet^+$ (Th1) MHC II $Tet^+$ $CD4^+$ T cell data. These data indicate a dysregulated $CD4^+$ T cell response to CR6 in *Stat1*$^{KO}$ mice. Given the importance of $CD4^+$ Th1 cells in coordinating antiviral responses, it is likely that Th17 cells are not able to help establish an appropriate immune response to a CR6 infection.

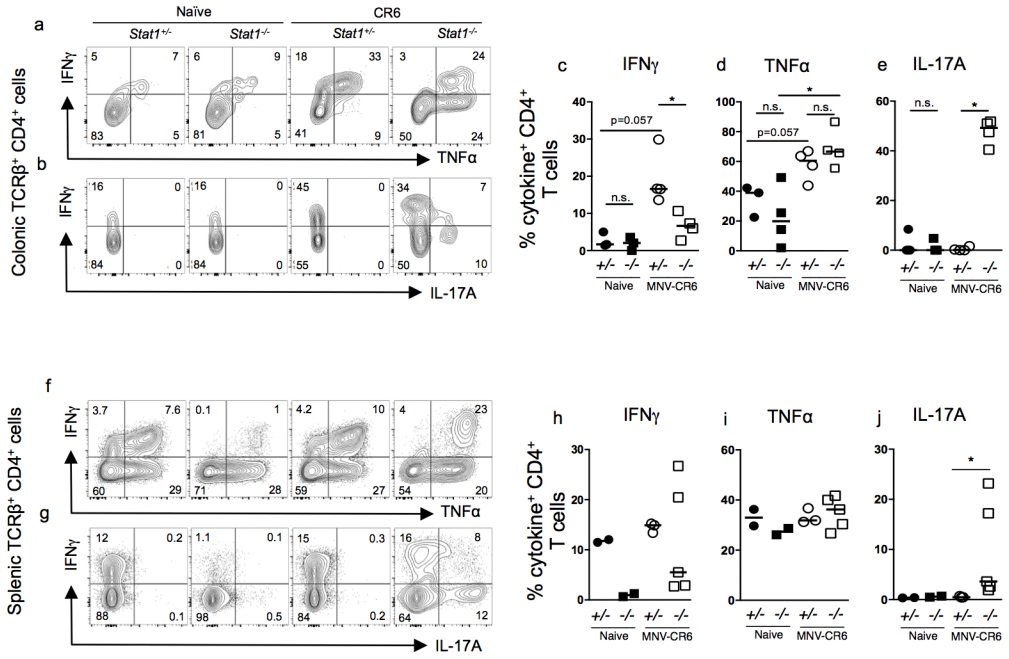


**Figure 3.7 STAT1-deficient Th cells produce IL-17A and do not produce IFNγ.** *Stat1*$^{het}$ *and Stat1*$^{KO}$ mice were given PBS or infected with $10^4$ pfu CR6 *p.o.* and analyzed on day 8 pi. LPLs and IELs were isolated from the colon and cecum and then stimulated with PMA and ionomycin, and stained for intracellular cytokines (a, c, d) IFNγ and TNFα (b, e) IL-17A. Splenocytes were collected, stimulated with PMA and ionomycin, and stained for intracellular cytokines (f, h, i) IFNγ and TNFα (g, j) IL-17A. Data in (a-e) are *n= 4* mice for infected group and are representative of three independent experiments with similar results. Data in (f-j) are *n=3-5* mice for the infected groups and are representative of two independent experiments. Data from one mouse are represented by individual symbols. Statistical significance was determined by Mann-Whitney test * = $p < 0.05$, n.s. = $p > 0.05$.

## 3.7 STAT1 directs CD4$^+$ T cell differentiation after receiving type 1-associated stimulation

To gain a better understanding of why CR6 infection promotes Th17 cell differentiation in *Stat1*$^{KO}$ mice, we sought to determine if cytokines known to be involved in directing Th differentiation to Th17 cells were present at higher levels in the serum and tissues of *Stat1*$^{KO}$

mice. Cytokines TGFβ and IL-6 act together on naïve $CD4^+$ T cells to promote Th17 cell differentiation during activation (Zhu and Paul, 2008). Therefore, we investigated if overall tissue mRNA transcripts of *Tgfb* and *Il6* differed between genotypes. However, *Tgfb* and *Il6* mRNA transcript levels from colonic tissues were similar in both infected $Stat1^{het}$ and $Stat1^{KO}$ mice (Fig 3.8a, b). Moreover, serum IL-6 levels do not differ significantly between infected groups, although IL-6 trended higher in $Stat1^{KO}$ mice (Fig 3.8c). These data suggest that the microenvironment in CR6-infected $Stat1^{KO}$ mice is no more conducive Th17 cell differentiation than in $Stat1^{het}$ mice.

Since Th17-differentiating cytokines were not in the serum and tissues of $Stat1^{KO}$ mice, we hypothesized that intrinsic $CD4^+$ T cell STAT1 signalling could be important for Th cell differentiation. To determine the intrinsic effect of STAT1 deficiency on $CD4^+$ T cell differentiation, splenocytes were activated *ex vivo* by αCD3 and αCD28 Ab stimulation (Ab against T cell activation receptors) under neutral (αCD3 and αCD28 mAb) and Th1 polarizing (αCD3/αCD28 Ab + IL-2, IL-12p70, and αIL-4 Ab) conditions. Five days after stimulation, supernatants from *in vitro* stimulated cells were analyzed for cytokine concentrations by cytometric bead array (CBA).

Following activation under neutral conditions, $CD4^+$ $Stat1^{KO}$ splenocytes produced a broad suite of Th1 (TNFα), Th17 (IL-17A, IL-22, and IL-17F), and Th2 cytokines (IL-5 and IL-13); however, activated $Stat1^{KO}$ $CD4^+$ T cells did not produce IFNγ (Fig 3.8d-j), suggesting a $CD4^+$ T cell intrinsic defect in IFNγ production. $CD4^+$ $Stat1^{het}$ splenocytes produced detectable levels of most cytokines under neutral stimulation (Fig 3.8d-j).

The addition of IL-2, IL-12p70, and αIL-4 Ab to the αCD3/αCD28 T cell activation assay created Th1 skewing conditions, emulating what would occur *in vivo* during a virus infection.

Under these conditions, *Stat1*$^{het}$ CD4$^{+}$ T cells skewed toward a Th1 phenotype and produced IFNγ and TNFα, but no other cytokines (Fig 3.8d-j). In comparison, without STAT1 signalling, CD4$^{+}$ T cells produced significantly less IFNγ than *Stat1*$^{het}$ CD4$^{+}$ T cells (Fig 3.8d). However *Stat1*$^{KO}$ cells produced detectable levels of Th17 cytokines (IL-17A, IL-22, and IL-17F) and Th2 cytokines (IL-5 and IL-13). Notably, both *Stat1*$^{het}$ and *Stat1*$^{KO}$ cells produced similar levels of TNFα indicating that not all cytokines are regulated by STAT1. In conclusion, these data suggest that when STAT1 is absent, activated CD4$^{+}$ T cells have a propensity to intrinsically differentiate toward Th17 and Th2-cytokine producing cells, and show a deficit in the ability to produce IFNγ.

Finally, these observations lead to the hypothesis that global dysregulation of CD4$^{+}$ T cells may be responsible for immunopathology, which could reflect the clinical signs of weight loss and histopathology observations in Fig 3.1-3.3.

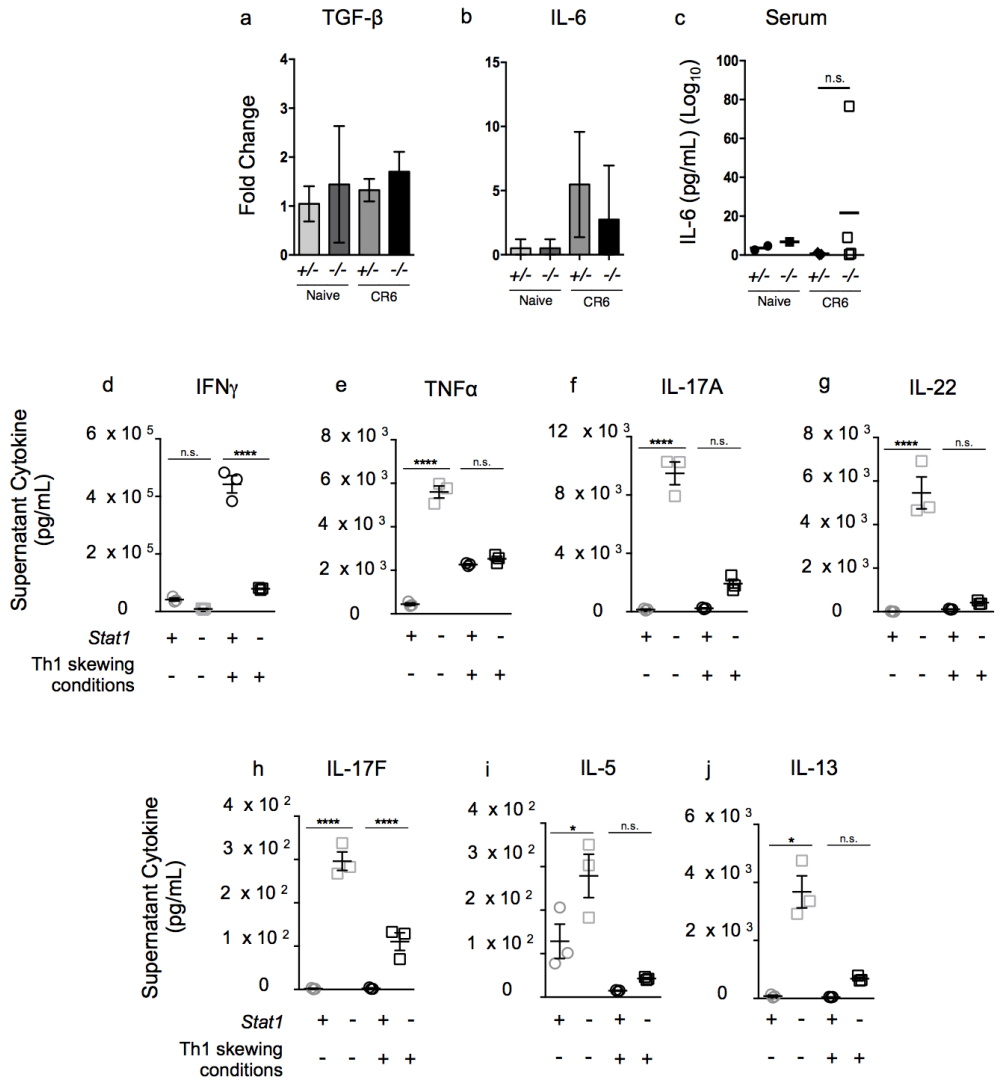


**Figure 3.8 Th1 skewing conditions directs away from type 1 cytokine production by *Stat1*$^{KO}$ CD4$^{+}$ T cells *in vitro*.**

(a) *TGFB1* and *IL6* transcript expression in colon as measured by qRT-PCR and normalized to *Hprt*. The values are represented as fold change relative to naïve *Stat1*$^{het}$. (b) Serum from CR6-infected mice were taken at day 8 *pi* and analyzed for cytokine levels by cytometric bead array. (c-j) Supernatants were taken at day 5, after *in vitro* stimulation of *Stat1*$^{het}$ and *Stat1*$^{KO}$ CD4$^{+}$ T cells, and analyzed for the labeled cytokine levels by cytometric bead array. Statistical significance was determined by Mann-Whitney Student's t test. * = $p < 0.05$, n.s. = $p > 0.05$.

### 3.8 IL-17A neutralization does not change clinical outcomes or immune signatures of CR6-infected *Stat1*$^{KO}$ mice

Our data indicate that in the absence of STAT1 signaling, CR6 infections promote the differentiation of naïve CD4$^{+}$ T cells into Th17 cells. Th17 cells typically coordinate immunity to extracellular bacterial and fungal infections. The role of Th17 cells and IL-17A in the context of intestinal CR6 virus infection, to our knowledge, has not yet been explored. In the context of lung virus infection, IL-17A production can induce immunopathology (Crowe et al., 2009). Moreover, our results found evidence of CR6 disseminating to the lungs of *Stat1*$^{KO}$ mice (Fig 3.2f), which provoked the hypothesis that IL-17A may promote immunopathology in CR6-infected *Stat1*$^{KO}$ mice. Reflecting our observations that RORγt$^{+}$ or IL-17A$^{+}$ CD4$^{+}$ T cells increased in numbers and frequency, serum Th17 cytokines IL-17A and IL-22 are significantly increased in CR6-infected *Stat1*$^{KO}$ mice (Fig 3.9a, b). Moreover, supporting the immunopathology hypothesis, we observed a moderate positive correlation between increased CR6 genome copies, which correlates with weight loss, and increased mRNA IL-17A transcripts from the spleens of infected *Stat1*$^{KO}$ mice (Fig 3.9c). To investigate if IL-17A causes immunopathology, we treated CR6-infected *Stat1*$^{KO}$ mice with either αIL-17A Ab or control isotype Ab, administered by intraperitoneal (i.p.) injection. Both treatment groups lost a similar percentage of weight (Fig 3.9d). IL-17A can act as a neutrophil chemoattractant, and we observed significant neutrophil infiltration in *Stat1*$^{KO}$ compared to *Stat1*$^{het}$ (data not shown); thus, we analyzed neutrophil infiltration in the colon and spleen of treated CR6-infected *Stat1*$^{KO}$ mice. There were no significant differences in neutrophil infiltration between treatment groups (Fig 3.9e, f). Moreover, IL-17A neutralization did not influence viral clearance (Fig 3.9g). Th17 differentiation and production of IL-17A is a feature of CR6-infected *Stat1*$^{KO}$ mice and is an

example of how STAT1 signalling is necessary to coordinate appropriate and effective immune responses to intestinal viral infections. However, contrary to the hypothesis that the pro-inflammatory cytokine, IL-17A, may contribute to immunopathology, IL-17A does not appear to influence CR6-induced weight loss, CR6 clearance, or abnormal immune features observed in infected *Stat1*$^{KO}$ mice.

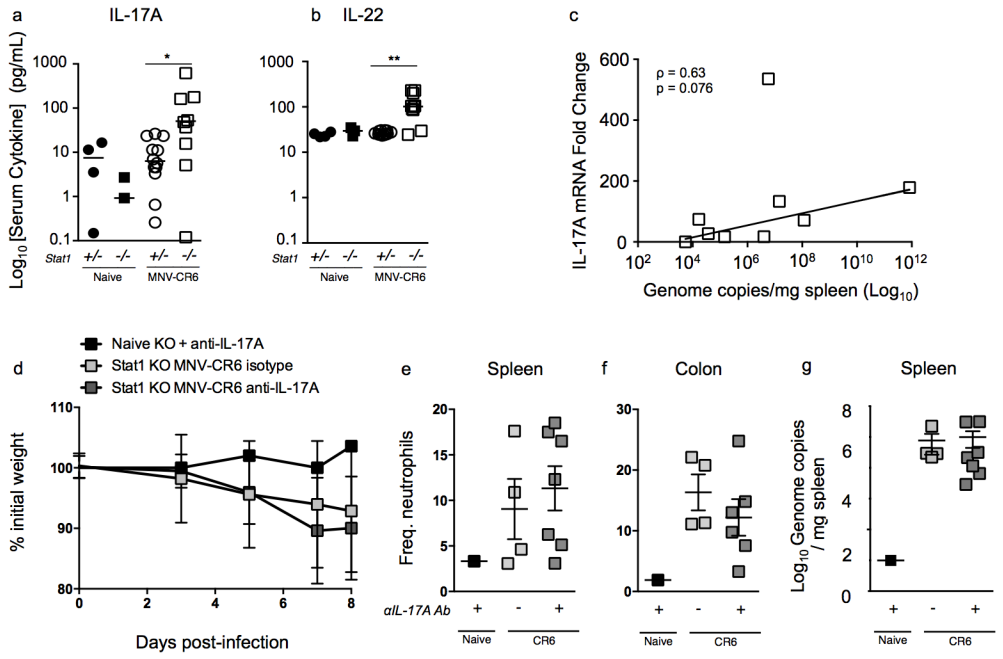


**Figure 3.9 IL-17A is not directly responsible for CR6-induced disease observed in *Stat1*$^{KO}$ mice.**

*Stat1*$^{het}$ *and Stat1*$^{KO}$ mice were PBS treated or infected with $10^4$ pfu CR6 *p.o.* and analyzed on day 8 pi Serum was collected and subjected to CBA for (a) IL-17A and (b) IL-22. (c) RNA was isolated from spleen tissue, qPCR was used to quantify MNV genome copies, normalized to mg tissue and *Il17a* transcripts were normalized to the reference gene *Hprt,* MNV genome copies were plotted against *IL17a* transcripts of the same spleen. Mice were given anti-IL17A Ab or isotype Ab i.p. post-CR6 infection. (d) weight change from day 0 was plotted over days. Neutrophils ($B220^-CD11b^+Ly6G^+$) in the (e) spleen and (f) colon. (g) Viral genome copies per mg spleen tissue. Data in (a and b) are compiled data from three independent experiments. Data in (c) are n=9 CR6-infected *Stat1*$^{KO}$ mice from two independent experiments. Data from one mouse are represented by individual symbols. Data in (d, e, f) are compiled from two independent experiments. Statistical significance was determined by Mann-Whitney test (a, b, d, e) and Spearman's coefficient test (d) * = $p < 0.05$, **=$p<0.01$, n.s. = $p > 0.05$.

### 3.9 STAT1 signalling regulates systemic cytokine production following CR6 infection

To broadly assess and characterize the systemic immune response to intestinal CR6 infection, serum cytokine levels were measured by cytometric bead array (CBA). Reflecting the controlled and localized response to CR6-infection observed in *Stat1*$^{het}$ mice, serum cytokine levels were not significantly increased in infected *Stat1*$^{het}$ mice, compared to naïve mice (Fig 3.10a-j). In comparison, CR6-infected *Stat1*$^{KO}$ mice displayed significantly increased antiviral cytokines, IFNγ, IL-2, and TNFα (Fig 3.10a, c, d). Moreover, CR6-infected *Stat1*$^{KO}$ mice displayed significantly increased Th17 cytokines, IL-17A and IL-22 (Fig 3.10f, g) and a trend toward increased anti-parasitic Th2 cytokines, IL-4 ($p=0.052$) and IL-5 ($p=0.10$) (Fig 3.10h, i). Finally, similar levels of the regulatory cytokine, IL-10, were measured between infected genotypes (Fig 3.10j). These data reflect the importance of STAT1 signaling in coordinating controlled and specific immunity to CR6 infections.

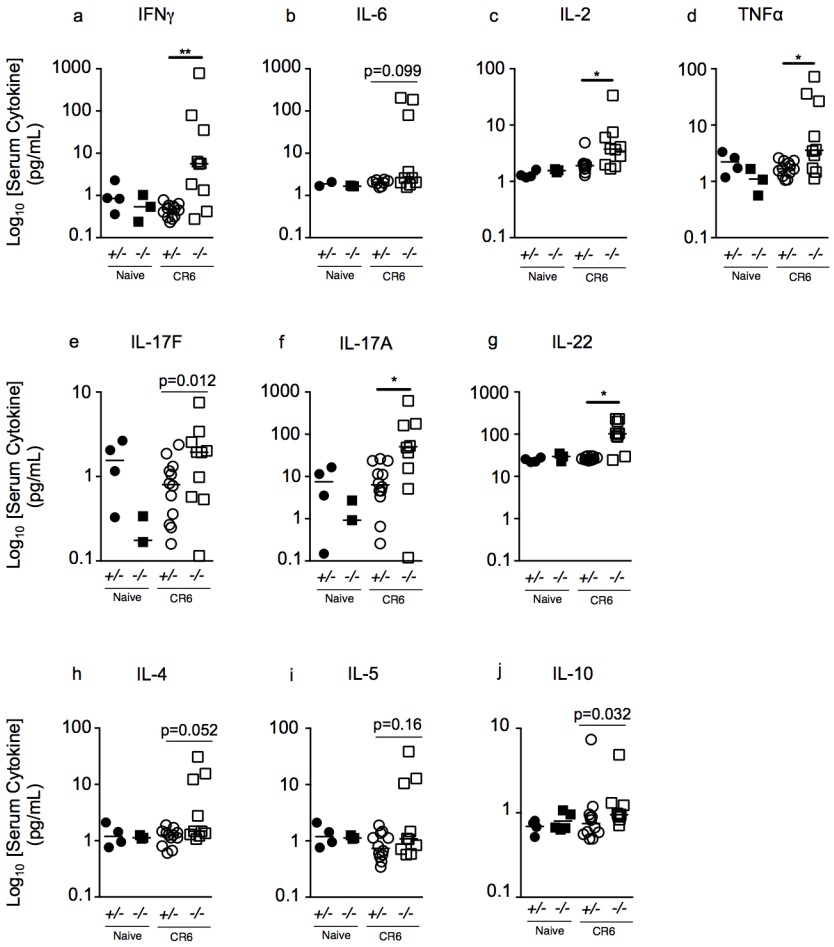


**Figure 3.10 CR6-infected *Stat1*$^{KO}$ mice have increased serum cytokines, compared to *Stat1*$^{het}$ mice**.

Serum from PBS or CR6-infected mice were taken at experiment end on day 8 pi and cytokine levels were analyzed by CBA. All data shown are compiled from three independent experiments. Data from one mouse are represented by individual symbols. Statistical significance was determined by Mann-Whitney test. * = $p < 0.05$, ** = $p < 0.01$.

### 3.10 STAT1 signalling does not regulate properties of Treg cells during CR6 infection

The immense dysregulation of cytokine responses in *Stat1*$^{KO}$ mice warrants investigation into Treg cell numbers and function, to ensure regulatory mechanisms are intact. Treg cells are key mediators of inflammation and produce cytokines, chiefly IL-10, which acts on multiple cell types through STAT3 to dampen the immune response to virus infections and promote proper adaptive memory formation (Zhu and Paul, 2008). If effector CD4$^{+}$ T cells significantly outnumber Treg numbers, this could indicate that the immune response is being poorly regulated. The ratios of activated T cells (CD44$^{hi}$) to T regulatory (Foxp3$^{+}$) cells are similar in CR6-infected *Stat1*$^{het}$ and *Stat1*$^{KO}$ mice (Fig 3.11a, b). To determine if Treg cells are producing IL-10, IL-10 was analyzed by flow cytometry and by RT-qPCR. There were significantly decreased frequencies of IL-10$^{+}$ splenic *Stat1*$^{KO}$ CD4$^{+}$ T cells compared to *Stat1*$^{het}$ CD4$^{+}$ T cells, which could simply reflect the active immune response to disseminated CR6 in *Stat1*$^{KO}$ mice, which is absent in the spleens of *Stat1*$^{het}$ mice (Fig 3.11c). Frequencies of IL-10$^{+}$ colonic IEL and LPL CD4$^{+}$ T cells were similar between genotypes (Fig 3.11d). Lastly, *il10* mRNA transcripts from spleens and colons were similar between *Stat1*$^{het}$ and *Stat1*$^{KO}$ mice, regardless of infection status (Fig 3.11e, f). These data do not support the hypothesis that Treg differentiation and function is dysregulated in CR6-infected *Stat1*$^{KO}$ mice; which suggests increased proinflammatory markers cannot be explained by the absence of, or decline in, Treg numbers and function.

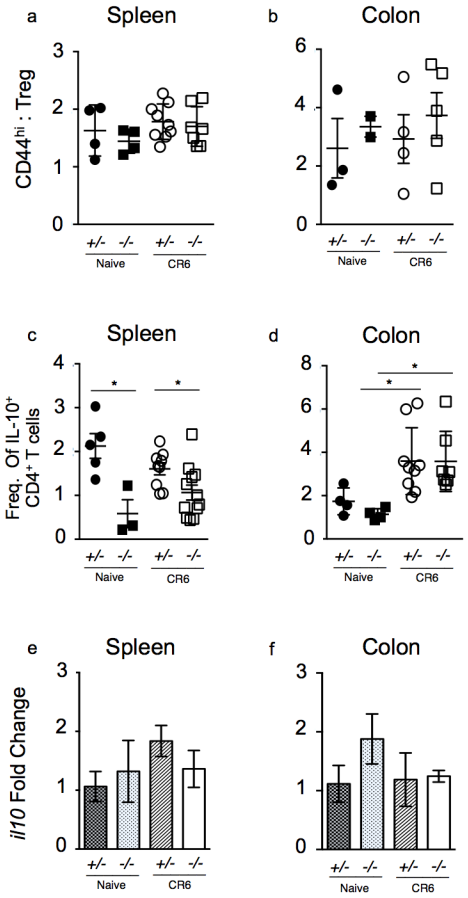


**Figure 3.11 Treg differentiation and function are not dependent on STAT1 signaling during CR6 intestinal infection.**

*Stat1*$^{het}$ *and Stat1*$^{KO}$ mice were given PBS or infected with $10^4$ pfu CR6 *p.o.* and analyzed on day 8 pi Splenocytes or pooled LPL and IELs were isolated and treated with PMA and ionomycin for 5 hours in the presence of BFA and monensin, cells were gated on $CD4^+$ and then stained intracellularly for IL-10 and Foxp3. (a, b) The ratio of $CD44^{hi}$ $TCR\beta^+$ vs. $Foxp3^+$ Treg cells. (c, d) Frequency of IL-10 producing $CD4^+$ T cells. (e, f) *IL10* transcript expression in spleen or colon as measured by qRT-PCR and normalized to *Hprt*. The values are represented as fold change relative to naïve *Stat1*$^{het}$. Data from one mouse are represented by individual symbols. Statistical significance was determined by Mann-Whitney test. * = $p < 0.05$, n.s. = $p > 0.05$.

### 3.11 Enteric CR6 infections do not cause a detectable disturbance in the intestinal barrier

Infiltrating IFNγ$^{+}$ CD8$^{+}$ IELs can negatively affect barrier integrity (Watson *et al.* 2005; Zufferey, Erhart, Saurer, & Mueller, 2009). Moreover, CR6 can infect and replicate in IECs (Lee et al., 2017). Finally, there are elevated levels of cytokines that are often involved in responses to mucosal fungal, bacterial, and parasitic infections, in CR6-infected *Stat1*$^{KO}$ mice (Fig 3.10e-i). This information provoked the hypothesis that without STAT1 signaling, CR6 may be causing intestinal barrier damage, which could prompt a secondary pathobiont infection. To investigate this hypothesis, expression of proteins that are important for mucosal barrier integrity were measured (Vaishnava et al., 2011; Wang et al., 2015). Significant increases in colonic mRNA transcripts, typically upregulated by mucosal infections, *Reg3b* and *Reg3g*, but not *Muc2*, were observed in infected *Stat1*$^{KO}$ mice, compared to *Stat1*$^{het}$ mice (Fig 3.12a, b, c). Previous studies have indicated that tight junction proteins are upregulated when barrier integrity is compromised (Brown et al., 2015; Gunzel & Yu, 2013). Therefore, we examined colonic transcripts of *Tight junction protein 1(Tjp1)*, *Claudin-2*, *Claudin-4*, and *Claudin-15* and found that they were similar regardless of infection status or genotype (Fig 3.12d-g). Barrier leakiness can also be assessed by measuring serum albumin that has crossed into the intestinal lumen (Wang et al., 2015). Serum albumin levels in fecal matter tended to be lowest in the infected *Stat1*$^{KO}$ group, although levels were not significantly different between genotypes (Fig 3.12h). In addition, gavaging mice with FITC-dextran can indicate a compromised intestinal barrier if it is detected in serum (Wang et al., 2015). Again, no significant differences in serum FITC-dextran levels were detected between genotypes (Fig 3.12i). Finally, CR6-infected *Stat1*$^{KO}$ mice were treated with antibiotics to deplete intestinal microbiota (Hill et al., 2010). Infected mice given vehicle control and antibiotics lost similar amounts of weight (Appendix C a). Moreover, similar frequencies of

CR6-specific $CD8^+$ IELs were collected in antibiotic treated mice (Appendix C b). Similar numbers of neutrophils were isolated from the spleens of both treatment groups (Appendix C c). Finally, ratios of Tbet to $ROR\gamma t^+$ $CD4^+$ T cells were similar in the spleen, LPL and IEL across treatment groups (Appendix C d, e, f). These data suggest that depleting microbes has no overall influence on the outcome, weight loss or immune response, of CR6-infected $Stat1^{KO}$ mice. Altogether, these data suggest that mucosal barrier integrity is maintained during CR6 infection, regardless of STAT1 signaling, supporting the hypothesis that abnormal immune responses in CR6-infected $Stat1^{KO}$ mice are because STAT1 signalling is required for coordinating an appropriate antiviral immune response.

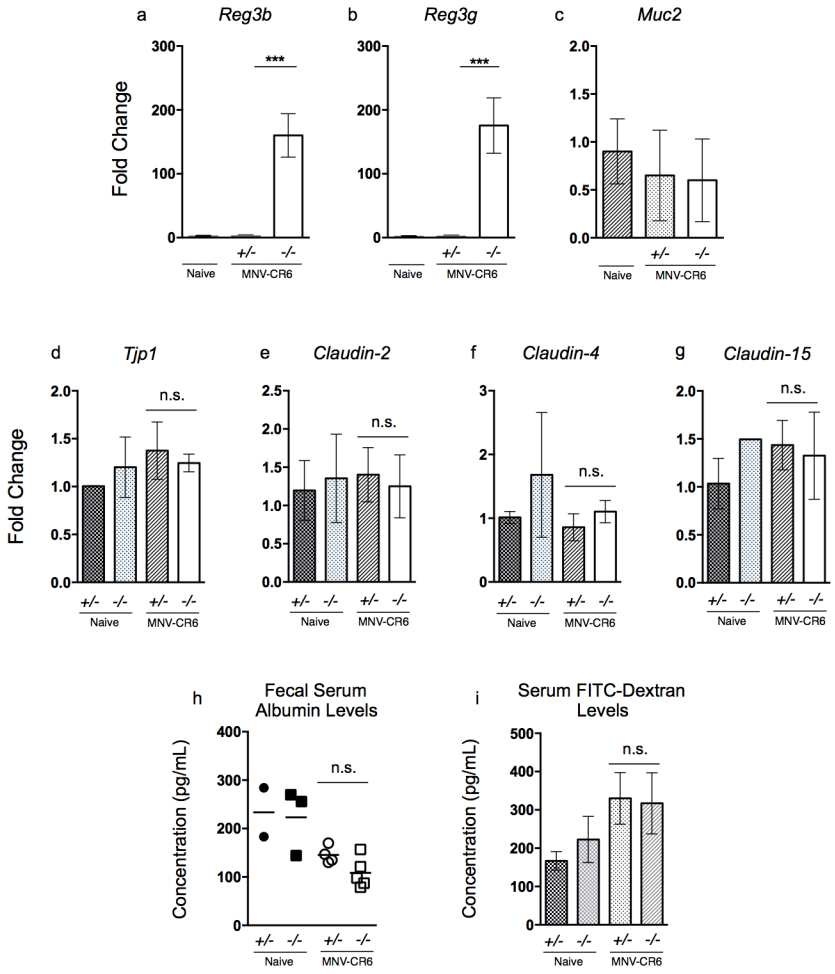


**Figure 3.12 Barrier integrity maintained during CR6 infection, regardless of STAT1 signaling.**

*Stat1*$^{het}$ *and Stat1*$^{KO}$ mice were given PBS or infected with $10^4$ pfu CR6 *p.o.* and analyzed on day 8 pi Fold change of colon transcript expression of (a) *Reg3g* (b) *Reg3b* (c) *Muc2* (d) *Tjpr* (e) *Claudin-2* (f) *Claudin-4* (g) *Claudin-15* as measured by qRT-PCR and normalized to *Hprt*. The values are represented as fold change relative to naïve *Stat1*$^{het}$ mice. (h) Colon luminal contents were collect at day 8 *pi* and analyzed via ELISA to quantify serum albumin concentration. (i) Serum was collected at day 6 pi and analyzed via ELISA to quantify FITC-dextran concentration. Data shown in (a-h) are representative of similar results from three independent experiments. Data in (i) are compiled from three independent experiments. Data from one mouse are represented by individual symbols. Statistical significance was determined by Mann-Whitney test. *** = $p < 0.0001$, n.s. = $p > 0.05$.

### 3.12 Antiviral treatment prevents clinical signs, but does not impair the immunological signature of CR6-infected *Stat1*$^{KO}$ mice

Thus far, we have determined that at day 8, a high percentage of CR6-infected *Stat1*$^{KO}$ mice exhibit symptoms of viral-induced disease (weight loss) and have high systemic viral burdens. These outcomes are associated with elevated levels of pro-inflammatory serum cytokines, increased IL-17A producing CD4$^{+}$ T cells, neutrophilia, and increased CR6-specific IFNγ$^{+}$ CD8$^{+}$ T cells. These characteristics prompted the investigation of whether immune-mediated tissue damage contributed to virus-induced disease. However, depleting CD4$^{+}$ and CD8$^{+}$ T cells and neutralizing IL-17A had no impact on the outcome of CR6-induced disease in *Stat1*$^{KO}$ mice. To determine if the cause of clinical signs and weight loss in *Stat1*$^{KO}$ mice could be narrowed to virus replication, and not immunopathology, *Stat1*$^{KO}$ mice were given an antiviral treatment with 2'-*C*-Methylcytidine (2CMC), which has been shown to inhibit both CW3 and CR6 replication (Rocha-Pereira et al., 2013, 2016). Our goal was to limit CR6 replication, but not completely clear it, to ensure a robust immune response would be initiated. Therefore, we altered the administration regimen to half the reported dose by i.p. injection, starting at either the day of infection, or 72 hours pi. Only one of the 2CMC treated CR6-infected *Stat1*$^{KO}$ mice had lost weight on day 8, and none succumbed to infection, whereas 4 of the 7 mice in the vehicle (PBS) treated group lost weight (Fig 3.13a). Of note, mice that did not begin 2CMC treatment until day 3 had begun to lose weight, but rebounded after the antiviral regimen was initiated (Fig 3.13a). The vehicle-treated *Stat1*$^{KO}$ mice that lost a significant amount of weight exhibited signs of virus-induced disease, high systemic viral burden and the associated immune parameters of elevated IL-17A and IFNγ. The 2CMC-treated *Stat1*$^{KO}$ cohort did not experience virus-induced weight loss and colonic viral burdens were significantly lower than vehicle-treated controls (Fig

3.13b). Virus titers were controlled in the spleens of antiviral-treated mice, compared to the mouse with clinical signs (Fig 3.13c). Immune parameters were measured to determine if controlling virus-replication would alter the immune response to CR6. If limiting virus replication does not influence immune parameters, but ameliorates weight loss, it would suggest that the immune response of CR6-infected *Stat1*$^{KO}$ is a byproduct of deficient STAT1 signalling, but does not cause immunopathology. CR6-specific $CD8^+$ IEL frequencies were expanded across all treatment groups (Fig 3.13d, e). There were no significant differences in splenic CR6-specific $CD8^+$ T cells and peptide-specific $CD8^+$ $IFN\gamma^+$ T cells between treatment groups, suggesting that these cells do not promote immunopathology (Fig 3.13e, f). Numbers of IL-$17A^+$ and $IFN\gamma^+$ $CD4^+$ T splenocytes were most increased in the PBS treated mouse that lost the most weight, however, all CR6-infected *Stat1*$^{KO}$ mice had CR6-specific IL-17A producing $CD4^+$ T cells (Fig 3.13g) and few IFNγ-producing $CD4^+$ T cells (Fig 3.13h). Finally, there were similar increases in neutrophils across all treatment groups (Fig 3.13j). Although pro-inflammatory cytokine-producing $CD4^+$ T cells are notably higher in the mouse that lost the most weight, $CD4^+$ depletion experiments indicated that depleting these cells does not prevent weight loss or mortality (Appendix D a). Moreover, $CD4^+$ depletion did not produce significant changes in neutrophil recruitment to the spleen and the colonic lamina propria and $CD8^+$ IEL and LPL T cells frequencies in infected *Stat1*$^{KO}$ mice (Appendix D b-c). These data indicate that uncontrolled virus replication, and not the significantly different adaptive immune response, is greatly responsible for clinical signs and mortality of CR6-infected *Stat1*$^{KO}$ mice.

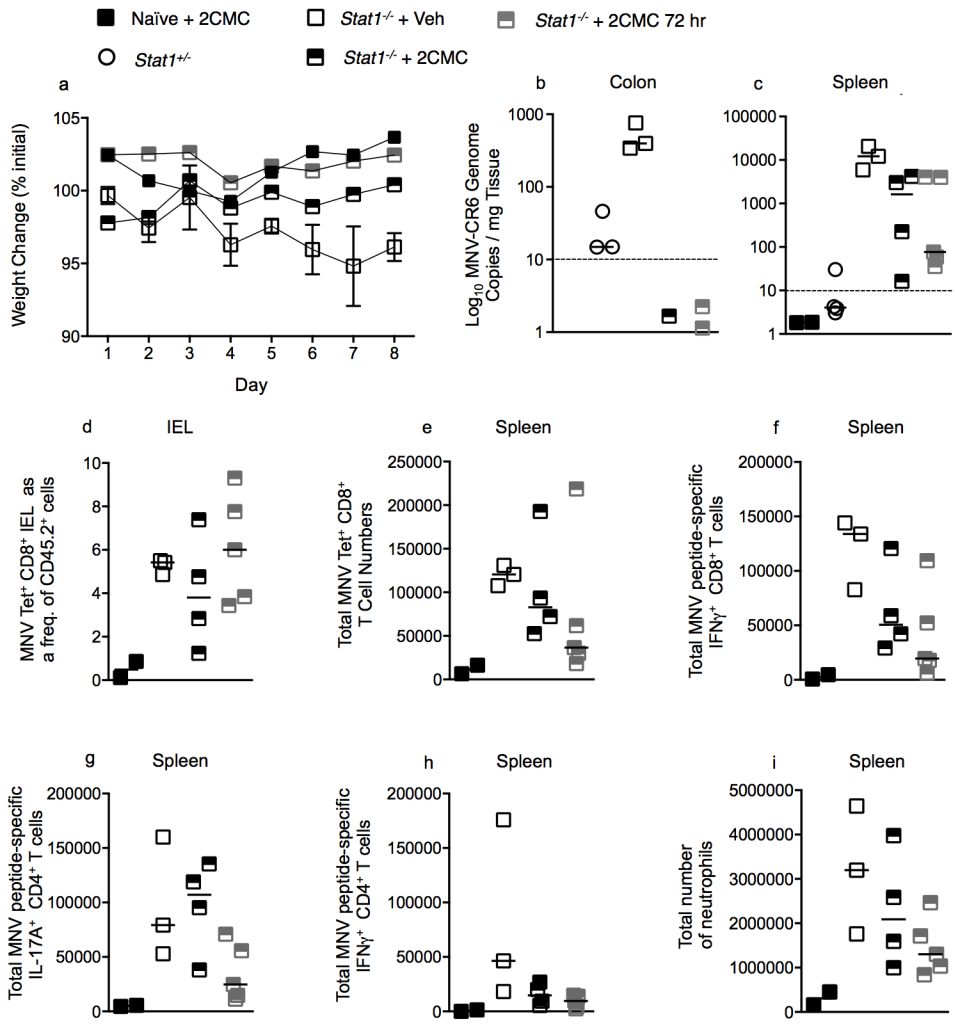


**Figure 3.13 Uncontrolled CR6 replication responsible for CR6-induced morbidity, but not altered immune responses observed in infected *Stat1*$^{KO}$ mice.**

*Stat1*$^{het}$ *and Stat1*$^{KO}$ were given PBS or infected with $10^4$ pfu MNV-CR6 *p.o.* and euthanized on day 8 pi (a) weight change as a percentage of initial weight at day 0. Viral genome copies per mg specified tissue (b) colon (c) spleen. MNV-CR6 Kb-P1$^{519F}$ Tetramer$^+$ CD8$^+$ T cells as a frequency of (d) CD45.2$^+$ IELs and total numbers in (e) spleen. (f) IFNγ$^+$ CD8$^+$ T cells responding to *ex vivo* MNV-specific peptide stimulation in the spleen. (g) IL-17A and (h) IFNγ$^+$ CD4$^+$ T cells responding to *ex vivo* MNV-specific peptide stimulation in the spleen. (i) Neutrophils (B220$^-$CD11b$^+$Ly6G$^+$) in the spleen. Data in are representative of two independent experiments. Data from one mouse are represented by individual symbols, the line representing the median. Statistical significance was determined by Mann-Whitney test * = $p < 0.05$, n.s. = $p > 0.05$.

# Chapter 4: Conclusion

## 4.1 Discussion

This study aimed to investigate the role of STAT1 in coordinating immune responses to CR6 infection. The data generated from my thesis project revealed that STAT1 signalling relays information from the eukaryotic virome, namely CR6, to the host's immune system. I uncovered that, while CR6 infections are asymptomatic in immunosufficient mice, CR6-infected *Stat1*$^{KO}$ mice can develop clinical signs, histopathological changes, and succumb to CR6 infection. Moreover, I was able to characterize CR6-specific T cell responses and conclude that STAT1 plays a major role in regulating $CD8^+$ and $CD4^+$ T cell function and response to enteric CR6 infections. Additionally, I found that STAT1 deficiency and the downstream consequences to immune responses likely do not impair the epithelial GI barrier during CR6 infections. Lastly, I uncovered a possible mechanism for how CR6 infections remain asymptomatic and persistent in immunosufficient mice: STAT1 enables the host to *resist* CR6 replication and dissemination to prevent virus-induced pathology. The concept of the host resisting CR6 infection is unanticipated because the relatively weak immune response raised against CR6 in immunosufficient hosts more closely resembles features of *tolerance* mechanisms for viral persistence.

All of the experiments I performed for my thesis project used littermate controls. Littermate controls were obtained by breeding *Stat1*$^{het}$ and *Stat1*$^{KO}$ mice to achieve 50% *Stat1*$^{het}$ and 50% *Stat1*$^{KO}$ offspring. By ensuring experimental mice have the same parents and that both genotypes are mixed together in one cage, we reduced environmental variables that could contribute to the observed phenotype. Cage by cage differences in microbiota metabolite production and composition, murine metabolism (due to cage temperature differences), water treatment, diet, and transport/handling of cages can all contribute to observed phenotypes.

Finally, parental microbiomes and genetics can influence offspring phenotypes (Stappenbeck and Virgin, 2016). Unfortunately, breeding in this way is not conducive to attaining WT mice. To ensure *Stat1*$^{WT}$ and *Stat1*$^{het}$ mice were phenotypically similar and that *Stat1*$^{het}$ mice are haplosufficient and appropriate to use in place of *Stat1*$^{WT}$ mice, I infected and analyzed the T cell response and viral burdens in a cohort of *Stat1*$^{WT}$ at the beginning of this project (data not shown). However, littermate controls considerably reduce environmental factors that could contribute to the outcome of CR6 infection in *Stat1*$^{KO}$ mice; therefore, I am confident that the observations and data presented in my thesis are a direct result of interactions between the host gene and CR6 infection, rather than environmental variables.

We were able to replicate data from past studies that found CR6 titers are elevated and disseminate systematically in *Stat1*$^{KO}$ mice compared to *Stat1*$^{het}$ or WT mice (Baldridge et al., 2015). However, although there was a trend toward increased CR6 genome copies in the colons of *Stat1*$^{KO}$ mice, my data found that the numbers of MNV genome copies per mg proximal colons of infected *Stat1*$^{KO}$ and *Stat1*$^{het}$ mice were not significantly different. Notably, the difference in genome copy numbers in the colon is similar when comparing my data to previously published data (Baldridge et al., 2015; Nice et al., 2015).

Mechanisms behind STAT1-dependent CR6 restriction to the colon are not currently understood. One study has shown that an amino acid difference in the VP1 capsid protein of CR6 and CW3 enables CW3 to disseminate systemically (Karst et al., 2014). It is possible that in *Stat1*$^{KO}$ mice, the absence of antiviral immune pressure mediated by STAT1 signalling, CR6 is able to mutate its capsid protein to overcome this restriction (Karst et al., 2003). Another possibility builds on knowledge from previous studies, which indicate that CW3-infected *Stat1*$^{KO}$ macrophages have defects in their capacity to kill virus and that DCs can traffic a persistent

MNV (strain CR3) to systemic organs (Elftman et al., 2013; Maloney et al., 2012). Consistent with this hypothesis, preliminary data I generated suggest there are increased CR6 genome copies in CR6-infected *Stat1*$^{KO}$ bone marrow-derived dendritic cells (BMDCs), compared to *Stat1*$^{het}$ BMDCs, which indicated a decreased ability to control viral replication and/or destroy virus particles (data not shown). Therefore, *Stat1*$^{KO}$ DCs with defects in the capacity to control CR6 infection, could traffic live virus to lymph nodes and spleen, where CR6 could infect APCs in systemic organs. In contrast, *Stat1*$^{het}$ DCs would have antiviral programming intact and control CR6 infection before trafficking to lymph nodes and the spleen to present CR6 antigens to the adaptive immune system. Future experiment could use fluorescent-labeled Ab against CR6 capsid proteins using fluorescence microcopy to track virus movement at different time points.

CR6 is an asymptomatic persistent infection in WT mice and in *Stat1*$^{het}$ mice. A prolonged (30 day) CR6 infection revealed that *Stat1*$^{KO}$ mice either eventually succumb to infection or spontaneously clear the infection; 81% of *Stat1*$^{KO}$ mice exhibited clinical signs and 69% succumbed to CR6 infection (Fig 3.1a, b). A previous study has reported spontaneous clearance of a persistent MNV strain (MNV-O7) in *Stat1*$^{KO}$ mice; however, this is a different strain of MNV and, although these mice had similar histopathology signs, these mice showed no clinical signs of disease (Shortland et al., 2014). Moreover, no explanation for the spontaneous clearance was given by this previous study (Shortland et al., 2014). Although the spontaneous clearance observed in *Stat1*$^{KO}$ mice and not *Stat1*$^{het}$ mice is perplexing, it could be due to administrating less than the $10^4$ CR6 pfu dose. Another possibility is that some *Stat1*$^{KO}$ mice received CR6 pfu of higher fitness than other *Stat1*$^{KO}$ mice received. A very small proportion of IECs are infected by CR6 and act as a reservoir for CR6 persistence; thus, administering viruses that are able to infect more IECs in immunodeficient mice could drastically increase viral

burdens and negatively impact host health (Lee et al., 2017). The data in figure 3.4 indicate that *Stat1*$^{KO}$ mice that lost the least amount of weight had high frequencies of CR6-specific CD8$^{+}$ T cells; thus, expanded effector CR6-specific CD8$^{+}$ T cells in combination with varying CR6 numbers and fitness, could provide an explanation for the delayed onset of symptoms or spontaneous clearance of CR6 by some *Stat1*$^{KO}$ mice.

In WT mice, CW3 infection is cleared by day 8 pi and promotes a robust CD8$^{+}$ T cell response that is important for CW3 clearance, whereas CR6 promotes a smaller and less functional antiviral CD8$^{+}$ T cell response at the same time point, and the virus persists and can be detected at high titers in the colon (Tomov et al., 2013). These data suggest that viral persistence could be due to CR6 infection promoting tolerant immune responses rather than the immune response resisting and clearing CR6. Additionally, the chronic LCMV model (a prototypic viral infection model that has informed much of our understanding of similar viral infections) persists because of immune-tolerant conditions. Chronic LCMV can be cleared by overcoming immune-tolerant conditions that are established by persistent type I IFN signaling associated with persistent infection; inhibition of type I IFN signaling results in increased levels of IFNγ, diminished IL-10 expression and viral clearance (Wilson et al., 2013). This collective knowledge of chronic viral infections provoked the hypothesis that the relatively weak antiviral immune response to CR6 infection could be a mechanism for CR6 asymptomatic persistence. In contrast to what was observed in chronic LCMV, both genotypes of CR6-infected mice displayed high IFNγ and relatively low IL-10 levels regardless of IFN signaling, and these antiviral responses were unable to clear CR6 unlike chronic LCMV. These data indicate that CR6 persistence is promoted by a different mechanism.

The perplexing nature of CR6 infections led me to investigate whether STAT1 enable mice to *tolerate* or *resist* CR6 infection. The concept of tolerance differs from that of resistance, in that resistance utilizes host immune defenses to actively limit pathogen burden, which protects the host from pathogens overtaking and causing disease (Schneider and Ayres, 2008). In contrast, tolerance aims to limit collateral host damage by regulating immune responses, which can allow for higher pathogen burdens to persist in the host, if this minimizes pathology caused by overt immune responses (Schneider and Ayres, 2008). Indeed, the data accrued from my experiments suggest that STAT1 signalling limits hyperinflammatory adaptive immune responses. However, the data from T cell depletion and cytokine neutralization experiments (αCD4, αCD8, αIL-17A) also suggest that hyperinflammatory $CD8^+$ T cell or unusual $CD4^+$ T cell responses do not contribute to the morbidity or mortality of CR6-infected STAT1-deficient mice. Importantly, $Stat1^{KO}$ mice with antiviral-controlled CR6 infections displayed similar dysregulated hyperinflammatory immune profiles observed in untreated $Stat1^{KO}$ mice, without signs of morbidity and mortality. These data suggest that STAT1 effectively limits pathogen burdens in immunosufficient mice to protect the host from CR6-induced morbidity and mortality. However, these experiments do not rule out the possibility that the innate system initiates a septic-like response once viral titers are significantly uncontrolled and contributes to morbidity and mortality.

While writing my thesis, a highly respected group in the MNV field published an article describing CR6 persistence (Lee et al., 2017). This article suggests CR6 persistence is due to CR6 tropism for a small number of IECs, which act as a reservoir for viral persistence. In infected IECs, a viral protein interferes with IFNλ-signalling, which enables replication; this mechanism of persistence is consistent with my data, which suggests CR6 persists due to a

failure in CR6 resistance and not due to a breakdown in tolerance. In other words, STAT1 signalling enables the host to *resist* CR6 replication and dissemination, but CR6 has developed a method to suppress STAT1 signalling by interfering with the IFNλ-signalling pathway to *persist* in the host. Thus, CR6 infection in WT mice is a good example of a balance between persistence and resistance. CR6 persists by interfering with the IFNλ-signalling pathway, while maintaining host health by allowing the host to restrict dissemination through IFNα/β signalling. If true, this indicates the virus has evolved a mechanism for propagation by targeting specific cell types and IFNλ-STAT1 signalling pathway to maintain persistence, but not impact host health. Importantly, it does not imply the host induces a tolerance response to maintain an asymptomatic and persistent infection. Indeed, my data indicate that without STAT1 signalling, the virus persists and loses intestinal restriction, which ultimately leads to the demise of the host and limits the propagation potential of CR6.

Few studies have investigated T cell responses generated against asymptomatic persistent enteric viruses and I wanted investigate T cell responses in this context. CR6-infection promoted different T cell responses in $Stat1^{KO}$ mice than $Stat1^{het}$ mice, which indicates that STAT1 regulates the generation of T cell responses to enteric infections. Fortunately, we had the necessary tools to investigate CR6-specific T cell responses. Moreover, my studies show that $Stat1^{het}$ mice added to our understanding of T cell interactions with the eukaryotic enteric CR6 infection at steady state.

We found that effector cytokine-positive $Stat1^{KO}$ CR6-specific $CD8^+$ T cells are increased in frequencies and numbers. $CD8^+$ T cells have been shown to be important for MNV clearance (Tomov et al., 2013). Our data show significantly increased CR6-specific $CD8^+$ T cell frequencies in $Stat1^{KO}$ mice compared to $Stat1^{het}$ mice. These results corroborate a previous

study that found STAT1 is important for limiting intrinsic $CD8^+$ T cells proliferation (Gil et al., 2012). Moreover, extrinsic signals can promote $CD8^+$ T cell responses, deficiencies in type I IFN-STAT1 signalling in DCs leads to efficient presentation and effective ($IFN\gamma^+$) $CD8^+$ T cell responses (Nice et al., 2016). Furthermore, I observed increased $IFN\gamma^+$ frequencies of CR6-specific $CD8^+$ T cells from infected *Stat1*$^{KO}$ mice, relative to littermate *Stat1*$^{het}$ mice, which could be due to increased STAT4 signalling (required for the production of IFNγ by $CD8^+$ T cells), when STAT1 is absent and/or increased extrinsic DC co-stimulatory signals when STAT1 is absent (Gil et al., 2012; Lawless et al., 2000; Nice et al., 2016). Despite the increase in functional CR6-specific $CD8^+$ T cells, *Stat1*$^{KO}$ mice failed to control viral burdens. There were also increased $CD4^-CD8^-$ cells that produced IFNγ. Although these cells were not specifically identified, other studies have shown that STAT1 negatively regulates IFNγ production in NK cells; thus, it is possible that the increased $IFN\gamma^+$ $CD4^-CD8^-$ cells are NK cells (Mack et al., 2011). These data suggest that increased functional cytotoxic cells are insufficient to resist CR6 infection. Finally, it was recently demonstrated that *Rag1*$^{-/-}$ mice showed higher CR6 titers in the colons of infected mice than WT mice, indicating that adaptive immune responses can partially suppress IEC CR6 infection, but cannot eliminate persistence (Lee et al., 2017). Taken together, this data suggests that increased functional CR6-specific $CD8^+$ T cells may help limit viral burdens to an extent, but cannot fully control the infection.

To our knowledge, this is the first study to investigate the $CD4^+$ T cell response to CR6 infection in both STAT1-sufficient and deficient hosts. We observed a small CR6-induced T-$bet^+$ Th1 response in the spleen and lymph nodes of immunosufficient hosts. CR6-specific $CD4^+$ T cells are difficult to analyze from the intestinal tract due to technically challenging protocols that involve magnetically enriching live MHC II $Tet^+$ $CD4^+$ T cells. However, because of the

localized nature of the $CD8^+$ T cell response in STAT1-sufficient mice, a better understanding of the T helper response in colonic tissues would help characterize the concerted immune response against CR6. Without STAT1 signalling, CR6-specific $CD4^+$ T cells lost Th1-skewing potential and expressed the Th17 transcription factor, RORγt, and generally stimulated (PMA/ionomycin) $CD4^+$ T cells produced IL-17A.

Upon $CD4^+$ T cell activation, Th1 differentiation is induced by STAT1 and STAT4; however STAT1 is preferentially recruited to the immunological synapse, which induces the expression of T-bet (Maldonado et al., 2009). STAT1 deficiency may allow other STAT molecules to enter the immunological synapse and direct Th differentiation to another subtype. This may explain increases in Th2 and Th17 serum cytokine levels in CR6-infected *Stat1*$^{KO}$ mice. Moreover, this could explain why *Stat1*$^{KO}$ CR6-specific $CD4^+$ T cells differentiate to RORγt$^+$ Th17 cells, whereas *Stat1*$^{het}$ CR6-specific $CD4^+$ T cells differentiate to T-bet$^+$ Th1 cells. Interestingly, the serum of CR6-infected *Stat1*$^{KO}$ mice shared a similar cytokine profile with *in vitro* stimulated *Stat1*$^{KO}$ $CD4^+$ T cells, even when those cells received Th1-skewing factors. This information provides evidence that without STAT1 signalling, $CD4^+$ T cells activated under Th1 skewing conditions differentiate to other subtypes. Since $CD4^+$ T cells help coordinate many facets of the immune response, this could have downstream consequences on the CR6-specific immune response. Future investigations into B cell responses in STAT1-sufficient and deficient mice with depleted $CD4^+$ T cells could determine if appropriately differentiated (Th1) CR6-specific $CD4^+$ T cells are important for generating an appropriate and effective CR6-specific B cell antibody response, shown to be important for controlling MNV infections (Chachu et al., 2008b).

IL-17A is typically not observed in high concentrations in peripheral tissues and can cause collateral immune-mediated damage. Thus, we explored if neutralizing IL-17A could alter the outcome of CR6-infected *Stat1*$^{KO}$ mice. However, we were unable to confirm IL-17A neutralization by differences in neutrophil levels or IL-22 mRNA levels. However, we did show a trend toward decreased serum IL-17A and IL-22 concentrations after IL-17A neutralization (Appendix E a, b) Since none of the above observations showed absolute differences after IL-17A neutralization we remain unable to definitively conclude whether IL-17A influences clinical disease. However, because depletion of CD4$^{+}$ T cells, a major source of IL-17A, did not rescue *Stat1*$^{KO}$ mice from CR6-induced disease and because antiviral treatment controls virus and rescues from CR6-induced disease these data suggest that IL-17A is not promoting disease. My experiments did not measure the function of innate lymphoid cells, which can produce IL-17A; thus, they remain another possible source of IL-17A.

CD4$^{+}$ Treg responses are important for resolving acute inflammation and promoting memory formation (Laidlaw et al., 2015). Treg cell ratios, IL-10 production, and frequencies were not significantly different in either *Stat1*$^{het}$ or *Stat1*$^{KO}$ mice post CR6-infection, indicating that Treg responses are normal in these mice.

CR6 infects the colon, an organ in which lymphocytes are in close proximity with a large number of microbes. During CR6 infections, there is a significant increases in infiltrating IFN$\gamma^{+}$ CD8$^{+}$ IELs, particularly in *Stat1*$^{KO}$ mice; these cells have been shown to impair mucosal barrier integrity (Watson et al., 2005; Zufferey et al., 2009). Moreover, in CR6-infected *Stat1*$^{KO}$ mice, I detected elevated levels of cytokines that are often involved in responses to mucosal fungal, bacterial, and parasitic infections. Thus, I hypothesized that without STAT1 signalling, CR6 may be causing intestinal barrier damage, which could prompt a secondary pathogen infection.

However, we observed no signs of histopathology or overt intestinal inflammation during CR6 infection, in either *Stat1*$^{het}$ or *Stat1*$^{KO}$ mice. We were also unable to detect signs of GI leakiness or a defect in barrier strength; however, there are potentially more sensitive assays that could be employed to determine more concretely if the barrier is functioning. I detected no differences in the expression of tight junction proteins, but I did not analyze localization of these proteins to appropriate areas during infection, which is a better indicator of whether there is a functional difference in tight junction proteins between genotypes or after infection. The data suggest that *Stat1*$^{KO}$ mice have an opportunity to promote stronger mucosal barriers due to increased Th17 cytokines, IL-17A and IL-22, which can act on colon epithelial cells by signalling through STAT3 to help protect the intestinal epithelium in the T cell-transfer colitis model (Zenewicz et al., 2008). In these experiments, overexpression of IL-22 can lead to increased MUC1, MUC3, and MUC13. Although I did not measure these mucins, this suite of mucins can enhance the mucus barrier (Sugimoto et al., 2008), and if promoted, the thick mucus layer could provide CR6-infected *Stat1*$^{KO}$ mice protection against commensal microbial translocation across the mucosal barrier.

Lastly, to determine if the microbiota could be contributing to the clinical signs of CR6-infected *Stat1*$^{KO}$ mice, I analyzed GI permeability and treated the mice with an antibiotic cocktail. Despite clear depletion of bacterial biomass in the feces of antibiotic-treated mice, I did not investigate the impact of the antibiotic cocktail on other members of the intestinal multibiome (ie fungi, protists). GF *Stat1*$^{KO}$ mice would be required to investigate the precise role other constituents of the intestinal microbiome play in the outcome of CR6 infections. These mice were unavailable at UBC at the time of these studies; however, I believe the data accrued from my project suggest that the microbiota contribute little to CR6-induced disease in *Stat1*$^{KO}$

mice. I hypothesize that CR6-infected GF *Stat1*$^{KO}$ mice would likely show relatively similar immunological features observed in conventionally raised *Stat1*$^{KO}$ mice.

## 4.2 Summary

In summary, STAT1 relays signals from an asymptomatic and persistent enteric virus, CR6, protects from CR6-induced disease, and coordinates CR6-specific immune responses. Moreover, STAT1 is critical to resisting viral burden, which can lead to death in infected mice. CR6 persists by inhibiting Type III IFNλ-STAT1 signalling in IECs, but likely does not target type I or II IFN pathways (Lee et al., 2017). Thus, immunosufficient hosts can restrict viral dissemination by establishing an antiviral state in APCs and avoid CR6-mediated disease observed when STAT1 signalling is absent. We characterized the chronic and acute outcomes of CR6 infection in STAT1-deficient mice (Nice et al., 2015). The majority of STAT1-deficient mice displayed clinical signs, histopathology, virus-induced weight loss, and immune dysregulation. Despite previous studies that looked at the role of STAT1 in individual circumstances (pathogen control, $CD4^+$ T cell differentiation, and $CD8^+$ T cell function) no study, to my knowledge, has systematically tested the relative contribution of these host-protective pathways to an enteric virus infection. Here, I tested the hypothesis that STAT1 acts to control CR6 infections and regulate the immune response to a persistent enteric eukaryotic virus, which establishes itself much like a commensal virus in immunosufficient hosts. My specific aims were to (1) evaluate CR6 infections and (2) characterize CR6-specific immune responses in *Stat1*$^{KO}$ and *Stat1*$^{het}$ mice. In the absence of STAT1, the ability of the host to restrict viral burdens is compromised and the virus replicates uncontrollably and disseminates systemically. I found that $CD8^+$ T cell responses were heightened in *Stat1*$^{KO}$ hosts and may contribute to

limiting CR6 burdens, but increased $CD8^+$ T cell activity was not sufficient to protect the host. Moreover, without STAT1 signalling the CR6-specific $CD4^+$ T cell response was skewed from antiviral Th1 to the Th17 subset. Thus, we hypothesized that immunopathology could be contributing to disease in these mice. However, when virus replication was controlled with antiviral treatments, $Stat1^{KO}$ mice exhibited no weight loss or clinical signs, yet continued to exhibit features of dysregulated $CD8^+$ and $CD4^+$ T cell profiles. These experiments suggest STAT1 plays a crucial role in coordinating antiviral immune responses, but that these adaptive immune responses are not sufficient to clear CR6 infection and do not contribute to the observed pathology. Therefore, STAT1-mediated control of virus replication is critical and without STAT1 signalling the virus can replicate to high titers and disseminate systemically, which can lead to tissue pathology. My data suggest that $Stat1^{KO}$ mice with high antiviral $CD8^+$ T cell numbers were able to control virus replication, for at least 8 days, and exhibited less weight loss than mice with lower antiviral $CD8^+$ T cell numbers. There is always the possibility that other immune cell types or factors that were not measured in my experiments might contribute to disease. The mechanism of CR6 systemic spread in STAT1-deficient hosts is still unknown, but I hypothesize that migratory DCs, unable to establish an antiviral state, have lost the ability to traffic live virus to lymph nodes and spleen. STAT1-dependent intestinal restriction of CR6 would be an interesting avenue to investigate as a future direction.

My thesis project sought to investigate how STAT1 signalling can influence CR6-induced disease and regulate CR6-specific immune responses. While I was able to describe and characterize T cell responses, many unanswered questions remain regarding innate immune responses. I was able to contribute novel findings and a new perspective to describe how CR6 persists asymptomatically in the host. This perspective provides a new framework that could help

shape future investigations in the field of host-virome interactions.

### 4.3 Research applications and future directions

My thesis project provides insight into the molecular mechanisms that are necessary for establishing immune homeostasis and dialog between host and virome. Research investigating the intestinal eukaryotic virome is exciting with many questions and hypotheses remaining unexplored. I have found that CR6 infections promote a subtle T cell response, mostly confined to the intestinal epithelium, but genetic mutations within the host can alter these responses and amplify the T cell response to CR6 infections. Animal models have shown that the intestinal virome contributes to the development and outcome of chronic immune conditions, depending on the host's genetic makeup (Cadwell et al., 2010; Hickman et al., 2014). A dysregulated T cell response to huNoV could theoretically lead to unnecessary acute or chronic inflammation.

Fludarabine—a STAT1 inhibitor—is an important chemotherapy treatment that can emulate genetic STAT1-deficiencies in humans. Fludarabine packaging warns patients that the drug causes immune system suppression, with a significant risk of adverse viral-infections. Fludarabine can cause gastrointestinal complications during treatment and severe virus infections (Elter et al., 2011). It is possible that Fludarabine may disrupt the ability of the gastrointestinal immune network to resist and restrict the eukaryotic virome, leading to clinical symptoms in these patients. Uncovering mechanisms of host-virome interactions, as I have explored in my thesis, can lead to designing more specific drug delivery systems for STAT1 inhibitor drugs or could suggest the use of a prophylactic antiviral treatment to prevent these inadvertent consequences of severe virus infections by this important chemotherapy agent.

My thesis project provides no evidence that an antiviral compound should be used against persistent huNoV infections, which can act as a reservoir for outbreaks. 2CMC inhibits huNoV

replication (Thorne et al., 2016), but was removed from the market as a Hepatitis C virus inhibitor due to adverse reactions in humans (Pierra et al., 2006). Moreover, depleting the murine virome with broad-spectrum antiviral treatment exacerbated DSS-induced colitis in wild type mice, indicating that a virome-host signaling pathway may provide tonic anti-inflammatory signals to the host (Yang et al., 2016). While broad-spectrum antivirals are not commonly used, it is worth noting that disrupting the commensal enteric virome could influence multibiome composition and/or alter immune homeostasis and influence inflammatory diseases. Clinical trials that treat huNoV with exogenous IFNλ would be an interesting next step, although it is possible that huNoV and CR6 have evolved distinct mechanisms of persistence. However, huNoV persistence is a likely source of new outbreaks and therapeutics to target persistent huNoV specifically could prevent many thousands of future infections and save lives (Gustavsson et al., 2017)

Discovering host-virome signalling pathways and interactions can inform future strategies for treating or preventing chronic inflammatory diseases. For example, the virome can trigger IBD in mice and there are reports of increased prevalence of IBS after community huNoV breakouts (Cadwell et al., 2010; Zanini et al., 2012). If more research in humans repeat these findings it could provoke the development of a vaccine or therapeutic against that member of the virome. Moreover, fecal matter transplants are being explored for the potential to treat various diseases and infections, but individual-variability in the virome and its influence on one's health has not been thoroughly considered. We may or may not deem the benefits of the procedure outweigh the costs of potential virome-host interactions, but more knowledge could aid in making informed decisions on this topic.

In conclusion, an asymptomatic and persistent enteric virus is restricted from causing disease by the host immune system in a STAT1-dependent manner.

**References**

Abt, M.C., Osborne, L.C., Monticelli, L.A., Doering, T.A., Alenghat, T., Sonnenberg, G.F., Paley, M.A., Antenus, M., Williams, K.L., Erikson, J., et al. (2012). Commensal Bacteria Calibrate the Activation Threshold of Innate Antiviral Immunity. Immunity *37*, 158–170.

Baldridge, M.T., Nice, T.J., McCune, B.T., Yokoyama, C.C., Kambal, A., Wheadon, M., Diamond, M.S., Ivanova, Y., Artyomov, M., and Virgin, H.W. (2015). Commensal microbes and interferon- determine persistence of enteric murine norovirus infection. Science. *347*, 266–269.

Baldridge, M.T., Lee, S., Brown, J.J., McAllister, N., Urbanek, K., Dermody, T.S., Nice, T.J., and Virgin, H.W. (2017). Expression of Ifnlr1 on intestinal epithelial cells is critical to the antiviral effects of IFN-lambda against norovirus and reovirus. J. Virol. *91*, JVI.02079-16.

Bartsch, S.M., Lopman, B.A., Ozawa, S., Hall, A.J., and Lee, B.Y. (2016). Global economic burden of norovirus gastroenteritis. PLoS One *11,* e0151219.

Basic, M., Keubler, L.M., Buettner, M., Achard, M., Breves, G., Schröder, B., Smoczek, A., Jörns, A., Wedekind, D., Zschemisch, N.H., et al. (2014). Norovirus Triggered Microbiota-driven Mucosal Inflammation in Interleukin 10-deficient Mice. Inflamm. Bowel Dis. *20*, 431–443.

Belkaid, Y., and Hand, T.W. (2014). Role of the microbiota in immunity and inflammation. Cell *157*, 121–141.

Bok, K., and Green, K. (2012). Norovirus gastroenteritis in immunocompromised patients. N. Engl. J. Med. *119*, 1831–1837.

Bouziat, R., Hinterleitner, R., Brown, J.J., Stencel-Baerenwald, J.E., Ikizler, M., Mayassi, T., Meisel, M., Kim, S.M., Discepolo, V., Pruijssers, A.J., et al. (2017). Reovirus infection triggers inflammatory responses to dietary antigens and development of celiac disease. Science. *356*, 44–

50.

Brestoff, J.R., and Artis, D. (2013). Commensal bacteria at the interface of host metabolism and the immune system. Nat. Immunol. *14*, 676–684.

Brown, a M. (2001). A step-by-step guide to non-linear regression analysis of experimental data using a Microsoft Excel spreadsheet. Comput. Methods Programs Biomed. *65*, 191–200.

Brown, E.M., Wlodarska, M., Willing, B.P., Vonaesch, P., Han, J., Reynolds, L.A., Arrieta, M.-C., Uhrig, M., Scholz, R., Partida, O., et al. (2015). Diet and specific microbial exposure trigger features of environmental enteropathy in a novel murine model. Nat. Commun. *6*, 7806.

Cadwell, K., Patel, K.K., Maloney, N.S., Liu, T.C., Ng, A.C.Y., Storer, C.E., Head, R.D., Xavier, R., Stappenbeck, T.S., and Virgin, H.W. (2010). Virus-Plus-Susceptibility Gene Interaction Determines Crohn's Disease Gene Atg16L1 Phenotypes in Intestine. Cell *141*, 1135–1145.

Carter, P.B., and Collins, F.M. (1974). The route of enteric infection in normal mice. J. Exp. Med. *139*, 1189–1203.

Chachu, K.A., LoBue, A.D., Strong, D.W., Baric, R.S., and Virgin, H.W. (2008a). Immune mechanisms responsible for vaccination against and clearance of mucosal and lymphatic norovirus infection. PLoS Pathog. *4*, e1000236.

Chachu, K.A., Strong, D.W., LoBue, A.D., Wobus, C.E., Baric, R.S., and Virgin, H.W. (2008b). Antibody Is Critical for the Clearance of Murine Norovirus Infection. J. Virol. *82*, 6610–6617.

Crowe, C.R., Chen, K., Pociask, D.A., Alcorn, J.F., Krivich, C., Enelow, R.I., Ross, T.M., Witztum, J.L., and Kolls, J.K. (2009). Critical Role of IL-17RA in Immunopathology of Influenza Infection. J. Immunol. *183*, 5301–5310.

Denning, T.L., Norris, B.A., Medina-Contreras, O., Manicassamy, S., Geem, D., Madan, R.,

Karp, C.L., and Pulendran, B. (2011). Functional Specializations of Intestinal Dendritic Cell and Macrophage Subsets That Control Th17 and Regulatory T Cell Responses Are Dependent on the T Cell/APC Ratio, Source of Mouse Strain, and Regional Localization. J. Immunol. *187*, 733–747.

Elftman, M.D., Gonzalez-Hernandez, M.B., Kamada, N., Perkins, C., Henderson, K.S., Núñez, G., and Wobus, C.E. (2013). Multiple effects of dendritic cell depletion on murine norovirus infection. J. Gen. Virol. *94*, 1761–1768.

Elter, T., Gercheva-Kyuchukova, L., Pylylpenko, H., Robak, T., Jaksic, B., Rekhtman, G., Kyrcz-Krzemie??, S., Vatutin, M., Wu, J., Sirard, C., et al. (2011). Fludarabine plus alemtuzumab versus fludarabine alone in patients with previously treated chronic lymphocytic leukaemia: A randomised phase 3 trial. Lancet Oncol. *12*, 1204–1213.

Filyk, H.A., and Osborne, L.C. (2016). The Multibiome: The Intestinal Ecosystem's Influence on Immune Homeostasis, Health, and Disease. EBioMedicine *13,* 46-54.

Gil, M.P., Ploquin, M.J.Y., Watford, W.T., Lee, S.H., Kim, K., Wang, X., Kanno, Y., O'Shea, J.J., and Biron, C.A. (2012). Regulating type 1 IFN effects in CD8 T cells during viral infections: Changing STAT4 and STAT1 expression for function. Blood *120*, 3718–3728.

Gracias, D.T., Stelekati, E., Hope, J.L., Boesteanu, A.C., Doering, T.A., Norton, J., Mueller, Y.M., Fraietta, J.A., Wherry, E.J., Turner, M., et al. (2013). The microRNA miR-155 controls CD8(+) T cell responses by regulating interferon signaling. Nat. Immunol. *14*, 593–602.

Gunzel, D., and Yu, A.S.L. (2013). Claudins and the Modulation of Tight Junction Permeability. Physiol. Rev. *93*, 525–569.

Gustavsson, L., Nordén, R., Westin, J., Lindh, M., and Andersson, L.M. (2017). Slow clearance of norovirus following infection with emerging variants of genotype GII.4 strains. J. Clin.

Microbiol. *55*, 1533–1539.

Handley, S.A., Thackray, L.B., Zhao, G., Presti, R., Miller, A.D., Droit, L., Abbink, P., Maxfield, L.F., Kambal, A., Duan, E., et al. (2012). Pathogenic simian immunodeficiency virus infection is associated with expansion of the enteric virome. Cell *151*, 253–266.

Hickman, D., Jones, M.K., Zhu, S., Kirkpatrick, E., Ostrov, D.A., Wang, X., Ukhanova, M., Sun, Y., Mai, V., Salemi, M., et al. (2014). The effect of malnutrition on norovirus infection. MBio *5*, e01032-13.

Hill, D.A., Hoffmann, C., Abt, M.C., Du, Y., Kobuley, D., Kirn, T.J., Bushman, F.D., and Artis, D. (2010). Metagenomic analyses reveal antibiotic-induced temporal and spatial changes in intestinal microbiota with associated alterations in immune cell homeostasis. Mucosal Immunol. *3*, 148–158.

Hirota, K., Turner, J.-E., Villa, M., Duarte, J.H., Demengeot, J., Steinmetz, O.M., and Stockinger, B. (2013). Plasticity of TH17 cells in Peyer's patches is responsible for the induction of T cell–dependent IgA responses. Nat. Immunol. *14*, 372–379.

Hofer, M.J., Li, W., Manders, P., Terry, R., Lim, S.L., King, N.J.C., and Campbell, I.L. (2012). Mice Deficient in STAT1 but Not STAT2 or IRF9 Develop a Lethal CD4+ T-Cell-Mediated Disease following Infection with Lymphocytic Choriomeningitis Virus. J. Virol. *86*, 6932–6946.

Hooper, L. V., Littman, D.R., and Macpherson, A.J. (2012). Interactions Between the Microbiota and the Immune System. Science. *336*, 1268–1273.

Hsu, C.C., Wobus, C.E., Steffen, E.K., Riley, L.K., and Livingston, R.S. (2005). Development of a microsphere-based serologic multiplexed fluorescent immunoassay and a reverse transcriptase PCR assay to detect murine norovirus 1 infection in mice. Clin. Diagn. Lab. Immunol. *12*, 1145–1151.

Ivashkiv, L.B., and Donlin, L.T. (2014). Regulation of type I interferon responses. Nat. Rev. Immunol. *14*, 36–49.

Jabri, B., and Ebert, E. (2007). Human CD8+ intraepithelial lymphocytes: A unique model to study the regulation of effector cytotoxic T lymphocytes in tissue. Immunol. Rev. *215*, 202–214.

Kahan, S.M., Liu, G., Reinhard, M.K., Hsu, C.C., Livingston, R.S., and Karst, S.M. (2011). Comparative murine norovirus studies reveal a lack of correlation between intestinal virus titers and enteric pathology. Virology *421*, 202–210.

Karst, S.M., Wobus, C.E., Lay, M., Davidson, J., and Herbert W. Virgin IV (2003). STAT1-Dependent Innate Immunity to a Norwalk-Like. Science. *299*, 1575–1578.

Karst, S.M., Wobus, C.E., Goodfellow, I.G., Green, K.Y., and Virgin, H.W. (2014). Advances in norovirus biology. Cell Host Microbe *15*, 668–680.

Kawashima, T., Kosaka, A., Yan, H., Guo, Z., Uchiyama, R., Fukui, R., Kaneko, D., Kumagai, Y., You, D.J., Carreras, J., et al. (2013). Double-Stranded RNA of Intestinal Commensal but Not Pathogenic Bacteria Triggers Production of Protective Interferon-β. Immunity *38*, 1187–1197.

Kernbauer, E., Ding, Y., and Cadwell, K. (2014). An enteric virus can replace the beneficial function of commensal bacteria. Nature *516*, 94–98.

Kolawole, A.O., Gonzalez-Hernandez, M.B., Turula, H., Yu, C., Elftman, M.D., and Wobus, C.E. (2016). Oral Norovirus Infection Is Blocked in Mice Lacking Peyer's Patches and Mature M Cells. *90*, 1499-1506.

Kolls, J.K., McCray, P.B., and Chan, Y.R. (2008). Cytokine-mediated regulation of antimicrobial proteins. Nat. Rev. Immunol. *8*, 829–835.

Kopf, M., Gros, G. Le, Bachmann, M., Lamers, M.C., Bluethmann, H., and Köhler, G. (1993). Disruption of the murine IL-4 gene blocks Th2 cytokine responses. Nature *362*, 245–248.

Laidlaw, B.J., Cui, W., Amezquita, R.A., Gray, S.M., Guan, T., Lu, Y., Kobayashi, Y., Flavell, R.A., Kleinstein, S.H., Craft, J., et al. (2015). Production of IL-10 by CD4+ regulatory T cells during the resolution of infection promotes the maturation of memory CD8+ T cells. Nat. Immunol. *16*, 871–879.

Lawless, V.A., Zhang, S., Ozes, O.N., Bruns, H.A., Oldham, I., Hoey, T., Grusby, M.J., and Kaplan, M.H. (2000). Stat4 regulates multiple components of IFN-γ-inducing signaling pathways. J. Immunol. *165*, 6803–6808.

Lee, S., and Baldridge, M.T. (2017). Interferon-Lambda: A Potent Regulator of Intestinal Viral Infections. Front. Immunol. *8*, 749.

Lee, J.S., Tato, C.M., Joyce-Shaikh, B., Gulan, F., Cayatte, C., Chen, Y., Blumenschein, W.M., Judo, M., Ayanoglu, G., McClanahan, T.K., et al. (2015). Interleukin-23-Independent IL-17 Production Regulates Intestinal Epithelial Permeability. Immunity *43*, 727–738.

Lee, S., Wilen, C.B., Orvedahl, A., McCune, B.T., Kim, K., Orchard, R.C., Peterson, S.T., Nice, T.J., Baldridge, M.T., and Virgin, H.W. (2017). Norovirus Cell Tropism Is Determined by Combinatorial Action of a Viral Non-structural Protein and Host Cytokine. Cell Host Microbe *22*, 449–459.

Levy, D.E., and Darnell Jr., J.E. (2002). Stats: transcriptional control and biological impact. Nat Rev Mol Cell Biol *3*, 651–662.

Mack, E., Kallal, L., Demers, D., and Biron, C. (2011). Type 1 interferon induction of natural killer cell gamma interferon production for defense during lymphocytic choriomeningitis virus infection. MBio *2*, e00169-11.

Maldonado, R.A., Soriano, M.A., Perdomo, L.C., Sigrist, K., Irvine, D.J., Decker, T., and Glimcher, L.H. (2009). Control of T helper cell differentiation through cytokine receptor

inclusion in the immunological synapse. J. Exp. Med. *206*, 877–892.

Maloney, N.S., Thackray, L.B., Goel, G., Hwang, S., Duan, E., Vachharajani, P., Xavier, R., and Virgin, H.W. (2012). Essential Cell-Autonomous Role for Interferon (IFN) Regulatory Factor 1 in IFN-γ-Mediated Inhibition of Norovirus Replication in Macrophages. J. Virol. *86*, 12655–12664.

McCartney, S.A., Thackray, L.B., Gitlin, L., Gilfillan, S., Virgin IV, H.W., and Colonna, M. (2008). MDA-5 recognition of a murine norovirus. PLoS Pathog. *4*, e1000108.

Monaco, C.L., Gootenberg, D.B., Zhao, G., Handley, S.A., Ghebremichael, M.S., Lim, E.S., Lankowski, A., Baldridge, M.T., Wilen, C.B., Flagg, M., et al. (2016). Altered Virome and Bacterial Microbiome in Human Immunodeficiency Virus-Associated Acquired Immunodeficiency Syndrome. Cell Host Microbe *19*, 311–322.

Moon, J.J., Chu, H.H., Pepper, M., McSorley, S.J., Jameson, S.C., Kedl, R.M., and Jenkins, M.K. (2007). Naive CD4+ T Cell Frequency Varies for Different Epitopes and Predicts Repertoire Diversity and Response Magnitude. Immunity *27*, 203–213.

Mowat, A.M., and Agace, W.W. (2014). Regional specialization within the intestinal immune system. Nat. Rev. Immunol. *14*, 667–685.

Mumphrey, S.M., Changotra, H., Moore, T.N., Heimann-Nichols, E.R., Wobus, C.E., Reilly, M.J., Moghadamfalahi, M., Shukla, D., and Karst, S.M. (2007). Murine Norovirus 1 Infection Is Associated with Histopathological Changes in Immunocompetent Hosts, but Clinical Disease Is Prevented by STAT1-Dependent Interferon Responses. J. Virol. *81*, 3251–3263.

Murphy, K.M., and Reiner, S.L. (2002). The lineage decisions of helper T cells. Nat. Rev. Immunol. *2*, 933–944.

Nelson, A.M., Elftman, M.D., Pinto, A.K., Baldridge, M., Hooper, P., Kuczynski, J., Petrosino,

J.F., Young, V.B., and Wobus, C.E. (2013). Murine norovirus infection does not cause major disruptions in the murine intestinal microbiota. Microbiome *1*, 1-11.

Nice, T.J., Baldridge, M.T., McCune, B.T., Norman, J.M., Lazear, H.M., Artyomov, M., Diamond, M.S., and Virgin, H.W. (2015). Interferon-λ cures persistent murine norovirus infection in the absence of adaptive immunity. Science *347*, 269–273.

Nice, T.J., Osborne, L.C., Tomov, V.T., Artis, D., Wherry, E.J., and Virgin, H.W. (2016). Type I Interferon Receptor Deficiency in Dendritic Cells Facilitates Systemic Murine Norovirus Persistence Despite Enhanced Adaptive Immunity. PLoS Pathog. *12*, e1005684.

Orchard, R.C., Wilen, C.B., Doench, J.G., Baldridge, M.T., McCune, B.T., Lee, Y.-C.J., Lee, S., Pruett-Miller, S.M., Nelson, C.A., Fremont, D.H., et al. (2016). Discovery of a proteinaceous cellular receptor for a norovirus. Science. *353*, 933–936.

Osborne, L.C., Monticelli, L.A., Nice, T.J., Sutherland, T.E., Siracusa, M.C., Hepworth, M.R., Tomov, V.T., Kobuley, D., Tran, S. V., Bittinger, K., et al. (2014). Virus-helminth coinfection reveals a microbiota-independent mechanism of immunomodulation. Science. *345*, 578–582.

Owen, R.L., Piazza, A.J., and Ermak, T.H. (1991). Ultrastructural and cytoarchitectural features of lymphoreticular organs in the colon and rectum of adult BALB/c mice. Am. J. Anat. *190*, 10–18.

Pensabene, L., Talarico, V., Concolino, D., Ciliberto, D., Campanozzi, A., Gentile, T., Rutigliano, V., Salvatore, S., Staiano, A., Di Lorenzo, C., et al. (2015). Postinfectious Functional Gastrointestinal Disorders in Children: A Multicenter Prospective Study. J. Pediatr. *166*, 903–907.e1.

Pierra, C., Amador, A., Benzaria, S., Cretton-Scott, E., D'Amours, M., Mao, J., Mathieu, S., Moussa, A., Bridges, E.G., Standring, D.N., et al. (2006). Synthesis and pharmacokinetics of

valopicitabine (NM283), an efficient prodrug of the potent anti-HCV agent 2′-C-methylcytidine. J. Med. Chem. *49*, 6614–6620.

Quigley, M., Huang, X., and Yang, Y. (2008). STAT1 signaling in CD8 T cells is required for their clonal expansion and memory formation following viral infection in vivo. J. Immunol. *180*, 2158–2164.

Ramana, C. V, DeBerge, M.P., Kumar, A., Alia, C.S., Durbin, J.E., and Enelow, R.I. (2015). Inflammatory impact of IFN-gamma in CD8+ T cell-mediated lung injury is mediated by both Stat1-dependent and -independent pathways. Am. J. Physiol. Lung Cell. Mol. Physiol. *308*, L650-7.

Reese, T.A., Wakeman, B.S., Choi, H.S., Hufford, M.M., Huang, S.C., Zhang, X., Buck, M.D., Jezewski, A., Kambal, A., Liu, C.Y., et al. (2014). Helminth infection reactivates latent -herpesvirus via cytokine competition at a viral promoter. Science. *345*, 573–577.

Richardson, S.J., and Horwitz, M.S. (2014). Is type 1 diabetes "going viral"? Diabetes *63*, 2203–2205.

Rocha-Pereira, J., Jochmans, D., Debing, Y., Verbeken, E., Nascimento, M.S.J., and Neyts, J. (2013). The Viral Polymerase Inhibitor 2'-C-Methylcytidine Inhibits Norwalk Virus Replication and Protects against Norovirus-Induced Diarrhea and Mortality in a Mouse Model. J. Virol. *87*, 11798–11805.

Rocha-Pereira, J., Van Dycke, J., and Neyts, J. (2016). Treatment with a nucleoside polymerase inhibitor reduces shedding of murine norovirus in stool to undetectable levels without emergence of drug-resistant variants. Antimicrob. Agents Chemother. *60*, 1907–1911.

Schneider, D.S., and Ayres, J.S. (2008). Two ways to survive infection: what resistance and tolerance can teach us about treating infectious diseases. Nat. Rev. Immunol. *8*, 889–895.

Schroder, K., Hertzog, P.J., Ravasi, T., and Hume, D.A. (2004). Interferon- y : an overview of signals , mechanisms and functions. J. Leukoc. Biol. *75*, 163–189.

Sheridan, B.S., and Lefrançois, L. (2010). Intraepithelial lymphocytes: To serve and protect. Curr. Gastroenterol. Rep. *12*, 513–521.

Shortland, A., Chettle, J., Archer, J., Wood, K., Bailey, D., Goodfellow, I., Blacklaws, B.A., and Heeney, J.L. (2014). Pathology caused by persistent murine norovirus infection. J. Gen. Virol. *95*, 413–422.

Sim, G.C., Wu, S., Jin, L., Hwu, P., and Radvanyi, L.G. (2016). Defective STAT1 activation associated with impaired IFN-γ production in NK and T lymphocytes from metastatic melanoma patients treated with IL-2. Oncotarget. *7*, 36074–36091.

Stappenbeck, T.S., and Virgin, H.W. (2016). Accounting for reciprocal host–microbiome interactions in experimental science. Nature *534*, 191–199.

Stappenbeck, T.S., Hooper, L. V, and Gordon, J.I. (2002). Developmental regulation of intestinal angiogenesis by indigenous microbes via Paneth cells. Proc. Natl. Acad. Sci. U. S. A. *99*, 15451–15455.

Stockinger, B., and Omenetti, S. (2017). The dichotomous nature of T helper 17 cells. Nat. Rev. Immunol. *17*, 534-544.

Sugimoto, K., Ogawa, A., Mizoguchi, E., Shimomura, Y., Andoh, A., Bhan, A.K., Blumberg, R.S., Xavier, R.J., and Mizoguchi, A. (2008). IL-22 ameliorates intestinal inflammation in a mouse model of ulcerative colitis. J. Clin. Invest. *118*, 534–544.

Swain, S.L., Weinberg, a D., English, M., and Huston, G. (1990). IL-4 directs the development of Th2-like helper effectors. J. Immunol. *145*, 3796–3806.

Thorne, L., Arias, A., and Goodfellow, I. (2016). Advances Toward a Norovirus Antiviral: From

Classical Inhibitors to Lethal Mutagenesis. J. Infect. Dis. *213*, S27–S31.

Tomov, V.T., Osborne, L.C., Dolfi, D. V., Sonnenberg, G.F., Monticelli, L.A., Mansfield, K., Virgin, H.W., Artis, D., and Wherry, E.J. (2013). Persistent Enteric Murine Norovirus Infection Is Associated with Functionally Suboptimal Virus-Specific CD8 T Cell Responses. J. Virol. *87*, 7015–7031.

Toubiana, J., Okada, S., Hiller, J., Oleastro, M., Gomez, M.L., Becerra, J.C.A., Ouachée-Chardin, M., Fouyssac, F., Girisha, K.M., Etzioni, A., et al. (2016). Heterozygous STAT1 gain-of-function mutations underlie an unexpectedly broad clinical phenotype. Blood *127*, 3154–3164.

Vaishnava, S., Yamamoto, M., Severson, K.M., Ruhn, K.A., Yu, X., Koren, O., Ley, R., Wakeland, E.K., and Hooper, L. V. (2011). The Antibacterial Lectin RegIII  Promotes the Spatial Segregation of Microbiota and Host in the Intestine. Science. *334*, 255–258.

Wang, L., Llorente, C., Hartmann, P., Yang, A.-M., Chen, P., and Schnabl, B. (2015). Methods to determine intestinal permeability and bacterial translocation during liver disease. J. Immunol. Methods *421*, 44–53.

Watson, C.J., Hoare, C.J., Garrod, D.R., Carlson, G.L., and Warhurst, G. (2005). Interferon-gamma selectively increases epithelial permeability to large molecules by activating different populations of paracellular pores. J. Cell Sci. *118*, 5221–5230.

van Wijk, F., and Cheroutre, H. (2010). Mucosal T cells in gut homeostasis and inflammation. Expert Rev. Clin. Immunol. *6*, 559–566.

Williams, M.A., Tyznik, A.J., and Bevan, M.J. (2006). Interleukin-2 signals during priming are required for secondary expansion of CD8+ memory T cells. Nature *441*, 890–893.

Wilson, E.B., Yamada, D.H., Elsaesser, H., Herskovitz, J., Deng, J., Cheng, G., Aronow, B.J.,

Karp, C.L., and Brooks, D.G. (2013). Blockade of chronic type I interferon signaling to control persistent LCMV infection. Science *340*, 202–207.

Woodward, J.M., Gkrania-Klotsas, E., Cordero-Ng, A.Y., Aravinthan, A., Bandoh, B.N., Liu, H., Davies, S., Zhang, H., Stevenson, P., Curran, M.D., et al. (2015). The Role Of Chronic Norovirus Infection In The Enteropathy Associated With Common Variable Immunodeficiency. Am. J. Gastroenterol. *110*, 320–327.

Yang, J.Y., Kim, M.S., Kim, E., Cheon, J.H., Lee, Y.S., Kim, Y., Lee, S.H., Seo, S.U., Shin, S.H., Choi, S.S., et al. (2016). Enteric Viruses Ameliorate Gut Inflammation via Toll-like Receptor 3 and Toll-like Receptor 7-Mediated Interferon-β Production. Immunity *44*, 889–900.

Yin, Z., Dai, J., Deng, J., Sheikh, F., Natalia, M., Shih, T., Lewis-Antes, A., Amrute, S.B., Garrigues, U., Doyle, S., et al. (2012). Type III IFNs Are Produced by and Stimulate Human Plasmacytoid Dendritic Cells. J. Immunol. *189*, 2735–2745.

Zanini, B., Ricci, C., Bandera, F., Caselani, F., Magni, A., Laronga, A.M., and Lanzini, A. (2012). Incidence of post-infectious irritable bowel syndrome and functional intestinal disorders following a water-borne viral gastroenteritis outbreak. Am. J. Gastroenterol. *107*, 891–899.

Zenewicz, L.A., Yancopoulos, G.D., Valenzuela, D.M., Murphy, A.J., Stevens, S., and Flavell, R.A. (2008). Innate and adaptive interleukin-22 protects mice from inflammatory bowel disease. Immunity *29*, 947–957.

Zhao, M., Stoler, M., and Liu, A. (2000). Alveolar epithelial cell chemokine expression triggered by antigen-specific cytolytic CD8+ T cell recognition. J. Clin. Invest. *106*, 49–58.

Zhu, J., and Paul, W.E. (2008). CD4 T cells: Fates, functions, and faults. Blood *112*, 1557–1569.

Zhu, S., Regev, D., Watanabe, M., Hickman, D., Moussatche, N., Jesus, D.M., Kahan, S.M., Napthine, S., Brierley, I., Hunter, R.N., et al. (2013). Identification of Immune and Viral

Correlates of Norovirus Protective Immunity through Comparative Study of Intra-Cluster Norovirus Strains. PLoS Pathog. *9*, e1003592.

Zhu, S., Jones, M.K., Hickman, D., Han, S., Reeves, W., and Karst, S.M. (2016). Norovirus antagonism of B-cell antigen presentation results in impaired control of acute infection. Mucosal Immunol. *9*, 1559–1570.

Zufferey, C., Erhart, D., Saurer, L., and Mueller, C. (2009). Production of interferon-gamma by activated T-cell receptor-alphabeta CD8alphabeta intestinal intraepithelial lymphocytes is required and sufficient for disruption of the intestinal barrier integrity. Immunology *128*, 351–359.

# Appendices

**Appendix A  Flow cytometry gating strategy used in experiments.**
This sample is of colonic and cecal IELs from CR6-infected *Stat1*$^{KO}$ mouse.

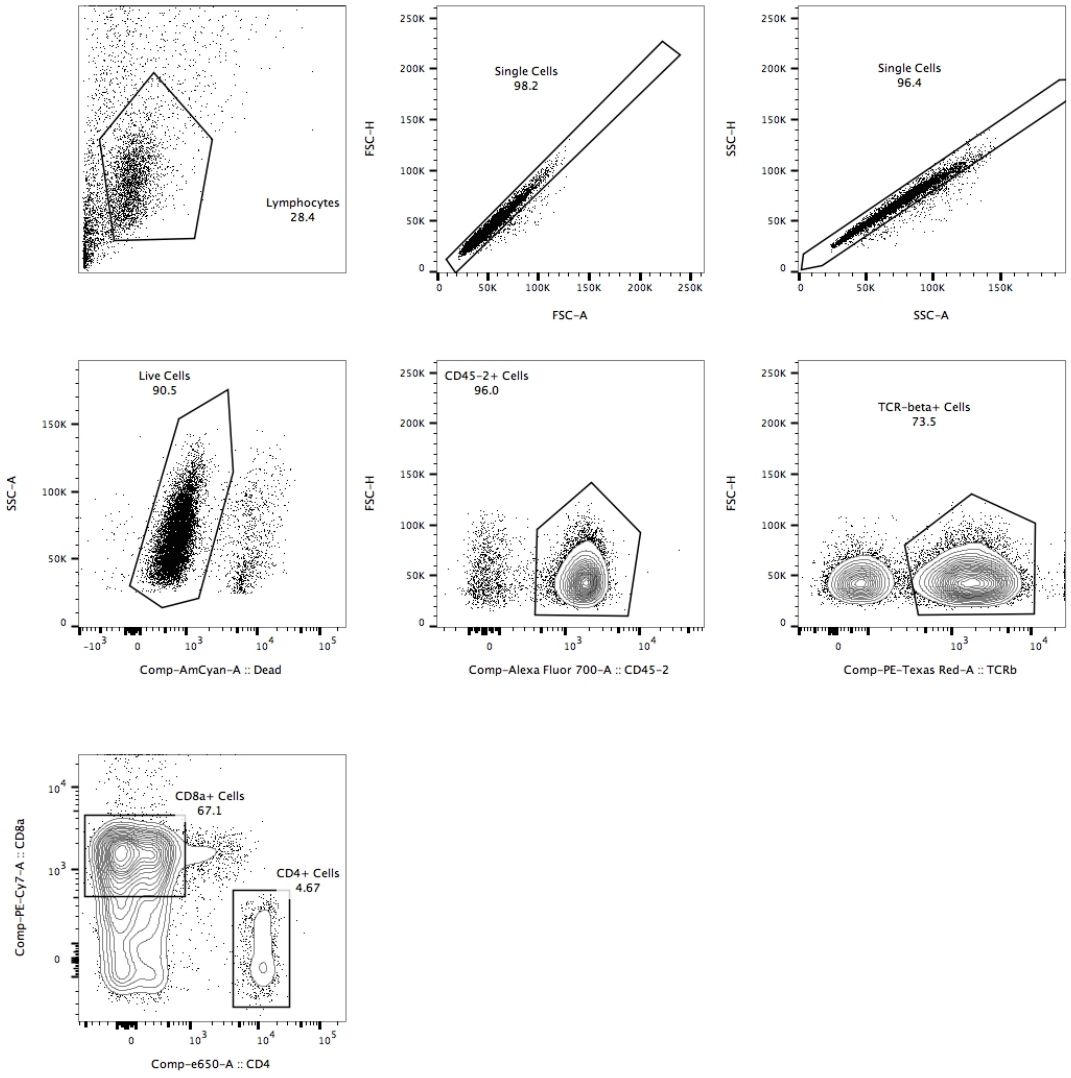

**Appendix B CD8$^+$ T cell frequencies expanded in CR6-infected *Stat1$^{KO}$* mice, but do not display a role in protection or immunopathology.**

*Stat1$^{het}$ and Stat1$^{KO}$* were given PBS or infected with $10^4$ pfu CR6 *p.o.* and analyzed on day 8 pi MNV-CR6 Kb-P1$^{519F}$ Tetramer$^+$ CD8$^+$ T cells as a frequency of CD8$^+$ in the (a) spleen and (b) LPL. (c) Survival curve of CR6-infected *Stat1$^{KO}$* mice, treated i.p. with αCD8 Ab or control Ab. Data in (a, b) are compiled data from two independent experiments. Data in (c) are from one independent experiment. Data from one mouse are represented by individual symbols, the line representing the mean. Statistical significance was determined by Mann-Whitney test (a, b).

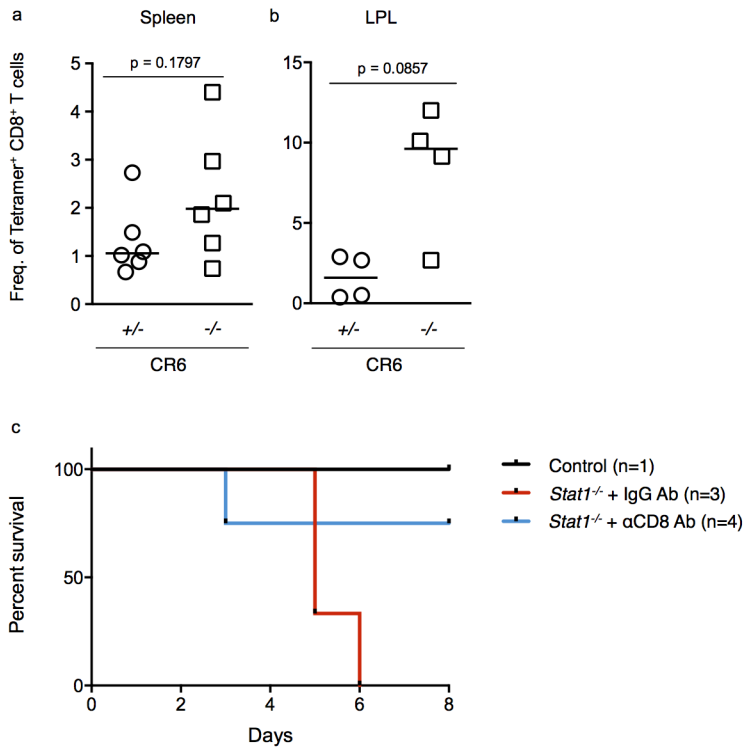

**Appendix C Antibiotic treatment does not change CR6-induced morbidity or altered immune responses observed in infected *Stat1*$^{KO}$ mice.**

*Stat1*$^{het}$ *and Stat1*$^{KO}$ mice were sham infected or infected with $10^4$ pfu CR6 *p.o.,* and given antibiotics (ABX) in drinking water over the course of infection, and analyzed on day 8 pi (a) weight change as a percentage difference from of initial (100%) (b) MNV-CR6 Kb-P1$^{519F}$ Tetramer$^+$ CD8$^+$ T cells as a frequency of CD45.2$^+$ IELs. (c) Neutrophils (B220$^-$CD11b$^+$Ly6G$^+$) in the spleen. Ratio of T-bet$^+$ TCRβ$^+$ CD4$^+$ to RORγt$^+$ TCRβ$^+$ CD4$^+$ T cells in (d) spleen (e) LPL (f) IEL. Data in (a) are n=6 treated or non-treated CR6-infected *Stat1*$^{KO}$ mice compiled from two independent experiments. Data in (b, c, d, e, f) are n=3 treated or non-treated CR6-infected *Stat1*$^{KO}$ mice and are representative of two independent experiments. Data from one mouse are represented by individual symbols. Statistical significance was determined by Mann-Whitney test.

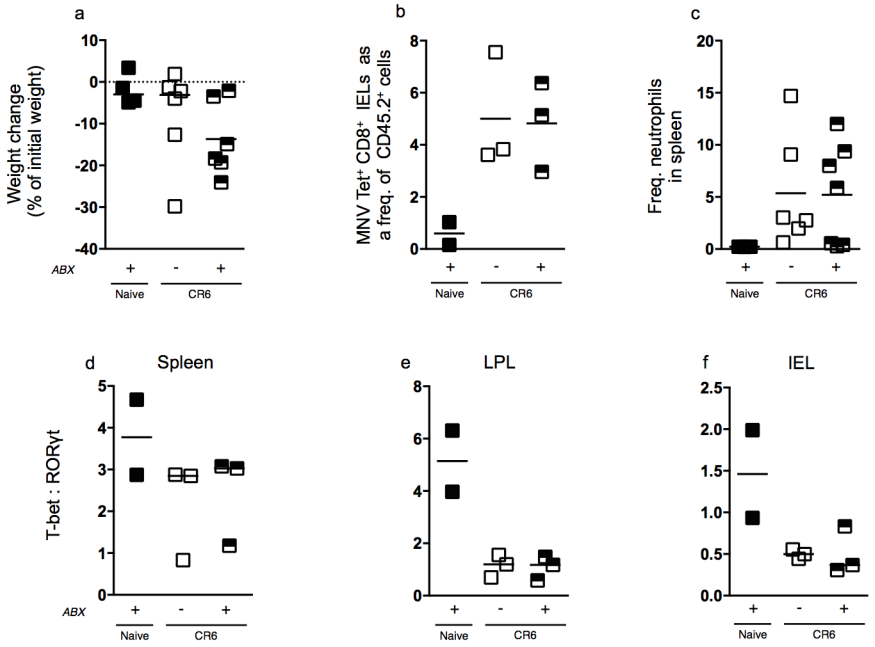

**Appendix D CD4 T cells not responsible for CR6-infection induced morbidity or altered immune responses.**

*Stat1*$^{het}$ *and Stat1*$^{KO}$ were given PBS or infected with $10^4$ pfu MNV-CR6 *p.o.* and euthanized on day 8 pi (a) weight change as a percentage of initial weight at day 0. Neutrophils (B220$^-$ CD11b$^+$Ly6G$^+$) in the (b) LPL and (c) spleen. Number of IL-17A$^+$ cells responding to *ex vivo* MNV-specific peptide stimulation in the spleen of (f) CD4$^+$ (g) TCRβ$^+$ (h) CD45.2$^+$. Data in are representative of one independent experiment. Data from one mouse are represented by individual symbols, the line representing the mean. Statistical significance was determined by Mann-Whitney test.

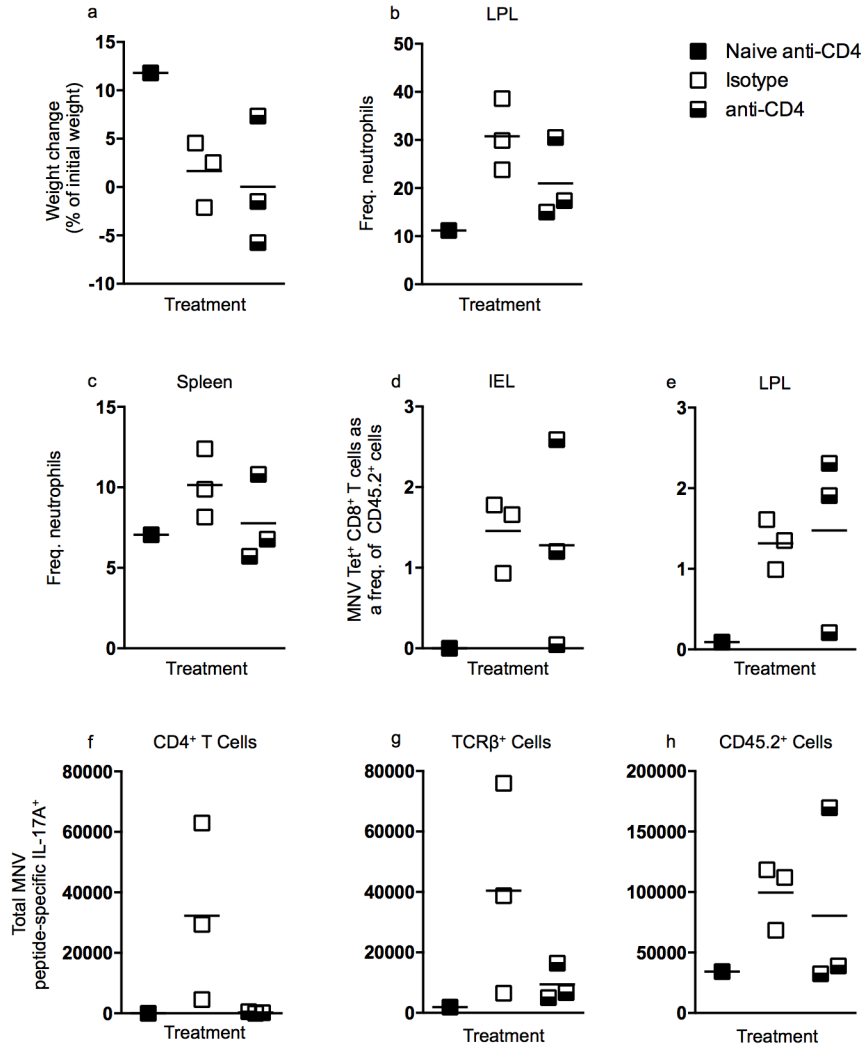

**Appendix E IL-17A-neutralization in CR6-infected *Stat1$^{KO}$* mice reduced Th17 serum cytokines, compared to control treated mice.**

*Stat1$^{het}$ and Stat1$^{KO}$* were given PBS or infected with $10^4$ pfu CR6 *p.o.,* mice were given three 400 μg/treatment Ab injections i.p. Serum from CR6-infected mice were taken at experiment end on day 8 pi and cytokine levels were analyzed by CBA. Data shown in (a) are representative of two independent experiments and (b) are compiled from two independent experiments. Data from one mouse are represented by individual symbols. Statistical significance was determined by Mann-Whitney Student's t test.